CONSORZIO RFX
Ricerca Formazione Innovazione

2007 ACTIVITY REPORT

INDEX

1. Introduction
2. RFX-mod
3. Theory and modelling studies
4. Collaborations
5. Diagnostics
6. ITER and Broader Approach
7. Cold plasma application
8. List of collaborations
9. Education and information to the public
10. List of publications 2007

1. INTRODUCTION

The programme of Consorzio RFX for the year 2007 has been presented and discussed at the 17th meeting of the RFX Technical-Scientific Committee on 14 November 2006.

The programme has been endorsed by the Board of Directors of Consorzio RFX on 5 December 2006 and by the Steering Committee of the Euratom-ENEA Association on 15 December 2006.

The final approval of the programme and of the relevant budget was given by the Consorzio Partners on 21 December 2006.

The key objectives of the 2007 programme were:

- "to extend the RFX-mod results previously obtained, both in terms of active control of MHD instabilities and of improvement of confinement properties, to a higher current range";
- "to advance the design of the ITER Neutral Beam Injector, in collaboration with the other EU Associations and in strict contact with the ITER Organization, and to start construction of the Test Facility".

The planned experimental schedule included 33 weeks of operation and the main scientific lines were: optimization of the MHD active control schemes to reduce plasma-wall interaction and transport, improvement of plasma confinement by expanding scaling studies, optimizing QSH control, continuing OPCD experiments and utilizing pellet injection.

Increase of plasma current to the 1.5-2.0 MA range was planned, as well as experiments on RWM stabilization and on the interaction between plasma and externally applied perturbations.

RFX operations ran smoothly during the whole year, confirming the excellent reliability of the machine and of its power supplies, diagnostics, control and data acquisition system. A total of 140 experimental days have allowed producing more than 2600 pulses, 1800 of them being useful for plasmas physics.

A significant effort has been dedicated to the improvement of the plasma control algorithms and devices. Owing to the high flexibility of the new MHD control system, the most important results in terms of quality of confinement have been obtained by implementing a new control scheme, called "Clean Mode Control", which could improve the effectiveness of the external action on the plasma dynamo modes. A better plasma control has been also obtained by pellet injection.

Section 2 describes the main results of the physics programme in RFX. According to plans, the plasma current has been raised up to 1.5 MA, close to the original target level of 2 MA.

The smoother plasma-wall interaction obtained by improving the magnetic boundary allowed to obtain long (up to 0.5 s), well controlled pulses, with electron temperatures close to 1 KeV in standard operation and even higher when Oscillating Poloidal Current Drive is applied. It has also been observed that the high current favours the onset of Quasi-Single Helicity states, which is a promising feature for future performance.

MHD simulation has been the main focus of the theory and modelling activity (Section 3): the implementation of a new code will allow a better description of the tearing mode behaviour, in the presence of passive structures and feedback. Kinetic calculations confirmed the differences between

Tokamak and RFP in terms of ITG stability, whereas diffusion-convection models allowed to better interpret anomalous transport.

Section 4 gives an overview of the main results of scientific and technological collaborations: it's worthwhile noting that the links with the Tokamak community have been further promoted by Consorzio RFX in 2007, by starting a new programmatic line on "Tokamak Physics". Of course, the collaboration with the other RFP laboratories has been still very active.

RFX is already characterized by a good diagnostic coverage; nevertheless, a significant effort, (Section 5) has been dedicated in 2007 to the completion of new diagnostics, in particular the reflectometer, the FIR polarimeter, the active spectroscopy by mean of the diagnostic neutral beam injector.

The second pillar of the programme regarded the ITER Neutral Beam Injector design. A key strategic decision has been taken in 2007: the Neutral Beam Test Facility, to be built in Padova, besides being aimed to develop and test the NBI before installation on ITER, will also serve as a test bed in parallel to ITER operation, with a wide scope regarding performance optimization, reliability improvement, availability verification. Consorzio RFX carried out a substantial design work in 2007 (Section 6), which contributed to two key decisions by the ITER IO: the adoption of the RF-driven ion source and of a new scheme for the power supplies. A significant milestone has been the start of the final design of the NBTF buildings by a civil engineering company. The year 2007 has been also characterized by an increased effort on source and beam modelling, with the aim of enforcing the competence of the group on neutral beam injection physics.

Section 6 also describes the work done on ITER diagnostics and for the Broader Approach, where RFX is in charge of a part of JT-60 SA power supplies.

Finally, Section 7 describes the recent results of a small effort dedicated to cold plasma applications, Section 8 gives a list of the ongoing collaborations and Section 9 reports on the educational activities, where a key achievement has been the start of the new joint research doctorate in fusion science and engineering.

2. RFX MOD

2.1 Technical improvements

2.1.1 Pellet injector

The cryogenic injector has been optimized by defining setting-up parameters that prevent pellet self-firing. Electronic problems due to EM interference at high current have also been solved. On-line codes that compute pellet parameters and trajectory have been modified for the new acquisition system. Many experiments have been performed with pellet injection to improve plasma performance, to study density transport and assist discharge setting-up (pellet at start-up).

2.1.2 *Preparation for high current operation*

The high current experimental campaigns which have been planned for 2007 and 2008 require the Magnetizing Winding Current to be increased up to the nominal design value of 50 kA.

As a consequence, the mechanical stresses due to electrodynamic loads on the coils and on the busbars are expected to be increased by a factor of two with respect to those applied in the previous high-current campaigns at 35 kA.

As a precautionary measure, it was decided to install a system of sensors suitable to measuring the displacement of the coil terminals and busbars in the central part of the Magnetizing Winding, which is indeed the most severely stressed part of the system.

In fact these sensors are intended to be used for two purposes:

a) as displacement measuring devices for a reliable determination the level of stress of the most critical components during normal operation

b) as protection devices suitable to reveal abnormal displacements which could be caused by a progressive delamination of the fibreglass insulation of coils and busbars. This is particularly important since in vacuum-impregnated fibreglass insulation systems, catastrophic electrical failures are often the consequence of the progressive degradation of a minor mechanical failure.

The main requirements of such a measurement system are the following:

1. measurement range > 5mm
2. linearity: < 0.1mm
3. accuracy: < 30μm
4. acquisition frequency: < 1 kHz
5. electrical insulation: 35 kV
6. electromagnetic compatibility up to 4T .

Theses requirements exclude the use of direct contact sensors (such as linear transducers and strain gauges)

After a comparison of sensors based on several different measurement principles, sensors based on confocal chromatic technology have been chosen. A polychromatic white light is focused onto the target surface by a multi-lens optical system, which disperses the beam in such a way that each specific wavelength is focused at its own specific distance. Only the light which is focused on the target is used for the measurement. The distance between the lens and the target can be determined by measuring the wavelength of the light reflected by a target.

The confocal measurement system consists of a controller connected to the lens by simple fibre optic. The electronic controller is placed 50 m away from the lens in order to prevent any interference due to the electric and magnetic field.

2.2 MHD mode physics and active control

Introduction

In 2007 a significant upgrade of the MHD control system has been realized. This upgrade allows improving the VS scheme, which was used since the beginning of RFX-mod operations.

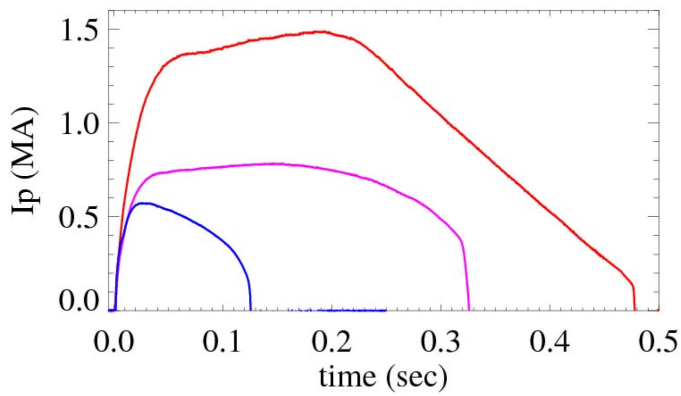

Fig. 2.1: time traces of plasma current. Red is obtained with the Clean Mode Control algorithm described here. The magenta curve refers to a discharge whose boundary was controlled with Virtual Shell algorithm. The blue discharge is performed without active control.

While this scheme in its old version was able to completely stabilize the Resistive Wall Modes (RWM), the action on the edge value of the tearing modes (TMs) has been found to be less effective due to a systematic error. The origin of the error is in the aliasing phenomenon affecting the measured magnetic field harmonics: this is due to the high poloidal and toroidal mode number sidebands produced by the discrete coils grid.

Such aliasing effect has been identified and corrected in real time, obtaining a clean Fourier spectrum. A new control scheme, named *Clean Mode Control (CMC)*, has therefore been implemented. Experiments aiming at optimizing the feedback laws applied to the clean Fourier spectrum have been performed and new physics results have been obtained. In particular, it has been observed that:

a) Tearing Modes amplitudes can be systematically reduced, more than with the previous scheme;
b) mode rotation and consequently locking of the modes from the wall can be obtained in a reproducible way;
c) the non-axisimmetric deformations of the plasma column can be significanty reduced, and this allowed to reach a plasma current level of 1.5 MA, , as can be observed in Fig. 2.1.

In the following more details on the new algorithm and on the results are given.

The systematic error due to the aliasing of sidebands

In the VS scheme, the control system determines the currents flowing into the saddle coils in order to keep the measurement of the corresponding sensor coils as close as possible to zero. This condition implies that all the Discrete Fourier Transform (DFT) harmonics of the measurements of radial field are almost zero. The sampling theorem states that the DFT harmonics correspond to Fourier harmonics only if the aliasing phenomenon does not occur; while this condition is met when the spectrum of MHD modes in RFX-mod is measured without any active action from the cols, this is not true when the saddle coils generate a field. Due to their discrete size, the field that they produce is characterized by a rich spectrum of high *n* sideband harmonics, whose aliasing pollutes the DFT spectrum: therefore zeroing the DFT harmonics does not imply that the Fourier harmonics are zero, i.e. that the edge amplitude of TMs or error fields are cancelled. The effect of this systematic error is shown in Fig. 2.2: the average spectrum of the radial DFT harmonics for a standard Virtual Shell controlled discharges is shown as open triangles, while the Fourier harmonics (obtained by subtracting the aliasing of the sidebands from the DFT harmonics) are the full triangles.

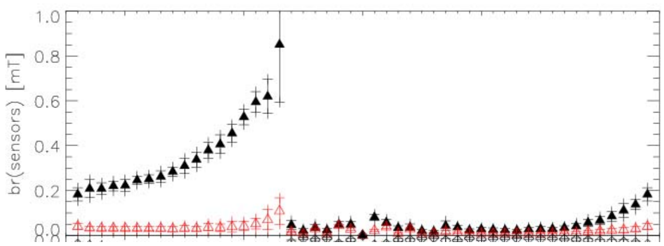

Fig. 2.2: the toroidal spectrum of the radial component of the magnetic field is shown. Open triangles: Discrete Fourier Transform; Full triangles: Fourier harmonics, obtained by subtracting from the DFT harmonics the aliasing of the sidebands produced by the saddle coils.

Another source of systematic error is the distance between the radial field sensors and the plasma edge.

Correction of the sidebands aliasing

While the sidebands generation is unavoidable, because it is due to the geometry of the saddle coils, the aliasing can be eliminated with two approaches: increasing the number of sensors or correcting the measurements. As the first option is not feasible in RFX-mod, a cylindrical model has been developed [Zanca07] in order to compute the aliasing of sidebands and subtract it from the measurements. This model requires the simultaneous measurement of the currents flowing into the coils and assumes that the passive structures between the coils and the sensors are continuous.

Once tested, this model has been implemented in real time, so that the feedback variables are the Fourier harmonics and not the aliased measurements. This required a significant upgrade of the control system hardware, because of the increased number of signals to be digitized in real time (192 currents flowing into the saddle coils), and because of the heavier computations to be performed at each control cycle.

A further enhancement of the control system, consisting in the acquisition of 4x48 toroidal field measurements, allowed the computation of the radial field at the plasma edge.

Initial results obtained with Clean Mode Control

With the new Clean Mode Control scheme a hybrid scenario has been explored so far: a group of modes, set by the operator, is controlled with the Fourier harmonics, leaving the other modes controlled using the DFT harmonics. More optimizations and simulation work is necessary in order to find optimal gains for all harmonics.

The choice of the gains is found to have important consequences also on the time evolution of the mode phases: spontaneous rotations up to 100Hz have been observed in experiments. Moreover, it was possible to find a proportional gain value to reduce the edge value of the TM to a threshold, after which modes begin to rotate. The ability of the CMC scheme of keeping the edge amplitudes to a low level and simultaneously inducing rotations of the TM phases has been used to decrease the non axis-symmetric displacement of the plasma produced by the TM radial amplitude at the edge. This allows to reduce the plasma-wall interaction. The control scheme has also important consequences on the plasma resistivity and on energy confinement. At intermediate currents (Ip < 850 kA), during the flat-top phase, the average on axis loop voltage is lower in CMC discharges compared to standard VS [Zanca07] at the same density as shown in Fig. 2.3. The adoption of the CMC scheme allowed performing a preliminary campaign of experiments with plasma currents up to 1.5MA. Even though a further decrease in loop voltage has not been observed in this regime, the energy confinement found during such operation is the best ever achieved in RFX-mod.

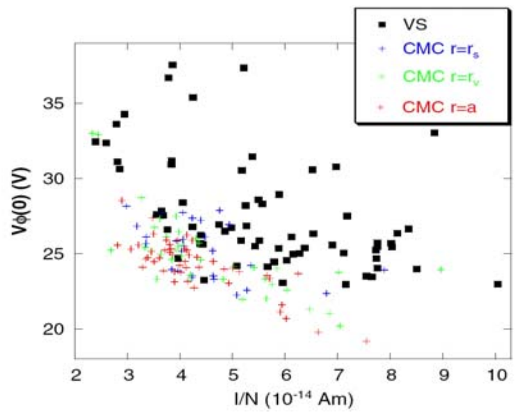

Fig. 2.3: On-axis value of the toroidal loop voltage as a function of the quantity I/N. These quantities are averaged between 60 and 140 ms. black squares represents standard Virtual Shell discharges, while coloured plus signs refer to Clean Mode Control discharges.

2.2.3 Resistive wall mode physics and control

In order to progress on Resistive Wall Mode (RWM) understanding, the 2007 activity in this area focused on systematic studies

(a) of growth rates under different experimental conditions and
(b) of interactions between RWM and external perturbations.

The first point lead to a statistical characterization of RWM growth rates measured under well-controlled conditions and in different plasma conditions. In particular the dependence on plasma current, electron density, and reversal parameter F has been analyzed. In this study, only shots where typical RWM helicities (m = 1, $|n|$ = 2, 3, 4, 5, 6) were excluded from the active control system have been used. An automatic procedure was developed in order to detect

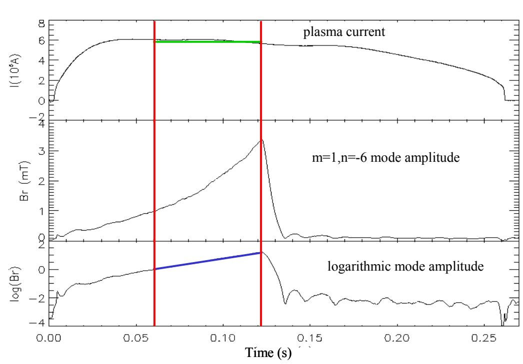

Fig.2.4: Analysis of a single RWM growth rate. The time interval selected is between the two red vertical lines.

and interpolate, with a single exponential fit, sufficiently long phases of mode amplitude free growth. An example of such interpolation is given in fig. 2.4. The high precision of the fit demonstrates that in the RFP configuration the growth of a RWM can be studied under well controlled experimental conditions and that it is possible to exclude the influence of interactions with other instabilities or of damping mechanisms on the RWM growth rate. This provides an interesting playground for numerical codes that, before facing the more complicated tokamak case, can test their accuracy with a quantitative comparison with RFP data. The clearest result of the statistical elaboration of growth rates is that the main drive for RWM destabilization in the RFP is the current profile. This is in very good agreement with theory. This result is shown in fig. 2.5, where the dependence of the internal, non-resonant, (m=1,n=-5) mode growth rate on the F parameter is plotted. It is clear that internal non-resonant RWMs are more unstable at shallower F values (i.e. with flatter current profiles). Similar plots for external non-resonant modes show, as expected, the opposite tendency, i.e. a growth rate increasing at deeper F values (corresponding to more peaked current profiles).

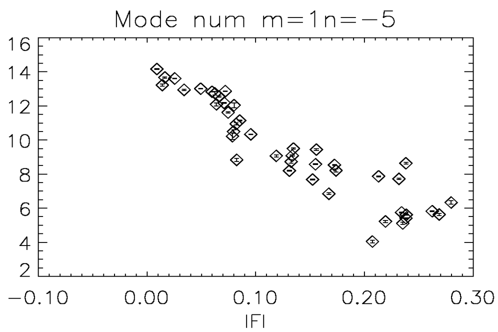

Fig.2.5: Growth rate (1/s) vs. |F| for the (1,-5) RWM.

A new set of experiments was devoted to the study of RWM interaction with external controlled perturbations. The main aim of this new set of experiments, performed in collaboration with scientists from the Max-Planck Institut für Plasma Physik in Garching (Germany), was the investigation of the main torque mechanisms acting on RWMs in the case of a Reversed Field Pinch plasma. To this purpose, the amplitude of selected unstable RWMs was only partially controlled by decreasing the proportional gain on the active control system in order to get an unstable mode with constant amplitude. The result of a scan on proportional gain is shown in figure 2.6. These studies are also interesting for the field of active RWM control, when the power allowed for the control is insufficient (with might be the case in future experiments).

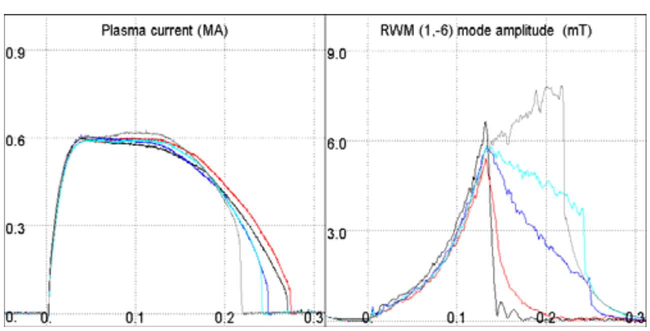

Fig.2.6: Example of proportional gain scan on the (1,-6) RWM control. Plasma current and mode amplitude are shown.

On the constant amplitude RWM was then applied a new feedback control strategy, with constant proportional (real) gain, but with different imaginary amplitude. In this way we studied the reaction of a RWM to an external perturbation with the same helicity, but with a non-zero torque between the two. First analyses of experimental results indicate that in this way the RWM, always wall-locked in the RFP case, can be unlocked and accelerated with a phase velocity that reaches a constant value and that depends only on the phase difference between the mode and the external perturbation. The induced mode rotation frequency found in these first experiments is low (a few Hz); a model to interpret these results is being developed.

2.3 Operation at High Current

In 2007 the plasma current in RFX-mod has been raised from approximately 1.1 to 1.5 MA [Marrelli 07]. 1.5 MA is the highest current ever reached in a Reversed Field Pinch and is also an important step towards the original target level of 2 MA for RFX-mod. In the older version of the device it was recognized that plasma wall interaction associated to locked modes represented an operational limit preventing the achievement of high current regimes. This problem was solved during the 2007 successful operation thanks to the exploitation of the sophisticated active magnetic boundary system that characterizes RFX-mod. In particular the latest version of the algorithm that drives the actuators of the artificial shell, the Clean Mode Control (see Sect. 2.2), has allowed to significantly reduce the maximum displacement of the plasma column induced by m=1 modes and to control its position around the torus. This reduced the plasma-wall interactions and opened the way to the high current operations.

In this first RFX-mod attempt to rise the current above 1 MA, the region of the parameter space with low density and shallow F has been mainly explored. It has been found in fact that F=-0.04 to -0.06 corresponds to a minimum loop voltage in a selected database, though such a dependence is to be confirmed by further experiments. Low density regimes also are characterized by lower toroidal loop voltage and have been accessed by He Glow Discharge Cleaning.

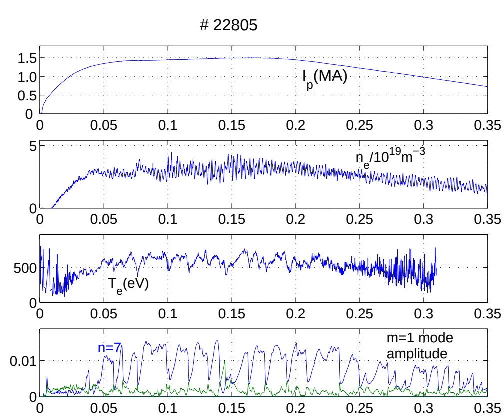

Fig. 2.7 Example of 1. MA discharge in RFX-mod. From top to bottom: plasma current, electron desnity,eElectron temperature amplitude of (blu) m=1n=-7 and (green) m=1 and n=-8 modes.

One of the discharges with the highest plasma current obtained up to now is shown in the Fig.2.7. In that pulse the flat-top sustainment was stopped at 180 ms and the discharge landed smoothly lasting around 400ms. This duration is well beyond the shell resistive time, thanks to the complete stabilization of the RWMs. The stationary flat-top electron temperature was between 0.7 and 0.8 keV with a density stably around $3x10^{19}$ m^{-3}. The bottom frame of Fig. 2.7 shows a typical phenomenon occurring at high current, that is the spontaneous development of a Quasi Single Helicity (QSH) state, where the amplitude of the innermost resonating tearing mode (m=1, n=-7) increases, while the amplitude of all of the other secondary m=1 modes decreases. [Valisa07].

Part of the high current campaign has been devoted to technical issues such as the study of the start-up phase, where a compromise is to be sought between equilibrium control, breakdown and density control. Pellet injection has proved very useful to aid the fuelling in the phases between breakdown and RFP formation. Here a strong fuelling is required to sustain the fast current ramp up; the standard and less efficient gas puffing would instead compromise the degree of gas wall-loading for the subsequent discharges. Indeed recycling control remains an important operational limitation affecting experimental sessions, whereas the discharges easily derive towards high density and less controllable conditions.

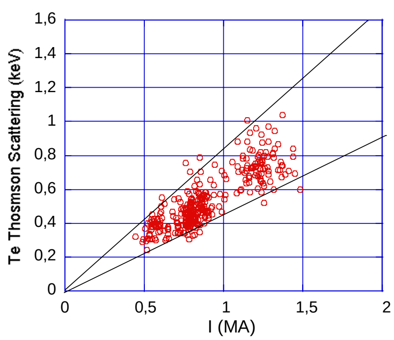

Fig.2.8 Electron temperature from Thomson scattering as a function of plasma current (all densities)

The current increase is accompanied by higher temperatures, as shown in Fig. 2.8. The highest values exceed 1 keV and are obtained during Oscillating Poloidal Current Drive (OPCD) operations, where single helicity structure and strong thermal barrier at the edge develop systematically (see Sect. 2.4). In the standard conditions, for any given density the correlation between current and temperature is linear and no signs of saturation of the temperature increase have been seen.

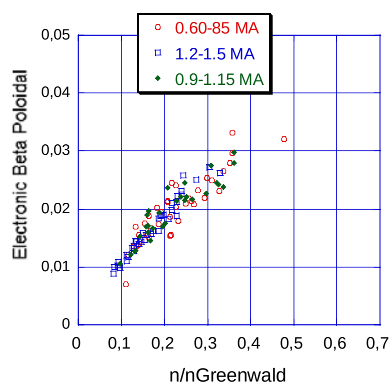

Fig.2.9 Beta Poloidal as a function of the normalized desnity. Color code for different current level is indicated in label..

An important result in the perspective of higher current operations is that the poloidal beta does not decrease with current. This is shown in Fig. 2.9 where the poloidal beta is plotted as a function of the normalized electron density for groups of discharges of different current. The three groups overlap, implying that no degradation is occurring at higher currents. Energy confinement improves as well with plasma current, with the highest values reached during transient events such as those produced with OPCD. Confinement scaling has not been studied yet given the preliminary and still not yet optimized nature of the high current operation.

Improvements are expected on various fronts, especially from further optimization of the m=1 and m=0 modes and better recycling control. Maximum confinement time achieved in 2007 is of the order of 2.5 - 3 ms, pending a deeper investigation on value of the loop voltage during transient events, which now suffers from large "noise" and needs a more careful analysis

2.4 Oscillating and Pulsed Poloidal Current Drive experiments

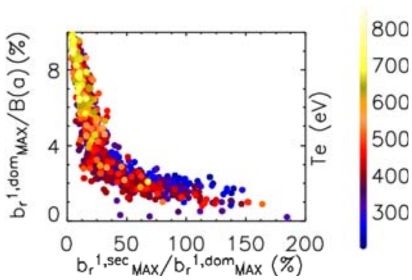

Fig. 2.10 Correlation between the maximum electron temperature, the dominant mode normalized amplitude and the secondary modes normalized amplitude.

In the experimental campaign dedicated to poloidal current drive techniques (OPCD and PPCD), new waveforms and circuit control programming have been adopted providing significant improvement in the already good results obtained in the previous years. Both OPCD and PPCD discharges have been programmed using the open loop control of the reversal parameter *F,* providing in this way a better control of the time evolution of the edge toroidal field and allowing current drive experiments at plasma currents up to 1.3 MA.

The operation at higher plasma current and the optimization of the waveforms with respect to previous campaigns allowed to reach record electron temperatures for RFX-mod, up to 1 KeV [Terranova07]. The enhanced plasma performance is obtained in QSH states, that are systematically induced by the OPCD: figure 2.10 shows the correlation between the normalized amplitude of the dominant MHD mode vs. the amplitude of the secondary modes (normalized to that of the dominant). Colour coding corresponds to electron temperature measured by the double filter diagnostic. Higher temperatures are obtained when the dominant mode is larger, and correspondingly the secondary are smaller. The magnetic field line topology has been investigated by means of a new field line tracing code (FLiT, [Innocente07]) that has been developed starting from the eigenfunctions of the tearing modes reconstructed in toroidal geometry. Figure 2.11 (left) shows the Poincaré puncture plot and the corresponding temperature profiles in a QSH state induced by the OPCD. Besides these typical asymmetric profiles, it was possible to induce even larger QSH states by superimposing to the OPCD a small rotating perturbation with the same helicity of the dominant mode (right frames of Fig. 2.11). This allows obtaining a magnetic island that expelled the separatix, then forming a new magnetic equilibrium with a helical hot core over a larger section of the plasma, as shown by the electron temperature profile. These new magnetic equilibrium has a single helical magnetic axis.

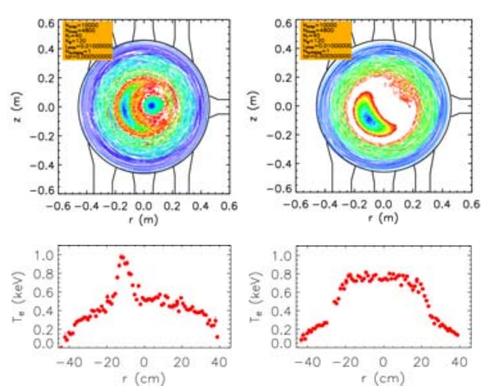

Fig.2.11 FLiT reconstruction of internal magnetic field line topology and electron temperature profiles in a QSH (left) and SHeX (right) state.

This operation with OPCD plus a small rotating perturbation are useful also for particle transport studies. The position of the induced helical structure is in fact known at any time. This allows injecting a pellet inside it, then providing a known particle source in a structure that otherwise would not be distinguishable from the background plasma. The first results give some indication that also the particle confinement is affected by these structures, but further investigation is required in order to optimize the synchronization between the pellet and the position of the structure.

While OPCD experiments aimed at optimizing plasma performance, PPCD experiments were dedicated to a comparison with the results obtained in the MST experiment in Madison (Wisconsin), In particular, we tried to reproduce similar values of induced electric field and loop voltage waveforms in the two devices. The preliminary results obtained in this limited campaign gave some indication on a possible explanation (linked to the stability of m=0 modes) for the different performances obtained in the two machines and provided important information for the organization of a joint experimental campaign dedicated to this topic involving all the RFP community for next year.

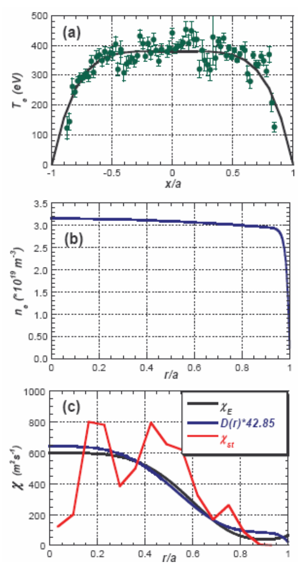

Fig.2.12 Electron temperature (a) and density (b) profile of 1 MA discharge.
Graph (c) compares the experimental thermal diffusivity (black line), the particle diffusivity times 42.85 (blue line) and the estimate of the theoretical χ by means of the FLiT code (red line).

2.5 Particle transport

2.5.1 Core particle transport in standard plasmas (MH)

A fraction of the experimental activity has been dedicated to a deeper investigation of core particle in standard RFP conditions, where magnetic perturbation is not mitigated.

According to the theory of the transport in a stochastic magnetic field [Rechester78] the electron thermal conductivity and the particle diffusivity coefficients are proportional to the magnetic line diffusivity via the ion and electron thermal velocity: $\chi_e = v_{th}^i D_M$, $D = v_{th}^e D_M$, where D_M is the magnetic diffusivity. The ratio between χ_e and D is proportional to the square root of the ratio between the ion and electron mass (≈40). In order to check this theory both the experimental particle diffusivity and thermal conductivity have been calculated by means of the transport code TED for a selection of 1 MA discharges, using the electron temperature profile measured by the Thomson scattering and the density profile obtained from the inversion of the interferometer data. The ion temperature is assumed equal to the electron one. The typical density and electron temperature profiles in those discharges are shown in figure 2.12. The magnetic field line diffusivity D_M has been calculated by means of the field line tracing code FLiT that has been developed starting from the eigenfunctions of the tearing modes reconstructed in toroidal geometry.

Figure 2.12-c shows a good agreement between the experimental thermal conductivity, the experimental particle diffusivity times 42.85 and the estimate of the theoretical χ_e which is found in

high current discharges. The agreement is worse when a similar analysis is done on discharges at lower current (600 kA), where the curves differ by a factor 2-3.

2.5.2 *Density limit*

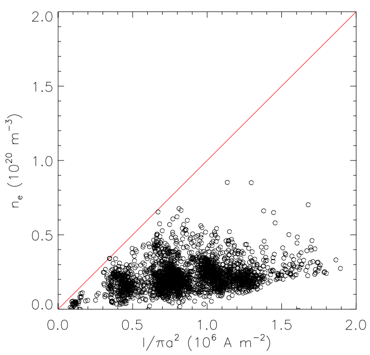

Fig.2.13 Electron density, plotted as a function of the Greenwald parameter $n_G=I/\pi a^2$ for a large database of RFX-mod discharges. The red, solid line represents the Greenwald limit $n=n_G$.

In RFX-mod an upper density limit has been found, well described by the Greenwald's law that holds for Tokamaks. In the RFP this limit is not accompanied by major disruptions, but has the form of a soft landing of the plasma current [Valisa2006]: high density discharges are difficult to sustain and have a decaying current ($n_G=I/\pi a^2$ is the Greenwald density). In any case, no discharges are found with $n/n_G > 1$ (see Fig. 2.13).

This empirical limit in RFX-mod is believed to be associated to the physics of the edge, and in particular to the development of a local thermal instability. In RFX-mod, highly radiating poloidal rings have been detected by the bolometric tomography. This occurs beyond a critical density well before the Greenwald limit, at n/n_G >0.35. It is noticeable that the same threshold marks a change in the electrostatic turbulence character at the edge in the sense of a reduction of the associated diffusivity.

These high radiation rings are toroidally localized and poloidally symmetric, having therefore an m=0 symmetry. The toroidal extension is of about 90°. The ring is often found in the region where the last-closed flux surface (LCFS) is shrunk. This is the region where the toroidal non-axisymmetric shift $\delta_{m=0}$ is less than 0, as a consequence of the action of m=0 modes. The emissivity in this region can be easily of the order 10 MW/m^3, and half of the total radiated power is emitted within the ring (on average, 5 MW over the total 9 MW at high density). Since the ohmic power is on average 20 MW, and the ring covers about one quarter of the whole torus, this means that the local ohmic input power is on average 5 MW (20MW/4), i.e. almost equal to the power radiated by the ring.

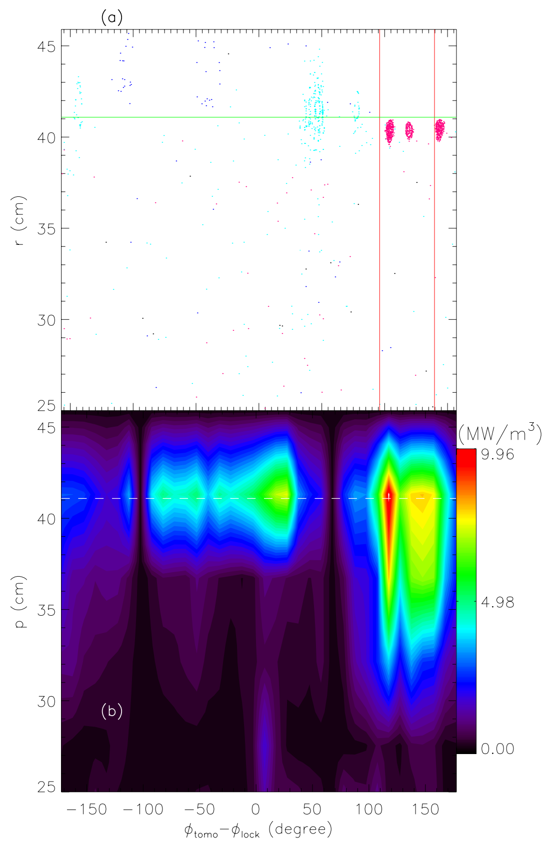

Fig.2.14 (a) Poincaré plot (equatorial cut, toroidal angle as x-axis, radius as y-axis), showing the magnetic field line topology and associated edge m=0 islands; (b) total radiation emissivity with the same coordinates. It is evident the correspondence between m=0 islands and localized radiation rings

This simple evaluation suggests that the density limit in the RFP can be seen as a radiation limit within the ring.

Regarding the physics of the radiation, it is well known that the region where $\delta_{m=0}<0$ is characterized by the presence of magnetic islands, almost poloidally symmetric (so, almost m=0). These islands have a great importance in the edge transport, since they determine a transport barrier with an associated temperature gradient, and are probably related to the interplay between magnetic-dominated transport and electrostatic transport at the edge [Spizzo 06]. The same islands can play a fundamental role in determining the density limit in the RFP, as shown in Fig.2.14, evidencing the correspondence between well-conserved islands (red in the picture) and radiation rings, which have the same symmetry.

The radiative instability could be explained in terms of a local decrease of particle diffusivity inside the island, which fills up with electrons and/or impurities. This local confinement of impurities can be triggered by the decrease of the turbulent diffusivity of electrostatic eddies, which is also found at n/n_G >0.35 [Scarin07].

2.6 Energy transport

2.6.1 Core energy transport in standard plasmas (MH)

The effect of VS on thermal properties of RFX-mod during standard, MH states is evident on the core electron temperature T_e^{core}, defined as the average temperature in the central region of the plasma column ($|r/a|$<0.5, where a is the minor radisu). The scaling of T_e^{core} as a function of I_p (see figure 2.15) is shown at I/N~4·10^{-14}Am for

- RFX-mod virtual shell - VS (full circles),
- RFX-mod standard - SD (empty diamonds), and
- RFX (empty triangle) discharges.

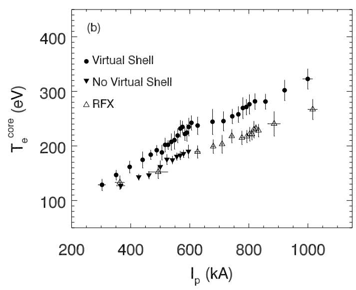

Fig. 2.15: T_e^{core} vs. I_p at I/N = 4·10^{-14}Am in MH states in RFX (empty triangles), RFX-mod without VS (full triangles) and RFX-mod with VS (full circles) in typical plasma discharges.

During initial RFX-mod experiments with plasma current up to 600 kA, the active MHD control was not used and SD pulses are similar to those of the RFX device, with comparable T_e^{core} values. In particular, confinement properties in RFX-mod SD are slightly lower than in RFX; this is because, in absence of feedback control, the penetration of the radial field through the thin shell of RFX-mod leads to more pronounced plasma-wall interaction and consequently to higher loop voltage (+25%, up to 40V). Performance is also deteriorated by wall- and phase-locking of m=1 and m=0 tearing modes, whose amplitude grows in time. By activating the saddle coil system for active control of MHD modes, the radial field penetration is canceled: plasma-wall interaction is strongly reduced, and the lower loop voltage (25-30Volts), accounts for an increase of ~20-25% in T_e^{core}. With respect to RFX, the improvement is maintained also at higher currents, up to 1 MA. The increased core temperature during VS operations is present also at other I/N values: this is interpreted as a more efficiently confined energy in the plasma in VS than in SD and RFX operation.

As customary in RFP's, RFX is powered through ohmic heating only. Local gradients are thus representative of local heat diffusivity χ_e, both in the core ($\nabla T_{e,core}$) and at the reversal surface ($\nabla T_{e,rev}$). These gradients are obtained through a linear fit of measured points at $|r/a|$~0.5-0.7 and $|r/a|$>0.75 respectively. $\nabla T_{e,rev}$ in VS discharges is higher than in SD (~60%), and as current increases above 600kA, it almost saturates. As far as $\nabla T_{e,core}$ is concerned, there is a weak but systematic positive trend with I_p, despite the low values, with steeper gradients (~30%) in VS operation. These trends are not influenced by the value of the axisimmetric displacement of the last closed flux surface, which is in the range 0-2 cm.

Steeper edge and core gradients are indicative of a decrease of electron heat transport during VS:

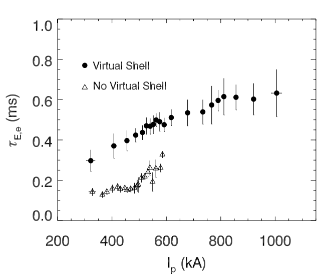

Fig. 2.16 Electron confinement time vs I_p in MH states at I/N= 4·10^{-14}Am in RFX-mod with (full circles) and without (empty triangles) VS.

we calculated the heat diffusivity adopting a 1D single fluid approach and solving the power balance equation, χ_e^{PB}. Edge and core χ_e^{PB} are both reduced during VS operation, at all currents available. In particular, the heat conductivity shows the same features of T_e gradients: $\chi_{e,rev}$ significantly decreases as VS is active, then becoming almost unvaried as plasma current exceeds 600kA; $\chi_{e,core}$ is 2 to 3 time lower than in SD, then still decreases as current rises up. The saturation at the reversal could be due to the role of m=0 modes, whose control with the present feedback system has still to be improved.

The reduction of electron heat diffusivity is tightly correlated to the increase of electron confinement time $\tau_{E,e}$ (with $\tau_{E,e} \sim L^2/\chi$, L being the typical gradient scale length): confinement time is here calculated through the poloidal beta parameter $\beta_{\theta,e}$, $\tau_{E,e} = \beta_{\theta,e} I^2/(8P_\Omega/3R\mu_0)$. This is shown in figure 2.16 as a function of I_p at I/N~$4 \cdot 10^{-14}$Am. At 600kA $.16_{E,e}$ nearly doubles with respect to SD, being about 90% larger and with about 0.6ms peak values of $.16_{E,e}$ in best MH discharges; at 1MA, during MH VS states, $\tau_{E,e}$ is about 70% larger than in RFX. Nevertheless improvements are available further mitigating the plasma–wall interaction, since $\tau_{E,e} \sim$ 0.8ms has been measured at 1.1MA in best MH discharges by active rotation of m=1 modes.

2.6.2 Energy transport in helical structures

An explanation of the strong heating observed in the core of a reversed-field pinch in the quasi-single-helicity state has been studied. During a QSH state, a magnetic helical structure is formed, in which the heat transport coefficient is much smaller than in the surrounding chaotic sea, because of the formation of well defined magnetic surfaces. The values of the thermal conductivity obtained with the M1TEV 2D [Annibaldi07] dimensional transport code (χ_i=9–30 m^2/s) are in good agreement with the estimates of the ion diffusion coefficient inside the island, given by a Hamiltonian guiding center code, D=2–7 m^2/s. In these simulations, transport inside the island is larger for ions, due to the presence of a population of helically trapped ions, which is a neoclassical effect. Heat transport is therefore dominated by ions, and the heat diffusion is $\chi \approx \chi_i = 5/2 D_i$=5–17.5 m^2/s, which is a factor of 2 smaller than the M1TEV estimates. Moreover, the values of thermal conductivity are in the tokamak range, and are consistent with the peak temperatures measured in RFX-mod. The effect of the helical structure width and of the different level of power deposited inside the structure on the final temperature peak has been also investigated: an inverse dependence on the width and and a linear dependence on the power is found.

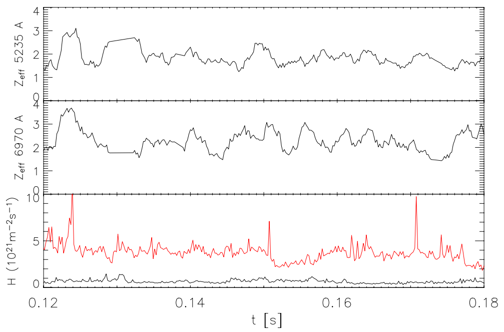

Fig.2.17 Top and centre: plasma effective charge versus time measured after boronization (#22724) from bremsstrahlung continuum at λ=5235 Å and λ=6970 Å. Bottom (black curve) hydrogen influx measured along a vertical diameter during the same discharge and in a similar discharge before boronization (in red #21944)

2.7 Impurity behaviour

Low impurity content (Z_{eff} ~1.8 from Bremsstrahlung continuum at λ=5235 Å and 6970 Å) is found in RFX-mod after

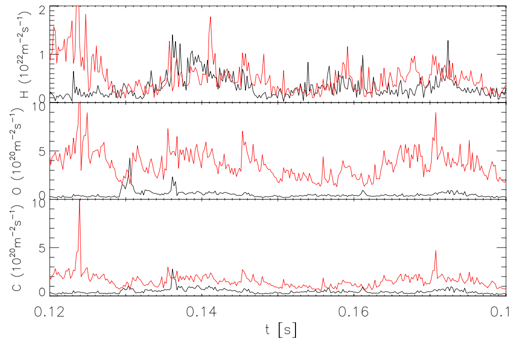

Fig 2.18 Hydrogen, Oxygen and Carbon influxes plasma versus time measured in two similar discharges after boronization (in black #22724) and before boronization (in red #21944) along an external line of sight.

d... ice of high re... continuum re... idered not re...

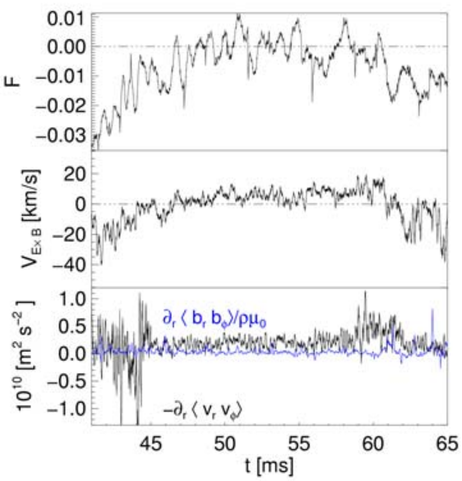

2.

D... omentum transport in the edge region has continued, w... ds and Maxwell in driving sheared flows also in non-st... ch includes the role of fluctuations in the momentum tr... e average of the momentum balance equation:

Fig.2.19: From top to bottom: (top) Reversal parameter F (middle) electric drift velocity ExB (bottom) Radial derivative of Reynolds stress (black) and Maxwell Stress (blue)

$$\partial_t \overline{V}_\phi + \partial_r \langle \tilde{v}_r \tilde{v}_\phi \rangle = \partial_r \left(\frac{\langle b_r b_\phi \rangle}{\rho \mu_0} \right) + \partial_r \left(\frac{\overline{B}_r \overline{B}_\phi}{\rho \mu_0} - \overline{V}_r \overline{V}_\phi \right) + \nu \nabla^2 \overline{V}_\phi \quad [1]$$

w... ating part, and ν is the kinematic vi...

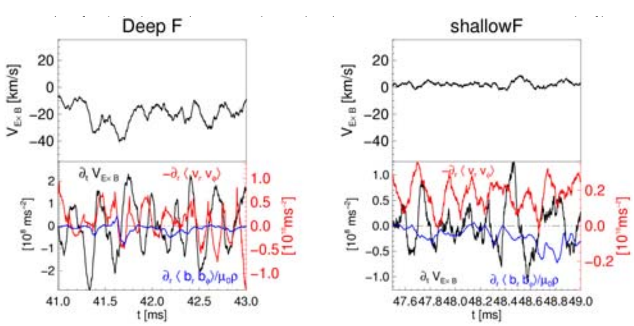

is ... etic components are referred also as E... tively.

D... ng sheared flow has been already

Fig.2.20: Two snapshot taken at two different values of the reversal parameter. In both cases in the top panels show the traces of ExB velocity whereas the bottom panels show in black line the time derivative of ExB velocity, in red line the radial derivative of Reynolds stress gradient, in blue line the radial derivative of Maxwell stress

demonstrated during the low-current operation of RFX-Mod. Similar analysis has been performed also during transient phenomena, in particular during the controlled variation of the reversal parameter F. In fig. 2.19 a snapshot of the observed behavior is reported. Starting from a deep *F* condition and moving towards a shallower profile the ExB velocity is found do decrease in absolute value becoming almost zero or slightly positive, restoring its initial value when the *F* return start to decrease again. Correspondingly strong modification on the radial derivative of Reynolds stress is observed. A zoom of the two different behavior are reported in figure 2.20. It can be clearly observed indeed that in both the cases, i.e. during the deep reversal condition and during the shallower one, the time traces of the radial derivative of Electrostatic Reynolds stress and of the time derivative of plasma velocity are well correlated. This demonstrates that in both cases the electrostatic fluctuations are the main driving term of plasma flow at the edge. It is worth to note that the main difference resides on the value of the coupling $\left\langle \tilde{v}_r \tilde{v}_\phi \right\rangle$ which is lower by a factor of two in the shallower condition.

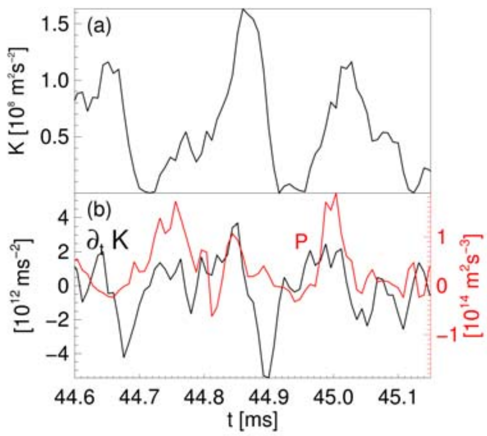

Fig.2.21: Top panel kinetic energy associated to mean plasma flow. Lower panel time derivative of kinetic energy K and production term

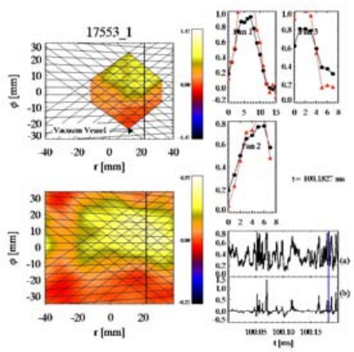

Fig 2.22: example of one coherent structure that flow in the GPI field of view. Left: 2D pattern reconstructed with the two different algorithms. Right: line integrals and time behavior of the GPI signal

The observed behavior suggests the existence of an energy exchange process between fluctuating and mean flow energy. The process is regulated through the production term

$$P = \left[\left\langle \tilde{v}_r \tilde{v}_\phi \right\rangle - \frac{\left\langle \tilde{b}_r \tilde{b}_\phi \right\rangle}{\overline{\rho}\mu_0} \right] \partial_r \overline{V}_\phi$$

as from fluctuations to mean flow.

As observed in figure which represents the amount of energy transferred for unit time and unit m 2.21 mean kinetic energy is found to oscillate in time, and in correspondence of this strong oscillation the production term is found to increase

2.9 Edge particle transport and coherent structures

2.9.1 Coherent structures characterization and transport

Coherent structures with eddy features or density blobs emerging from electrostatic turbulence background have been detected in the edge region of several fusion experiments including tokamaks, stellarators and reversed field pinches (RFP).

It is believed that these structures play a major role in driving the transport in the edge region.

These structures have been detected in the edge region of the RFX-mod, where in order to gain insight into their presence and features fluctuations of different plasma parameters are monitored at high time resolution mainly by insertable probes and Gas Puffing Imaging diagnostics.

The Gas Puff Imaging (GPI) diagnostic [Cavazzana04] measures the emission fluctuations of the neutral Helium puffed in the plasma edge, and it allows to characterize the edge turbulence and in particular the coherent structures that are considered the main cause of anomalous transport in the edge of the magnetic configurations. Two tomographic algorithms to obtain the 2D pattern of the edge structures from the line-integrated signals have been developed [Serianni07], and one typical result is shown in Fig 2.22. It is visible a coherent structure in the field of view of the GPI. The tomographic inversion has been obtained by expressing the emissivity of the plasma edge in a two dimensional Fourier series. Hence it is possible to characterize the turbulence properties by studying the time behaviour of the Fourier modes.

In particular, from the time derivative of the toroidal phase of the reconstructed modes, it is possible to obtain the toroidal velocity of propagation of the edge turbulence with high time resolution. In fig.2.23 this result for one RFX-mod discharge is reported. The toroidal phase of the dominant reconstructed mode has a linear dependence as a function of the time; the toroidal velocity can be evaluated with a time resolution up to 1 μs, which is necessary in order to study the turbulent phenomena. In this way it has been developed a simple tool to analyze the 2D images of the edge turbulence measured by the GPI. In fact a lot of physical information from the energy and the phase of the reconstructed modes can be obtained without the need of complicate image analysis technique.

The insertable probe system, dubbed 'U-probe' allows measuring both magnetic and electrostatic fluctuations simultaneously and on the same location with a high time resolution. It consists of two sets of electric and magnetic probes toroidally spaced by 88 mm. Each set is equipped with a 2-D array of Langmuir probes and a radial array of 3-axial magnetic coils. So that fluctuations of velocity patterns and relative vorticity, of density and pressure gradients and of current density directly measured trough magnetic field circuitation are available simultaneously.

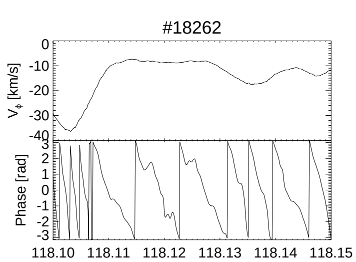

Fig 2.23: time behaviour of the toroidal velocity of the edge turbulence (top) obtained from the time derivative of the toroidal phase of the tomographic mode (bottom)

Statistical methods have been applied in order to detect structure-related bursts in the turbulence. It has been found that in the cross-field plane bursts, often referred in literature as density 'blobs', exhibit both electrostatic feature as vortices, and magnetic features as current density bursts. An example is shown in fig. 2.24.

These structures are characterized by pressure peaks associated to current density filaments mainly oriented along the magnetic field, confirming what theoretically postulated by [Bergmans01, Myra07] and travelling according to the local E×B flow. It is worth noting that analogous filamentary structures have been observed also in the boundary region of tokamak experiments [Kirk06].

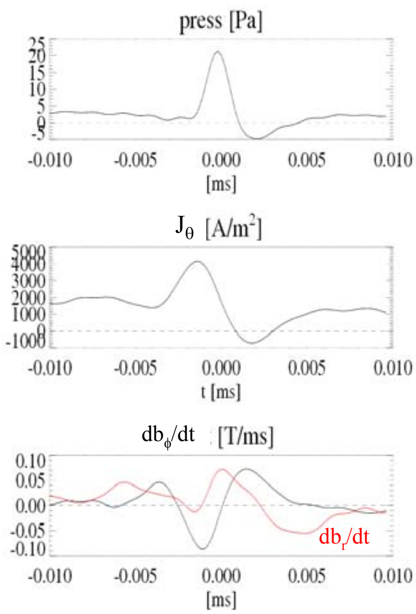

Fig.2.24 Conditional average on intermitted bursts of pressure fluctuations (top panel) and corresponding peaks detected on poloidal current density (middle panel) and relative features of the radial and toroidal components of dB/dt (bottom panel) measured by the 'U-probe' inseratble system

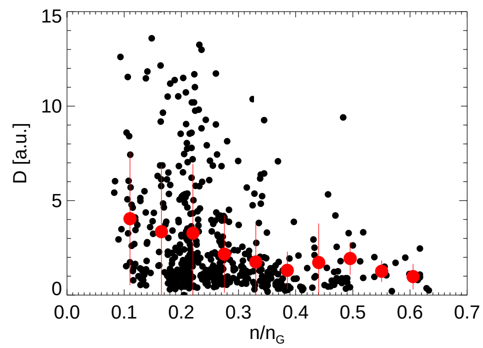

Fig.2.25: Diffusivity of the plasma trapped in the coherent structures as a function of the normalized plasma density

In RFX-mod the contribution of coherent structures emerging from turbulence background has been found to account for the 50% of the total edge diffusivity [Spolaore04].

In particular the behaviour of the diffusivity of the plasma trapped in the coherent structures has been studied with GPI as a function of the normalized plasma density n/nG. The diffusivity D_p is evaluated as $D_p \propto f_p^{\,2}\, u\, \Delta s$, where f_p is the packing fraction [Spolaore04], i.e. the area of the edge plasma occupied by coherent structures, *u* is the relative speed of the structures and Δ_s is their toroidal width, evaluated with the GPI without the need of the frozen-turbulence hypothesis. All these quantities are computed for a selected database of RFX-mod discharges. In Fig.2.25 the diffusivity as a function of the normalized plasma density is shown. The black dots are the experimental measurements and the red ones are the ensemble average. It is clear that D_p depends on n/n_G, and that it decrease with the normalized density. In particular there is a decrease of D_p between $0.1< n/n_G<0.35$ and then a saturation at higher density.

2.9.2 *Edge fluctuations statistical properties*

The large amount of emission fluctuation data collected by the Gas Puff Imaging (GPI) diagnostic [Cavazzana04] in RFX-mod allows the statistical approach to the analysis of the edge turbulence. It has been shown that the edge signals are intermittent, i.e. they are characterised by large events at short time scales occurring sporadically but more often then predicted from a Gaussian distribution.

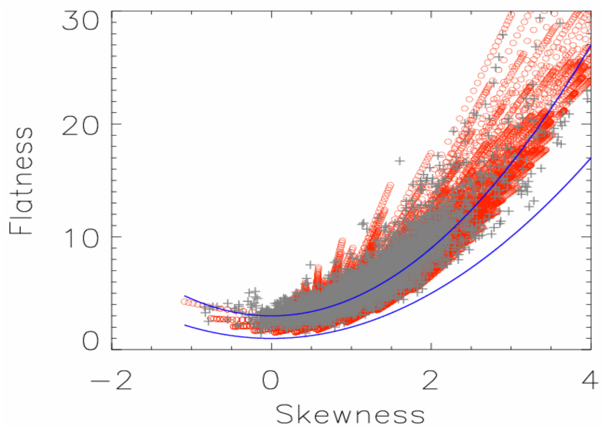

Fig.2.26 Flatness as a function of the Skewness for the experimental GPI data of RFX-mod (grey crosses) and the same quantities for the two Gamma functions. The two blue lines delimited the region of the plane that represent the Beta function.

We have shown that the PDFs of the edge fluctuation data display large tails, that are approximately exponential. All these PDFs from RFX-mod can be fitted with a linear combination of two Gamma functions [Sattin06]: one is related to the background uncorrelated turbulence, and the other to the coherent bursts.

This statistical analysis has been made for thousands discharges in different plasma conditions, and in Fig.2.26 the fourth order moment (Flatness) of the PDF as a function of the third order one (Skewness) is reported for the experimental data (red circles), compared with the same quantities for the theoretical two Gamma functions (black points). The "theoretical" data well reproduce the experimental ones, confirming that the two Gamma can reproduce quite well all the GPI data from RFX-mod edge. In the same graph the two blue lines delimit the region of the plane Skewness-Flatness that represents the Beta function. In fact in [Labit07] the fluctuations of the ion saturation current measured in TORPEX device with Langmuir probes are shown to be fitted with a Beta function. In RFX-mod, thanks to the good statistics we can demonstrate that the two Gamma better represent the experimental data of emission fluctuations measured by the GPI than the single Beta.

The same statistical analysis has been carried out also for TPE-RX reversed field pinch experiment and the two Tokamaks NSTX and Alcator C-mod. All these four experiments are equipped with a GPI diagnostic to study the edge fluctuations. Making the previous graph for the data of all the four experiments, we obtain the curves as reported in Fig. 2.27. All the points stay in the same region of the one occupied by the RFX-mod data. This result shows a common PDF for the edge fluctuations in different plasma devices, plasma conditions and magnetic configurations,

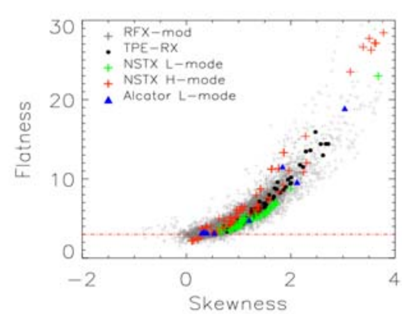

Fig2.27 Flatness and Skewness of the GPI data for the four experiments analysed. Different symbol are explained in the legend

suggesting a universal behaviour of the edge fluctuations: in all the devices studied the PDFs can be fitted with two Gamma functions, one related to the coherent bursts and the other to the Gaussian background.

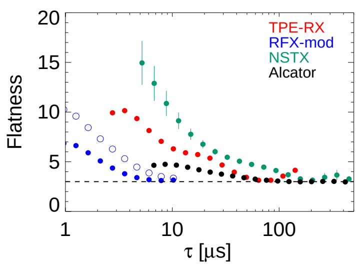

Fig 2.28 Flatness as a function of the time scale of the edge emissivity fluctuations for the four experiments analysed

A complementary approach is the one based on the wavelet transform, that allows studying the statistical properties of the fluctuations scale by scale [Farge92].

In the Fig 2.28 we show that the Flatness of the fluctuations varies with the scale of the fluctuations themselves: the statistical properties depend on the scale of the fluctuations. This behaviour is recovered for all the four devices analysed, the only difference is the absolute value of the Flatness and the time-scale range (in the figure the blue points regards RFX-mod: full is virtual shell discharges, empty is without). Again, this similar behaviour of the edge turbulence is a signature of common properties and origin of the phenomena.

2.10 Tokamak experiments

Well controlled and reproducible tokamak discharges have been obtained in RFX-mod, at a toroidal field of 0.45 T (corresponding to the maximum current of 12 kA to which the TFAT converters have been commissioned) and a plasma current of 80 kA, with $q_a \approx 3 \div 4$. A discharge duration of more than 500 ms has been achieved, limited only by constraints on energy dissipation in the toroidal field coils. An example of traces from a good tokamak discharge obtained in RFX-mod is shown in fig. 2.29. It can be seen that a constant 80 kA plasma current, giving $q_a = 3$, can be sustained with a loop voltage of about 1 V, at a density of 2×10^{18} m^{-3}, corresponding to a density normalized to the Greenwald density of 0.2. Higher densities can also be achieved, although the achievement of a long and stationary flat-top is not guaranteed, due to the mode locking phenomenon described below. Electron temperatures of 300-400 eV have been measured both with Thomson scattering and double filter diagnostics. Energy confinement times of several tens of milliseconds, in line with predictions from the Neo-Alcator scaling law for ohmic tokamaks have been calculated, although at densities much lower than densities obtained in RFP plasmas, due to the much lower plasma current, so

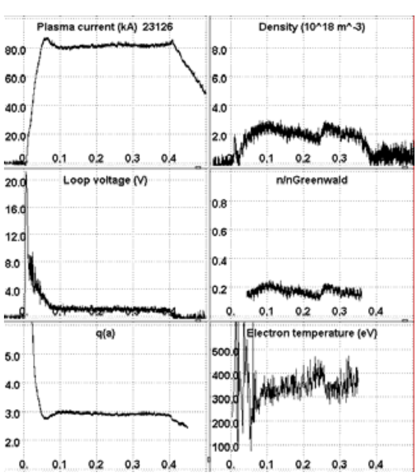

Fig. 2.29 Main traces of a good tokamak discharge.

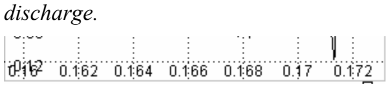

Fig. 2.30 Magnetic field measurements obtained by a poloidal array of probes belonging to the ISIS system (top) and time trace of a single signal, showing the slowing down and locking of the m=2/n=1 mode.

that the nτ product is almost comparable for the two configurations.

A tendency of the m=2/n=1 mode, normally present in the discharge and rotating at a frequency of several kHz, to lock to the wall. This phenomenology appears more frequently at higher densities. The magnetic field measurements obtained with a poloidal array of probes located behind the first wall graphite tiles, belonging to the ISIS system, is shown in the top frame of fig. 2.30, displaying the slowing down of the mode and its subsequent locking to the wall, which occurs at t = 149 ms. The time trace of a single signal, for a different discharge, is depicted in the bottom frame of the same figure. Also in this case it is possible to observe the locking, in this case at t = 169 ms. The events are associated to a "minor disruption", with a sudden drop of the plasma current and a negative spike in the loop voltage.

2.11 ULq Experiments

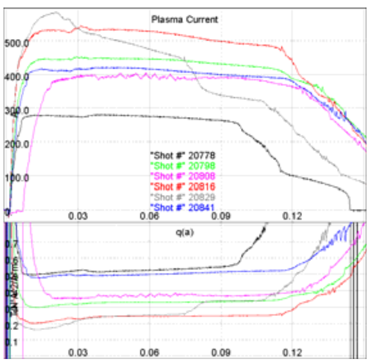

Fig. 2.31 Plasma currents and related safety factor q at the edge during ULq experiments

RFX has a high operational flexibility and, thank to this feature, in the end of 2006 and 2007 Ultra Low q (ULq) configurations have been set up in an easy way, by exploring different experimental conditions. ULq is a plasma configuration with a safety factor q at the edge ranging between 0 and 1 which is well known for its peculiar "stepwise" behavior of the plasma current in correspondence to the q rational values.

Plasma current I_p in the range between 250 to 600 kA and q in between 0.25 to 0.7 have been produced with pulse length over 100 ms. Fig. 2.31 shows typical waveforms of I_p and q at the edge.

The comparison of the ULq with the RFP configuration produced in RFX is significant, being both the configurations with low magnetic field at the edge, with ideal MHD modes at resonant surfaces but with different shear along the minor radius. Initial experiments show that:

- steady state ULq plasma currents obtained with a toroidal loop voltage between 30 to 40 V for times longer than the shell time constant, like in RFPs;
- different m,n mode rotations, measured with magnetic probes internal to the vessel (see Fig. 2.32) while MHD modes in RFPs plasmas are always locked to the wall;
- the possibility to operate at high densities, near the Greenwald limit, with sustained plasma current and peaked

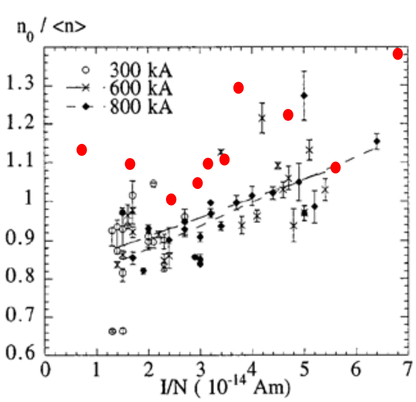

Fig. 2.33 Peaking factor vs. I/N for ULq (red dots) and RFP (black dots)

profiles, as summarized in Fig. 2.33;

- phases with reduced MHD activity followed by phases with very high resonant MHD modes, whose dynamics are in agreements with the results of theoretical analyses.

References

[Zanca07] P. Zanca, L.Marrelli, G.Manduchi, G.Marchiori, Nuclear Fusion, **47**, 1425 (2007)

[Marrelli07] L. Marrelli, P. Zanca, M. Valisa, G. Marchiori, A. Alfier, F. Bonomo, M. Gobbin, P. Piovesan, D. Terranova, and the RFX-mod team, Plasma Phys. Control. Fusion, **49**, B359 (2007)

[Marrelli 07] L.Marrelli et al ..., Plasma Phys. Contr. Fus. **xx**, pag (2007)

[Valisa 07] M. Valisa presentation at the 49th Conf. of the Plas. Phys Div. of APS, Orlando FL, 2007

[Terranova07] D. Terranova, et al., Phys. Rev. Lett. **99** 095001 (2007)

[Innocente07] P. Innocente, et al., Nucl. Fusion **47** 1092 (2007)

[Rechester78] A. B. Rechester and M.N. Rosembluth, et al., Phys. Rev. Lett. **40** 38 (1978)

[Valisa2006] M.Valisa, et al., *Edge transport properties of RFX-mod approaching the density limit,* in Proc. 21st IAEA Fusion Energy Conf., paper EX/P3-17, Chengdu, China, 2006, IAEA, Vienna. available online at http://www-naweb.iaea.org/napc/physics/FEC/FEC2006/papers/ex_p3-17.pdf

[Spizzo06] G.Spizzo, S.Cappello, A.Cravotta, D.F.Escande, et al., Phys. Rev. Lett. **96**, 025001 (2006).

[Scarin07] P.Scarin, et al., Bull. Am. Phys. Soc. **52**, 110 (2007).

[Annibaldi07] S. Annibaldi, F. Bonomo, R. Pasqualotto, G. Spizzo, A. Alfier, P. Buratti "Strong transport reduction in the helical core of the reversed-field pinch" Physics of Plasmas 14, 112515 (2007)

[Cavazzana04] R. Cavazzana et al., Rev. Sci. Instrum. **75** 4152 (2004)

[Serianni07] G. Serianni et al., Plasma Phys. Control. Fusion **49** 2075 (2007)

[Bergmans01] J. Bergmans, T.J. Schep Phys. Rev. Lett. **87**, 195002 (2001)

[Myra07] J. R. Myra, Plasma Phys. Control. Fusion 14, 102314 (2007)

[Kirk06] A. Kirk et al. Plasma Phys. Control. Fusion 48, B433 (2006)

[Spolaore04] M. Spolaore et al., Phys. Rev. Lett. 93 215003 (2004)

[Sattin06] F.Sattin et al., Plasma Phys. Control. Fusion, **48**, 1033, (2006)

[Labit07] B.Labit et al. Phys.Rev.Lett., **98**, 255002, (2007)

[Farge92] M.Farge, Annu.Rev.Fluid Mech., **24**, 395, (1992)

3. THEORY AND MODELING

The 2007 theory and modelling activity brought the following salient results. MHD simulations of the Ultra-Low q regime of RFX-mod recovered the experimentally found staircase-like evolution of the edge safety factor, bringing further confidence in this type of simulation. The ongoing implementation of the numerical code PIXIE3D that is designed to address extended MHD modeling is a turning point in our MHD simulation activity. Tearing mode evolution in the presence of the RFX-mod passive structures and feedback is now better described by accounting for the evolution of the flow profiles due to the electromagnetic torques, and for the non-linear interaction between several modes. Kinetic calculations confirmed that the RFP configuration has a larger ITG stability threshold than the tokamak because it has a stronger Landau damping due to the shorter connection length. Diffusion-convection models have been used a lot to interpret anomalous transport measurements; their domain of validity was made more precise. Differences in guiding center drifts proved to improve confinement for fast ions with respect to thermal ones in RFPs, in contrast to the tokamak.

3.1 Basic MHD dynamics and 3D simulations

The collaboration with LANL (L. Chacon et al.) led to the acquisition of the new advanced numerical code PIXIE3D, which is designed to address extended MHD modeling including energy balance, generalized Ohm's law, and toroidal geometry. Its implementation at RFX is presently underway. The first step of this task consisted in a successful benchmark of PIXIE3D with our previous code SpeCyl.

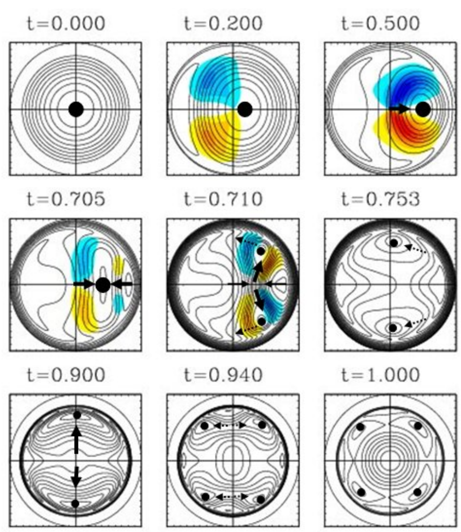

Fig.3.1 Evolution of the external kink in ULq (m=1, n=2): first row) typical kink displacement with formation of island at the resonant surface; second row) plasma core and original magnetic axis splits in two islands as result of strong convolution (m=2, n=4); third row) further splitting of the original plasma core in four little islands: tiny MHD activity with high m modes (m=4, n=8) following the development of kink

By using the SpeCyl code, a simulation study of the Ultra-Low q (ULq) configuration has been performed in 2007 [Bonfiglio07a, b, Cappello07a], as a support activity to the experimental ULq campaigns on RFX-mod. When driving the edge q-value, q(a), from RFP to tokamak-like conditions and vice-versa, a MHD phenomenology qualitatively similar to the experimental one is observed: a staircase-like evolution of q(a), with preferred edge q-values being about the major rational numbers (fig. 3.1). Each transition from a rational edge q-value to the next one is accomplished after a kink deformation of the plasma column, whereas the phases of constant q(a) are characterized by tiny MHD activity.

The efficient mechanism of QSH triggering by OPCD action, experimentally observed in RFX-mod, has also been addressed through SpeCyl simulations. So far, the systematic repetition of QSH states alternated by MHD crashes, which characterizes OPCD experiments, has been observed in numerical tests only when starting from already established QSH conditions. This needs to be further investigated. Simulations with the

DEBS code confirmed the measured level of magnetic fluctuations in RFX-mod with the Virtual Shell, and as a function of the wall resistivity for operation without control [Paccagnella07].

The equilibrium code FLOW [Guazzotto04, 05, 07], an ideal MHD code including the effects of anisotropy and arbitrary plasma rotation, was modified to allow modeling of RFP profiles in order to compute trapped particle fractions and bootstrap current profiles.

3.2 Active control of MHD modes

The ongoing experimental study of the Resistive Wall Mode (RWM) requires a reliable linear stability code. Collaboration with Dr. M. Chu in General Atomics (San Diego) led to an adaptation to the RFP of the equilibrium Chease code and of the Mars code. The latter is a linear simulation code written in the 3-D toroidal configuration for tokamaks, and includes the effects of resistive wall, finite beta, dissipation, plasma rotation, and feedback coils.

The effect of toroidicity and shell discontinuities on RWMs is being studied in collaboration with Y.Q. Liu (Chalmers University, Sweden) and F. Villone (Università di Cassino). The growth rate of these modes increases as a consequence of the shell gaps. Previous cylindrical estimates for the RWMs growth rates were confirmed by toroidal stability calculations using the MARS code with a homogeneous resistive wall. This collaborative computational effort enters the IMP2 (Nonlinear MHD) project within the Integrated Tokamak Modelling EFDA Task Force.

A new linear cylindrical model allowing the calculation of the coils and wall contributions to the measured total m=0 magnetic field was developed. The model was used to interpret results obtained in experiments where an asymmetric m=0 perturbation was applied to the plasma. It was found that, for the shallow F values at which these experiments have been done, the m=0 intrinsic plasma response is stable, and that it can mainly be interpreted as due to the nonlinear coupling of the dominant adjacent m=1 modes. However this is not true when a QSH oscillatory regime of the 1/-7 mode is present. In this case the m=1 n=-8 mode amplitude is also reduced and the computed nonlinear contribution is weaker than the m=0 measured field [Pizzimenti07].

Two models, based on Newcomb's equation solution, have been developed to describe the tearing mode evolution in the presence of the RFX-mod passive structures and feedback. The first one is a single mode stationary model, which was used to derive the clean-mode-control scheme [Zanca07a]. The second one complements the first one by accounting for the evolution of the flow profiles due to the electromagnetic torques, and considers the non-linear interaction between several m=0,1 modes [Zanca07b]. It is a generalization of a mode-locking model developed in collaboration with R. Fitzpatrick [Fitzpatrick02] that takes into account non-ideal boundary conditions.

3.3 Turbulence and transport modelling

The interest in drift-type instabilities driven by Ion Temperature Gradient (ITG) and/or trapped particle dynamics is currently rising in the RFP community, since the significant progress made in RFP operations leads to a strong reduction of the stochastic nature of the magnetic field. This is an important issue because these types of micro-turbulence might finally rule the energy confinement for the future RFPs. As a first step to understand the behaviour of ITG modes in RFP plasmas, last year their stability threshold in the limit of adiabatic electron and small Larmor radius was computed for the first time in a kinetic setting. This year these kinetic calculations were extended and found consistent with fluid calculations in appropriate limits [Guo07]. This fact confirmed that the RFP configuration has a larger ITG stability threshold than the tokamak because it has a stronger Landau damping due to the shorter connection length. The required temperature slope for

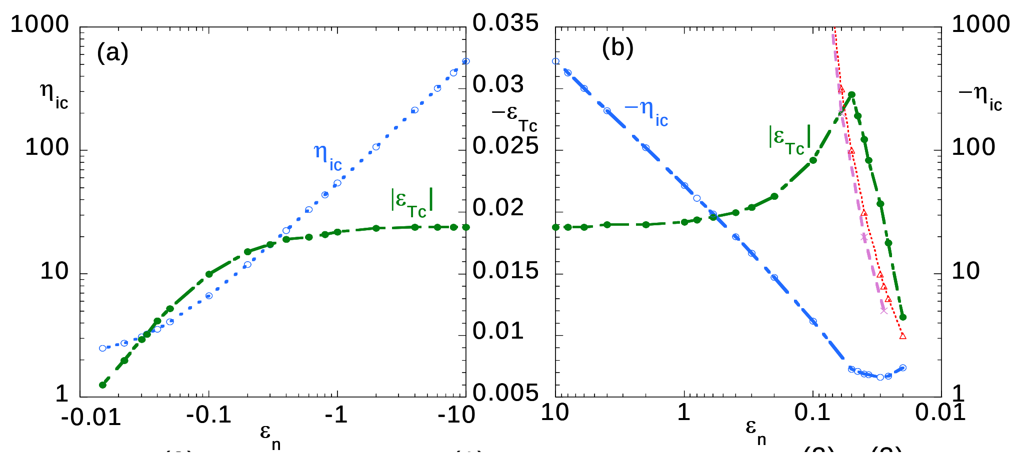

Fig. 3.2 In green: threshold ε_{Tc} for both (a) ε_n <0 and (b) ε_n >0 density profiles for typical RFX-mod parameters. The areas below the $|\varepsilon_{Tc}|$ curves are unstable to ITG mode, and stable above. The corresponding η_{ic} values are also plotted in blue (the regions above the η_{ic} curves are unstable). The red and pink curves correspond to fluid calculations for $|\varepsilon_{Tc}|$.

instability may be found only in the very edge of the plasma or near the border of the dominant magnetic island during quasi-single helicity states. In figure 3.2, $\varepsilon_n = L_n / R$ is the normalized density gradient length, $\varepsilon_T = L_T / R$, is the normalized temperature gradient length, and $\eta_i = L_n / L_T$ is their ratio. The "c" index corresponds to the critical or threshold value for ITG modes.

Fusion experimentalists have been using a lot of diffusion-convection models to interpret anomalous transport measurements. In the last few years there were growing claims that such models are incorrect, and that they should be substituted with fractional diffusion models incorporating nonlocal effects due to large flights in the radial transport, the so-called Lévy flights. The fact that these ideas were starting to impinge data analysis in the laboratory was an incentive to revisit this issue at RFX. Diffusion-convection models are special instances of the Fokker-Planck Equation (FPE). Our analysis allowed bettering evaluating the limits and the potentialities of FPE in describing anomalous transport [EscSatt07]. In particular, the kind of averaging performed over the data is of paramount importance. Depending on the kind of averaging, the same system may be found diffusive or dominated by its Lévy flights. The analysis brought another caveat to the experimentalists: a bump in a density profile may be the mere consequence of a localized particle source, and not of a diffusion-convection mechanism. A spin-off of this study was the reconsideration of particle transport in the RFP, and the derivation of a new FPE description of particle transport incorporating magnetic field perturbation profile and Coulomb scattering.

A kinetic approach to the derivation of the particle and energy fluxes in a plasma with a chaotic magnetic field was developed that takes into account the whole spectrum of particle velocities [Predebon07a]. With the simplifying hypothesis that the magnetic field has a diffusive nature, keeping as guidelines classical papers on the topic ([Rechester78] and [Harvey81]), the contribution of slow particle dynamics and collisional processes was shown to be relevant throughout the plasma, not only in the colder peripheral regions where collisional effects are expected to be dominant. Applied to the RFX-mod reversed field pinch, such a model turns out to modify the weight of the single terms in the fluxes, and to change particle flux by a factor about 2, even in the plasma core.

The two 1D transport codes RFXPORT and RITM already used at RFX were integrated in one single unit. In its original version, RFXPORT solves the MHD equations and the transport - continuity and heat balance – equations, and uses an ad hoc dynamo term in Ohm's law. RITM solves the transport equations for the main gas and impurities. In particular, taking into account the necessary atomic processes, it computes the densities of neutrals and impurities, the effective charge, and the radiation power. In the integrated code, RITM is used as a subroutine to compute the lacking terms in the transport equations of RFXPORT. To interpret the experimental results of RFX-mod, self-consistent transport models have been included: for example a stochastic transport model based on the classical papers [Rechester78] and [Harvey81], and on their recent extension indicated above [Predebon07].

In order to better understand turbulence in fusion plasmas, the energy reservoirs and the transfer coefficients in between have been analyzed. In the single fluid framework the possible energy reservoirs are: electromagnetic energy (E_{em}), kinetic energy (E_K), thermal energy (E_T), and a relative kinetic energy (E_J). The latter, which is proportional to the current density squared, is due to the relative motion of ions and electrons. From the single fluid equations (up to the second order moments) the energy fluxes between the reservoirs have been calculated. By dividing all the quantities in average and

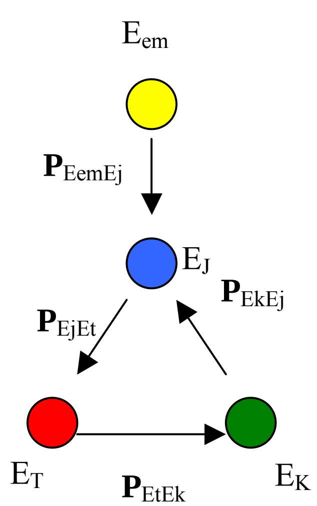

Fig. 3.3: Scheme of energy reservoirs and of the energy fluxes in between.

fluctuating parts, it was then possible to write expressions for the energy flows between the reservoirs due to plasma turbulence (see the schematic picture in Fig. 3.3). A preliminary attempt to evaluate some of these terms using experimental measurements of fluctuations was made: in particular, the energy transfer from electrostatic fluctuation to mean flow scales. Using this scheme it will be possible in the future to check the usually assumed proportionality between the collisional term and the current density, and between the viscosity tensor and the rate of strain tensor, and to test or to correct the usual closure approximations of MHD.

The interpretation of edge turbulence measurements in fusion devices is a difficult topic. Recently the Torpex group in Lausanne suggested analyzing fluctuating signals in terms of the flatness-versus-skewness (F-S) curve. Several physical mechanisms are claimed to produce these signals, each of them leading to a different analytical fit of the F-S curve. The best fit of RFX-mod signals obtained through the GPI diagnostic cannot be done by the same theory as that for the Langmuir probe data of the Torpex group. This raises the issue of the origin of this difference: an instrumental or a physical one?

The departure from equilibrium conditions of the GPI signal may be expected in the early stages of helium gas puffing. In order to deal with this case, a simulation of light emission using a time-dependent collisional-radiative model was carried out in collaboration with J. Abdallah (Los Alamos).

3.4 Particle transport

An RFP version of the ORBIT code has been used for several years to compute particle orbits and magnetic field lines. This year the code benefited from several improvements in the representation of the magnetic perturbation. In ORBIT, the perturbed radial field is defined by the scalar function α through the relation $\mathbf{b}=\nabla\times\alpha\mathbf{B}_0$ where $\mathbf{B}_0$ is the equilibrium magnetic field. In the past, the function α was obtained from the radial field perturbation computed in cylindrical geometry. It is now computed in toroidal geometry [Gobbin07a] by using the radial component of the magnetic field perturbations derived from Newcomb equation [Zanca04]. This improvement was motivated by the significant difference of the radial profiles of perturbation in cylindrical and toroidal geometries, due to toroidal coupling. This is particularly relevant for the $m=0$ modes. Another important improvement consisted in the removal of the systematic error due to the aliasing of sidebands produced by the actively controlled saddle coils [Marrelli07]. Newcomb equation in toroidal geometry is now solved by using as boundary conditions the measurements corrected for the effect of the aliasing of sidebands as described in [Zanca07a]. Finally, we also corrected the approximate representation of the $\alpha(r)$ function for the $m=1$ mode near the origin. It is now linear in r as predicted by the theory, which allows a more precise representation of magnetic field lines topology even in close proximity of the geometric origin.

Particle transport was computed with ORBIT for a multiple helicity (MH) state obtained as an output of SpeCyl and for magnetic field fluctuations typical of RFX-mod (b / Bθ (a) = 4% $\widetilde{b} / B_\theta(a) = 4\%$). The magnetic structure underlying the MH regime turns out not to be fully chaotic. Trapped particles diffuse slowly radially with their banana motion, while passing particles move radially by following magnetic field lines. Transport is found to be subdiffusive, but can be described by an appropriately modified Rechester-Rosenbluth formula [Spizzo07].

A Field Line Tracing code (FLiT) was developed to improve the geometrical description of the magnetic field structure in RFX-mod plasmas. In contrast to the ORBIT code, FLiT does not assume $\mathbf{b}=\nabla\times\alpha\mathbf{B}_0$, an assumption less correct in the RFP than in the tokamak. The code uses the internal tearing eigenfunctions in toroidal geometry for a force-free plasma with circular cross section computed by solving a system of Newcomb-like equations for the modes coupled by toroidicity [Zanca04]. The FLiT code works in toroidal geometry, and solves the field line equations in the same flux co-ordinates as the tearing eigenfunctions. The validity of the model used to evaluate the internal tearing eigenfunctions and of the field line integration was confirmed by two different geometrical comparisons.

Suprathermal ions in fusion plasmas have different confinement properties in tokamak and RFP configurations, because of differences in guiding center drifts. The kinetic safety factor profile $\widetilde{q}$ felt by fast ion guiding centers controls the resonant interaction with magnetic perturbations. It was calculated analytically in a setting adequate to both tokamak and RFP configurations. In the former case the main effect of perturbations is a radial shift of the orbit proportional to the magnetic field, while in the latter the toroidal drift generated by the poloidal field gradient and curvature is dominant. This is why $\widetilde{q} - q$ is larger and modifies more significantly the confinement of fast particles in RFPs than in tokamaks. Applications to experimental cases show better confinement properties for fast ions than thermal ones in RFPs, especially in helical regimes (Quasi Single Helicity and Single Helicity), in contrast to the tokamak [Gobbin07b].

References

[Bonfiglio07a] D. Bonfiglio, S. Cappello, R. Piovan, G. Spizzo, D. Terranova, oral contribution for the 12th IEA-RFP Workshop, Kyoto (2007).

[Bonfiglio07b] D. Bonfiglio, S. Cappello, R. Piovan, poster at the 12th European Fusion Theory Conference, Madrid (2007).

[Cappello07a] S. Cappello, D. Bonfiglio, R. Piovan, poster at the 49th APS DPP meeting, Orlando (2007).

[Cappello07b] S. Cappello, D. Bonfiglio, G. Spizzo, D. Terranova, R. B. White, poster at the 12th European Fusion Theory Conference, Madrid (2007).

[EscSatt07] D.F. Escande, F. Sattin, Phys. Rev. Lett. **99**, 185005 (2007)

[Fitzpatrick02] R. Fitzpatrick, P. Zanca, Phys. Plasmas **9,** 2707 (2002)

[Gobbin07a] M. Gobbin, et al., 34th EPS Conference (Warsaw, 2007)

[Gobbin07b] M. Gobbin, et al., submitted for publication

[Guazzotto04] L. Guazzotto, R. Betti, J. Manickam and S. Kaye, Phys. Plasmas **11**, 604 (2004)

[Guazzotto05] L. Guazzotto and R. Betti, Phys. Plasmas **12**, 056107 (2005)

[Guazzotto07] L. Guazzotto, J. P. Freidberg and J. Kesner, Phys. Plasmas **14**, 062501 (2007)

[Guo07] S. Guo, submitted for publication

[Harvey81] R. W. Harvey et al., Phys. Rev. Lett. 47, 102 (1981)

[Marrelli07] L. Marrelli, P. Zanca, et al., Plasma Phys. Control. Fusion, **49**, B359 (2007)

[Paccagnella07], R. Paccagnella, D. Terranova, P. Zanca, Nucl. Fusion **47** (2007) 990.

[Pizzimenti07] A. Pizzimenti, R. Paccagnella, submitted for publication

[Predebon07] I. Predebon and R. Paccagnella, Phys. Plasmas 14, 082310 (2007)

[Rechester78] A.B. Rechester and M.N. Rosenbluth, Phys. Rev. Lett. 40, 38 (1978)

[Spizzo07] G.Spizzo, R.B.White, and S.Cappello, Phys. Plasmas **14**, 102310 (2007)

[Zanca07a] P. Zanca, L. Marrelli, G. Manduchi and G. Marchiori, Nucl. Fusion 47, 1425 (2007)

[Zanca07b] P. Zanca, internal note NT FC/77

[Zanca04] P. Zanca, D. Terranova, Plasma Phys. Control. Fusion 46, 1115 (2004)

4. COLLABORATIONS WITH OTHER EXPERIMENTS (RFP AND TOKAMAK)

4.1 Collaborations on MHD

4.1.1 PPCD and MHD studies in MST

The high flexibility of the MST SXR tomography diagnostic, together with the possibility of easily removing the probes, allows using it in [illegible] configuration settings. The most common and exploited [illegible] called *normal* configuration, where all the Be foils mounted on the four probes have the same thickness [Franz2006]. [illegible] 2006 the *two-color* configuration has been developed and applied in PPCD measurements. In this case two pairs of Be foil thicknesses have been installed in the photocameras: a 303μm thickness in the probes SXR1 and SXR2 and a thicker one (761μm) in SXR3 and SXR4. The probes are coupled two by two, and cameras with the same Be foil thickness [illegible] displaced at 90deg each one from the other. Thus each pair of probes can be used to reconstruct the SXR emissivity through tomographic inversion in the two different energy ranges. By calculating the ratio of the two reconstructions, a two-dimensional map of T_e can be obtained (two-foil technique), with the time accuracy typical of the SXR measurements (up to tens of kHz). An example is illustrated in Fig.4.1: for each pair of probes (SXR1-2 and SXR3-4) the brightness profiles and contour plots of the emissivity distribution for a 550kA PPCD plasma are

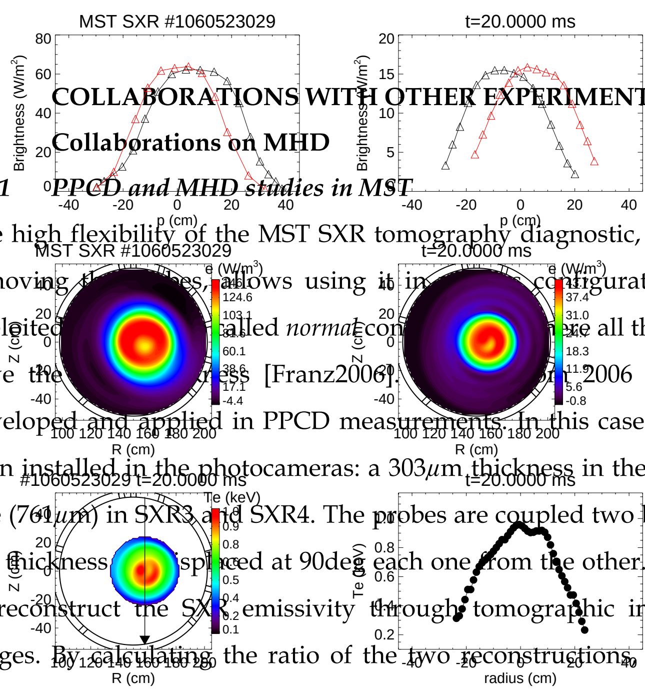

Fig.4.1: Example of SXR and Te estimation. Top: brightness radial profiles of SXR1 (black), SXR2 (red) and SXR3 (black), SXR4 (red). Middle: contour plots of the SXR emissivity distribution. Bottom: Te contour and radial profile along the vertical black arrow.

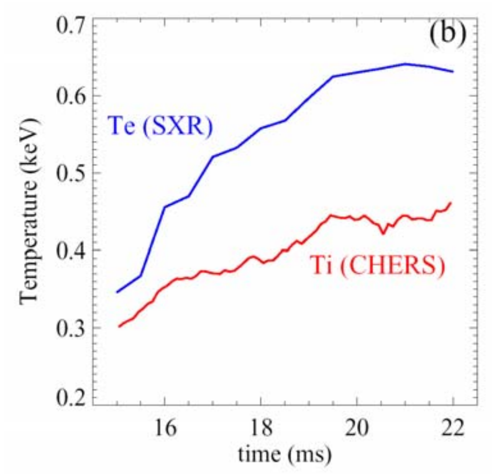

Fig.4.2: Temporal evolution of T_e and T_i in a pellet-injected high current PPCD plasma.

displayed. No evidence of a more localized emissive region is present (MH state), and the emissivity is symmetric in both energy ranges. The *Te* contour and radial profile along the black arrow are illustrated on the bottom of the figure. Both SXR and *Te* profiles indicate that plasma is shifted towards the outboard side of the vessel more than in standard discharges and that the application of PPCD can distort the plasma shape and make it poloidally asymmetric [Franz2007].

The SXR tomography has been also used in pellet-injected PPCD plasmas. The injection of pellets during PPCD allows reducing magnetic fluctuations and increasing the density up to 4 times the typical value. In Fig.4.2 an example of *Te* and *Ti* measurements is illustrated [Chap 2006]: the temporal evolution of the on-axis electron temperature (measured with the two-foil technique from the SXR measurements) increases during the PPCD application, between 14 and 24ms; also the ion temperature value (measured by CHERS) increases during the improvement period, but the effect is smaller.

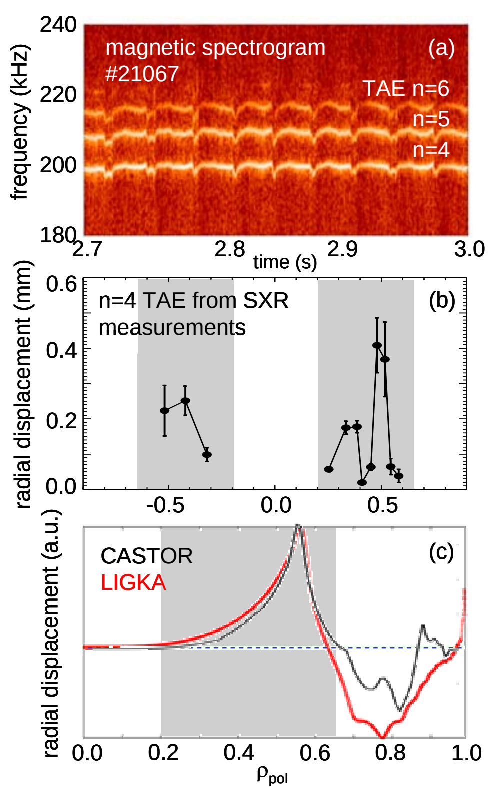

Fig.4.3: (a) Magnetic spectrogram, (b) total radial displacement of the n=4 TAE (b) from SXR and (c) predicted by CASTOR and LIGKA.

In the period of particle confinement after pellet ablation, at *Ip* larger than 500kA, density profiles can assume various shapes: the typical high current PPCD *ne* flat profile can be replaced by a peaked or a very hollow one. As a consequence, the SXR plasma emissivity distribution is different: a pellet plasma SXR emissivity distribution is peaked and the emitting plasma volume is focused on the axis of the plasma column, smaller than the case of a non-pellet discharge.

4.1.2 TAE and fast ion losses in Asdex UG

The internal structure of MHD instabilities driven by fast ions, such as Toroidal Alfvén Eigenmodes (TAEs), has been studied in collaboration with the ASDEX-Upgrade team by means of a new multichord soft x-ray diagnostic with high spatiotemporal resolution (32 lines of sight, 2MHz sampling rate, and 0.5MHz bandwidth) [Piovesan07]. A detailed knowledge of the TAE radial structure is important, since large amplitude TAEs can induce fast ion losses in present and future devices, including ITER. It is thus important to benchmark the available codes with accurate internal measurements, to make reliable predictions.

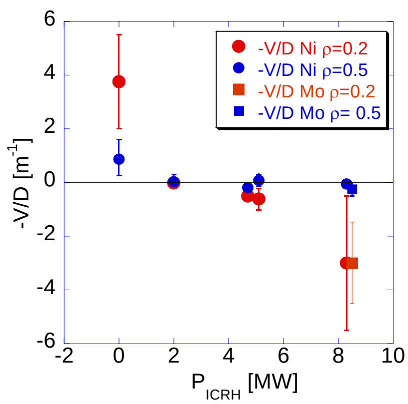

Fig.4.4 Ni peaking factors at ρ=0.2 and ρ=0.5 versus ICRF power for 6 JET discharges. Mo peaking factors are for a single JET discharge.

The high resolution of the new AUG soft x-ray diagnostic allowed us to reconstruct TAE eigenfunctions over a wide range of plasmas. Fig. 4.3 shows the result of these measurements for a discharge in which TAEs are destabilized through Ion Cyclotron Resonance Heating. The magnetic spectrogram in Fig. 4.3-(a) shows the presence of three dominant TAEs with toroidal mode number n=4,5,6. The measured total displacement profile of the n=4 TAE is shown in Fig. 4.3 -(b). This is computed as $\xi_r(\rho_{pol}) = \tilde{A}_{SXR} / \nabla_r A_{SXR}$, where $\tilde{A}_{SXR}(\rho_{pol})$ is the soft x-ray fluctuation brightness profile at the n=4 mode frequency. The n=4,5,6 TAEs are localized at mid radius and their amplitude fall in the range 0.1-0.4mm, which corresponds to a magnetic perturbation $\tilde{b}_r / B_0 = \xi_r / 2qR_0 = 0.1 - 5 \times 10^{-4}$. The experimental eigenfunctions have been compared with the predictions of two linear stability codes, the resistive MHD code CASTOR and the non-perturbative gyrokinetic code LIGKA, and reported in Fig. 4.3-(c). These simulations are based on accurate equilibrium reconstructions made with the CLISTE code, constrained by Motional Stark Effect measurements of the core magnetic field, and reflectometry and Lithium beam measurements of the density profile. The CASTOR and LIGKA predictions compare very well and a reasonably good agreement is found with the experimental profiles. In particular, theory reproduces very well the radial position and width of the TAE eigenfunctions. To account for line-integral effects in the eigenfunction reconstruction, simulations of the brightness signals have been made with the MHD-Interpretation Code, which simulates the soft x-ray measurements in the real AUG geometry with the theoretical eigenfunctions as an input [Piovesan07].

The effect of TAEs on the fast ion population is being investigated. To this aim a new powerful fast ion loss diagnostic (FILD) with high time, energy, and pitch-angle resolution has been recently developed in AUG. The FILD and the soft x-ray diagnostics have given interesting results on the correlation among high-frequency modes and fast ion transport, both for TAEs and for a mode recently observed in AUG, which very likely belongs to the branch of the Energetic Particle Modes [García-Muñoz2007]. ORBIT simulations are being developed to interpret these new measurements.

The experimental TAE eigenfunctions are used as inputs to the ORBIT code and the fast ion transport caused by them will be investigated in detail. A precise understanding of these effects may have impact on the prediction of fast ion transport in future burning experiments.

4.2 Collaborations on transport

4.2.1 Effect of radio-frequency heating on impurity transport at JET

Previous experiments on JET have shown that injection of radio-frequency (RF) power may generate an outward pinch for impurities, with corresponding flattening of the impurity density profiles [Puiatti 06]. Ni (A=28) and Mo (A=42) laser blow off (LBO) experiments have been performed in JET discharges featuring the injection of RF power at ITER relevant collisionality (Zeff<0.2), aiming at studying the effect of different power levels when ion cyclotron resonance frequency (ICRF) is applied to electrons. In the central plasma, hollow impurity profiles are found in discharges with strong centrally deposited ICRF applied to electrons (~8-9 MW), corresponding to an outward directed pinch velocity (see Fig 4.4). About 2 MW of RF injection results in flat Ni profiles; peaked profiles corresponding to an inward pinch are found when no RF is applied. A peaking factor very similar to that found for Ni has been evaluated for Mo at the higher values of ICRF power. Due to the high mass of Mo, this result is important in view of using W as plasma facing material. Small peaking factors are found in the more external region ρ=0.5, due to the higher values of the diffusion coefficient.

4.3 Collaborations on edge Physics

4.3.1 Edge Te and ne profiles during Type-I ELM mitigation experiments on JET

ELM mitigation experiments have been carried out at JET, with Type-I ELMs in H-mode plasmas mitigated through edge ergodization, produced by the ex-vessel error field correction coil (EFCC) system. The High Resolution Thomson Scattering (HRTS) diagnostic, which has recently become operational at JET, has been used to study the behavior of electron temperature, density and pressure profiles during the mitigation phase. We have modelled the edge transport barrier with a modified hyperbolic tangent function whose parameters are used to quantify edge barrier properties. In the case of an n=1 external field, the barrier position and height are found to be correlated to the choice of the toroidal direction of the perturbation. ELM mitigation correlates with a reduction of the edge pressure gradient due to a reduced height and an increased width of the edge pressure transport barrier, consistent with the linear ELM stability theory. Agreement between the barrier position measured by HRTS and obtained from plasma equilibrium reconstruction is also found: a main toroidally symmetric and a secondary toroidally asymmetric deformation of the plasma column are induced by the external perturbation. The detrimental effect of an ELM event on edge confinement is strongly reduced during ergodization. ELM mitigation is also obtained when the plasma column is far from the inner wall and in case of compound ELMs.

4.3.2. Gas Puffing Imaging in Alcator C-MOD

During 2007 a collaboration with Alcator C-MOD has been established with the aim of applying advanced analysis techniques on the data collected by the Gas Puffing Imaging (GPI) diagnostic. In particular a model to describe the Probability Distribution Function (PDF) initially developed for RFX-mod data [Sattin06] has been applied in order to distinguish the different dynamics of light emission signals in the region across the last closed flux surface (LCFS) location. The model tries to fit the data with two different Gamma functions

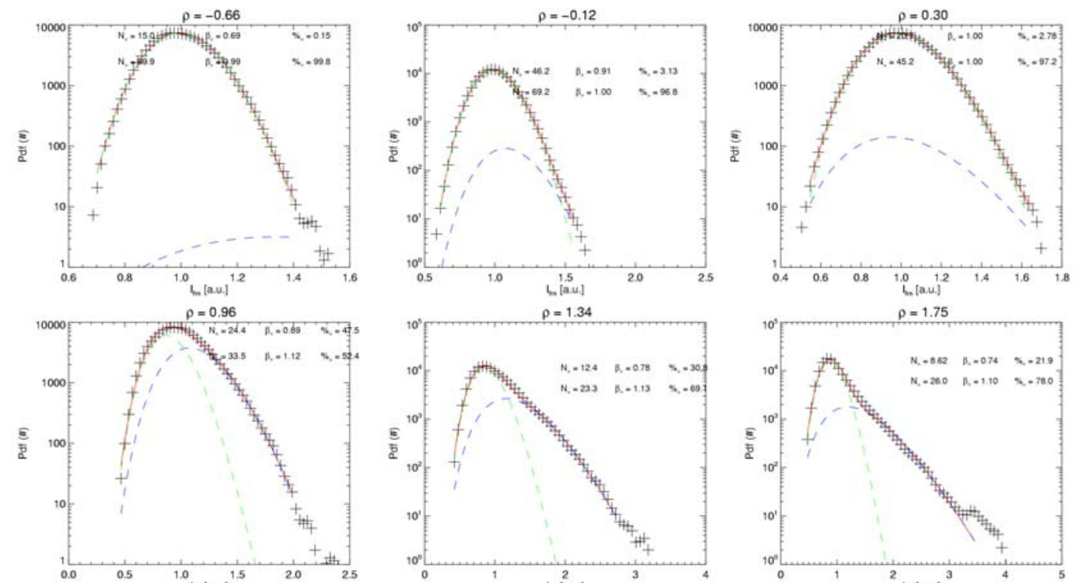

Fig.4.5 Probability distribution function of signals collected at different radial location. Together with the data, the results of the two-Gamma fit are also shown in red-line together with the two contributions (respectively in green and blue). Positive values of ρ refer to data in the SOL

$$P(x) = \frac{C_<(\beta_< N_<)^{N_<}}{\Gamma(N_<)} x^{N_< -1} \exp(-\beta_< N_< x) + \frac{C_>(\beta_> N_>)^{N_>}}{\Gamma(N_>)} x^{N_> -1} \exp(-\beta_> N_> x)$$

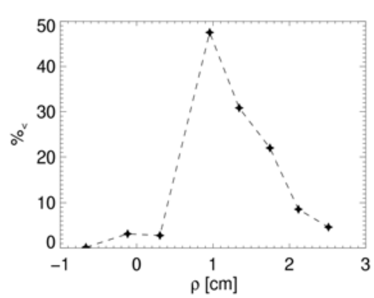

Fig.4.6 The fraction of PDF due to Gamma distribution with $N_<$ < 15

where in analogy of what is generally done in statistical mechanics $N_>$ and $N_<$ may be interpreted as effective degree of freedom of the two different population which constitute the probability density function, and to distinguish the contribution of $N_>$ from $N_<$. Indeed a hypothesis suggests that the two contributions are linked respectively to the uncorrelated and correlated part of the fluctuations. The results of the analysis at different radial positions with respect to the LCFS position is shown in fig. 4.5. It can be observed that the values of $N_>$ and $N_<$ are quite large in the confined plasma and up to approximately 1 cm into the SOL. Things change dramatically further inside the SOL where $N_<$

assumes values less than 15, contributing to a fraction up to 30 % of the total PDF. This can be observed in fig. 4.6, where the fraction of PDF due to $N_<$ < 15 is plotted versus ρ, the relative position with respect to the LCFS. This behavior may be compared to the radial profile of the packing fraction f_p, defined as the percentage of the signals occupied by the detected intermittent structures, and has been introduced as the ratio between the area occupied by blobs and the total edge area [Spolaore04]. The calculated packing fraction is shown in figure 4.7 as a function of ρ. Indeed the packing fraction clearly peaks approximately 1 cm inside the LCFS, in the same location where the relative fraction of minor-Gamma distributions is obtained, indicating that this region is clearly distinguished with respect to the other one as far as the statistical properties and dynamical behavior are concerned.

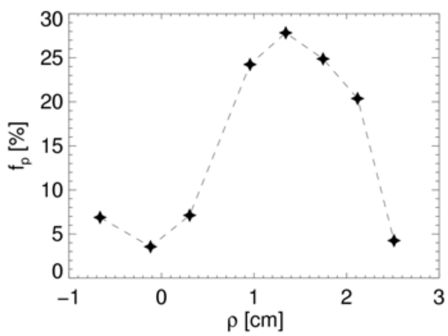

Fig.4.7: Packing fraction as a function of the distance from the separatrix

4.3.3 *Gas Puffing Imaging in NSTX*

In the National Spherical Torus Experiment (NSTX) a Gas Puffing Imaging (GPI) diagnostic [Maqueda03] is installed to study the edge turbulence.

A quantitative description of the difference in the number of edge structures between L-mode and H-mode has been carried out [Agostini07]. With a method based on the Wavelet Transform, the intermittent bursts are detected in the GPI time signals during the L and H-mode phase of plasma discharges, and their linear density N_s (number of structures per unit of time) is evaluated as shown in Fig.4.8. During the H-mode the linear density of bursts has a drastic decrease with respect to the L-mode phase for all the time scales (τ) of the fluctuations (fig. 4.8a). A complementary piece of information is shown in fig. 4.8b, where N_s is plotted as a function of the perpendicular velocity of the fluctuations (each point refers to one discharge). Every discharge exhibits a sudden decrease of the linear density of intermittent events in the H-mode with no significant change in the poloidal velocity. If these structures are considered to be responsible for most of the anomalous particle transport in the edge of the magnetic confinement devices, this measurement indicates that the drop in their density correlates with the presence of the H-mode.

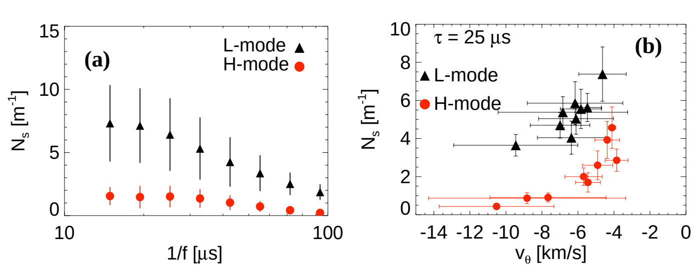

Fig4.8 linear density of edge structures (N_s) as a function of the time scale τ (left) and as a function of the perpendicular velocity of the edge fluctuations (right). Black dots are referred to L-mode and red ones to H-mode

4.4 JET Plasma Control Upgrade

The Plasma Control Upgrade (PCU) is one of the most important enhancements included in JET EP2: it was launched in 2005 in order to double the survivable ELM size in JET operation and to validate the vertical stabilization systems for ITER. The project was divided into four tasks. The third task, named "Vertical Stabilization Power Amplifier", was intended to study all the viable solutions for upgrading the Vertical Stability Power Supply.

In 2006, RFX developed the reference design for the new amplifier, which was used as technical basis for the preparation of the Technical Specifications and cooperated to the preparatory work for the Call for Tender and the Tender evaluations. The upgrade has been approved by the EFDA Steering Committee on 14 July 2006.

The contract for the amplifier procurement was signed in June 2007; the foreseen duration is 20 months up to February 2009, when the new amplifier should start operating.

During 2007, RFX contributed in particular to review the detailed design provided by the Supplier: analyses and numerical simulations were performed to verify the performance of the amplifier and relevant electric circuit in different operating conditions, and to check the effectiveness of the design choices proposed by the Supplier. Part of these activities have been performed by a young researcher who has been working full time at JET since October 07 and will remain there till February 2009 to closely follow all the design, manufacturing and testing activities.

In 2007 a substantial step ahead has been also done in the second task aimed at implementing the hardware and software infrastructure for the new real-time controller of the JET Vertical Stabilization. The status of the new controller implementation is very advanced and in the next year it will be commissioned. In this framework RFX has significantly contributed to some key activities such as the preparation of the multi-core target distribution and the development of the multi-core software architecture under Linux/RTAI which is a real-time extension of the Linux kernel. The successful results allow now running non-real-time applications under Linux on one core, while RTAI running on other cores take care of real-time activities. The software drivers for the ATM (asynchronous transfer mode) real-time network have been also developed and tested. The activities have been mostly carried out at the JET site by RFX professionals.

4.5 FT3

The target plasma of FT3 has been revisited during 2007 to strengthen the relevance of FT3 as an experiment for burning plasmas studies. In order to better match the dimensionless parameters of ITER, in fact, plasma current, toroidal magnetic field and minor radius have been slightly increased. The discharge duration has been instead relaxed to values that limit the cost of the device without affecting the objectives of the experiment, among which the study of the contribution of the fast particles to the instability spectrum. The new choice has also had an impact on the distribution of the field shaping coils, now closer to the plasma, on the torus dimensions and in part on the topology of the access ports.

Consorzio RFX has directly contributed to such process revisiting the issue of VDE instabilities related to the new equilibria, studying the requirements for stabilizing Resistive Wall Modes and evaluating, in some cases, the impact of the new access ports on the diagnostics.

[Agostini07] M. Agostini et al., Phys. Plasmas 14 102305 (2007).

[Carraro07] L.Carraro et al. Bulletin of the American Physical Society Vol. 52, 16, (2007) 217- 49th Annual Meeting of the Division of Plasma Physics, 12-17 Nov. 2007 Orlando FL

[Chapman2006] B.E.Chapman, *Improved confinement MST RFP plasmas with hot ions and high density*, October 30–November 3 2006, Philadelphia PA, 48th Annual Meeting of the Division of Plasma Physics.

[Franz2006] P. Franz et al., Phys. Plasmas **13**, 012510 (2006).

[Franz2007] P. Franz et al., *X-ray emission maps in the MST reversed field pinch*, November 12-16 2007, Orlando FL, 49th Annual Meeting of the Division of Plasma Physics.

[García-Muñoz07] M. García-Muñoz, H.-U. Fahrbach, S. Günter, V. Igochine, M.J. Mantsinen, M. Maraschek, P. Martin, P. Piovesan, K. Sassenberg, and H. Zohm, Fast ion losses due to high-frequency MHD perturbations, accepted for publication in Phys. Rev. Lett.

[Maqueda03] R. J. Maqueda et al., Rev. Sci. Instrum. 74 294 (2003).

[Piovesan07] P. Piovesan, V. Igochine, et al., EPS conference, Warsaw (2007); P. Piovesan, V. Igochine, P. Lauber, et al., TAE internal structure through high-resolution soft x-ray measurements in ASDEX-Upgrade, submitted to Nucl. Fusion (2007).

[Sattin06] F. Sattin et al., Plasma Phys. Control. Fusion, 48, 1033, (2006).

[Spolaore04] M. Spolaore et al., Phys. Rev. Lett., 93, 215003 (2004).

[Puiatti 06] Puiatti M.E. et al., Plasma Phys. Control. Fusion 45, 2011 (2006)

[Carraro 07] Carraro L. et al., 34th EPS Conf. On plasma Phys, paper O-4.028, Warsaw (2007)

[Coccorese04] V. Coccorese, et al., "Design of the new magnetic sensors for JET", Review of Scientific Instruments, **75**, 4311–4313 (2004).

[Peruzzo07] S. Peruzzo, et al., "JET Enhancements – Magnetic Diagnostics Project Summary", JW2-PS-EP-MAG-06, 31/07/2007.

5. DIAGNOSTICS

The 2007 activity on diagnostics entailed maintenance/improvement of operating diagnostics, such as the CO2 interferometer, the Thomson scattering, the SXR tomography, the pellet injector, ISIS and the GPI, work to complete/commission existing but still non operating diagnostics, such as the microwave reflectometer, the FIR polarimeter, the Edge Thomson scattering, the solid pellet injector and the CXRS with the DNBI, and the development of new measurements, such as the on-axis B from MSE and of new instruments, such as the Gundestrup probes, the Laser Blow-Off system, and the new fast CMOS camera. Finally, the work on the JET EP diagnostics, and in particular on the high resolution Thomson Scattering, has been the main activity among the collaborations to other experiments.

5.1 Maintenance/improvement of operating RFX diagnostics

5.1.1 CO2 Interferometer

In 2007 an extraordinary maintenance of the multi-chord interferometer was done, since some chords of the diagnostic were blinded by deposits on the optical components that face plasma. The windows and the in-vessel optical components were removed and inspected. Deposits were present on both, in particular on the accesses at poloidal angles +90° and -90°, which have large and short pipes. The analysis of the deposits showed they are made of graphite, even if further tests are under way to evaluate the presence of boron. The windows were replaced with new ones, whereas the in-vessel optics were cleaned and re-installed (all but one which was too damaged and was replaced). One of the CO_2 lasers has been replaced. The interferometer has been re-aligned and all the 14 channels have been operating during 2007. High plasma current operation induced EM interference on some components, in particular Bragg Cell drivers and chillers, and non-compensated vibrations of some mirrors, resulting in an enhanced measurement error. EM interference has been solved by a re-arrangement of the components on the structure of the interferometer. We are still seeking a solution to the problem of non-compensated vibrations. In autumn, the boronization of the wall deposited a thick boron layer on one of the windows, which practically eliminates one of the measuring chords. The window will be replaced, but a way to protect the windows and the internal optics during first wall treatments is under study.

5.1.2 Main Thomson Scattering System

A procedure for cleaning the inner surface of the 3 collection windows by laser ablation has been studied, since presently they deteriorate in time and have to be periodically replaced. It consists in sending the laser beam in a 1 mm optical fiber in order to bring its radiation directly to the installed window: laboratory tests have been done to determine the requirements of the system, in terms of laser power, laser frequency and laser spot size at the output of the fiber. The oscillator of Ruby laser used for the Edge Thomson Scattering (40mJ at 1Hz) has been found suitable for the purpose; a prototype is going to be designed.

The Nd:YLF laser has been completely re-aligned: optical components (lenses, mirrors, crystals, rods) have been substituted; new lamps of the main rod, which are not commercially available anymore, have been manufactured and installed by the company which provides maintenance of the Ruby laser. The laser is now capable of working at 6J for all of the 10 available pulses.

5.1.3 SXR tomography

During the April 2007 shutdown, the SXR photocameras of the tomography have been modified in order to include curved Be foils both in the pinhole and the filter wheel in substitution of the original flat ones. This will avoid the software processing of the signals due to the different thicknesses of the Be seen by each line of sight.

Progress in the diagnostic of the core plasma will also come from a new camera that will substantially increase the spatial resolution of the SXR tomography, adding a total of 65 channels organized in three rows. It will be installed on a horizontal porthole of the vacuum vessel, replacing the present tomography manipulator. Different beryllium foils will be installed in two rows, so that different energy spectra ranges could be measured simultaneously in the same plasma shot: this will allow following the temporal evolution (up to 100 kHz) of the plasma SXR emission and T_e profile with high accuracy.

5.1.5 *Integrated System of Internal Sensors*

In 2007 the electrostatic sensors of the Integrated System of Internal Sensors (ISIS) have started full operation, complementing the information of the magnetic sensors. This has been accomplished by realizing a differential-input circuitry in order to separate the ground loop between the experiment and the acquisition system. The complete system now provides measurements of electrostatic and magnetic fluctuations with sampling frequency of 1 MHz and 5 MHz respectively and with toroidal and poloidal space resolution. A first characterisation of the electrostatic fluctuations in the edge region has been carried out.

5.1.6 *Triaxial magnetic coils added to the GPI diagnostic*

Triaxial magnetic coils have been installed on the GPI flange (Fig.5.1) to observe the thermal He beam and study the magnetic structure of the emission bursts. The bursts detected by the GPI have a magnetic structure compatible with a current filament elongated along the poloidal direction and propagating toroidally and radially.

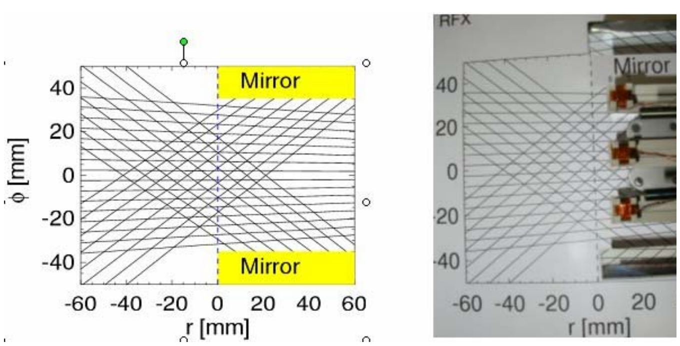

Fig. 5.1: Optical drawing of the GPI LoS net and picture of the triaxial coils

5.2 Completion/commissioning of RFX diagnostics

5.2.1 *Reflectometer*

Most of the activities needed for the installation of the diagnostic on the machine have been completed. A prototype has been successfully tested on the bench with the new acquisition system (4 channel at 1 GSample/sec, with 50 Msample of memory each) reaching a double frequency scan of 4 GHz in 500 ns (200ns each scan + 2 x 50 ns of dead time). The new circuitry has been engineered and is ready for production. The 4-fold increase of the frequency modulation rate (4 Mscan/s) from the previous 4 GHz/1 µs has been motivated by the observation that the Doppler-effect caused by medium scale density fluctuations introduces a significant shift of the measured position of the density cut-off layer. This effect is at the origin of the unrealistic non monotonous density profiles obtained with several reflectometers installed in different fusion experiments. Like in FM-Doppler radar, given a sufficient time resolution, this radial velocity can be measured and used to correct the reflecting cut-off layer position.

5.2.2 FIR Polarimeter

The re-commissioning of the 6-channel FIR polarimeter started in January 2007. The polarimeter has been modified to solve the problem that previously affected the measurements. A new frame for the system has been fixed to one of the RFX-mod inertial platforms. The frame holds two granite tables on which different optics have been mounted. One of these tables replaces the previous metallic box that suffered from vibrations due to electrodynamic forces. On its surface four plane mirrors have been installed, one of which is used to bend the horizontal beam coming from the laser room vertically towards the torus. The other table (the Beam-splitter Box, BSB) houses the optical components to split the FIR beam into 6 chords. Some of the optical devices of the BSB have been motorized to allow in-situ alignment of the system. The Detection Section (DS, composed, for each channel, of a motorised rotating half wave plate, a wire grid to split the two components of the radiation, a parabolic mirror to focalize the beam and a pyro-electric detector) has been maintained, except for substituting some damaged optics. A remote control for the motorised half-wave plate has been bought and the software for the control has been implemented in order to allow a shot-by-shot calibration of the system. The DS has been pre-aligned and then installed on top of the machine, fastened to the mechanical structure of the field shaping coils. The acquisition system has been also recommissioned. Most of the FIR line has been enclosed inside plexiglass boxes and connecting pipes to be kept at a 20 mbar over-pressure with nitrogen, which mitigates the attenuation of the FIR radiation by the air humidity. The entire optical path has been pre-aligned by a He-Ne laser. Recently a general maintenance of the laser system (CO_2 + FIR) has been started which is still under way. The final alignment of the diagnostic is scheduled during the January 2008 shut down.

5.2.3 Edge Thomson Scattering

The edge TS system has been completed. Stray light has been sufficiently reduced by developing a proper alignment technique; the remote controls of the mechanical structure and of the pumping system are now available. The system will run during next experiments.

5.2.4 *Non-cryogenic Pellet injector*

The development of a non-cryogenic pellet injector continued with the commissioning of pellet loading, unloading and launch systems. The design of the pellet injector interface to the RFX-mod device has been nearly completed: the non-cryogenic pellet injector will share the same port and vacuum system of the cryogenic injector. In parallel, the development of the Lithium handling and pellet preparation tools have been started to be ready for the planned 2008 Lithium pellet injection.

5.2.5 *CXRS with Diagnostic Neutral Beam Injector*

Charge exchange recombination spectroscopy is one of the important diagnostics which RFX has been waiting for. Several technical problems have delayed its exploitation in 2007. A fault in the communication electronics has been fixed by substituting the original Russian boards with RFX units. The modularity of the control software, based on java routines, allowed the software reconfiguration to accommodate the new drivers. On the other hand, it has also become clear that in RFX there are conditions that hamper this type of measurement. To investigate the underlying problems, many simulations have been carried out by means of the software recently developed by M. von Hellermann [vonHellermann07] of FOM. The main outcome is that the neutral density at the edge of the RFX plasma is large enough for the natural emission of the CVI CXRS line to overwhelm the one actively induced by the beam. According to simulations, some regions of the parameter space are better than others to achieve an adequate signal-to-background ratio. Such conditions include high temperature plasmas and low recycling walls; in addition, OVIII emission lines should be more favorable than CVI lines.

5.3 Development of new measurements on RFX

5.3.1 *Insertable probes*

During 2007, the insertable probe dubbed “Gundestrup” has been installed and commissioned in RFX-mod. The probe consists of a boron nitride case equipped with 8 directional graphite pins arranged on a circumference of 23 mm diameter, which can provide measurements of local plasma flow in the poloidal and toroidal directions. Two additional pins are also available for the local measurement of plasma density and temperature by a standard Langmuir probe technique. A radial position scan has been performed on a shot-by-shot basis: for plasma currents lower than 400kA, the probe can withstand up to 50 mm insertion. Two different configurations, with all the Gundestrup pins measuring either floating potential or ion saturation current, have been used in order to compare the results of the theoretical interpretation models providing the plasma flow. The data acquisition system has been arranged so as to get an easier probe configuration change and front-end isolation amplifiers, withstanding up to 1500 V rms, protect the acquisition system from possible over-voltages [Serianni04]. All signals have been sampled at 5 MHz.

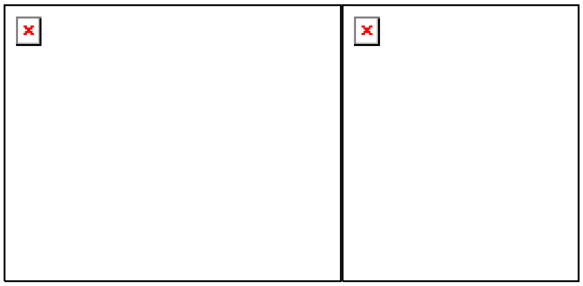

Fig. 5.2: lateral view of target (left) and plasma produced by the ablation process (right)

5.3.2 *Laser Blow-Off system*

The mechanical structure of the Laser Blow Off system has been built and is being presently installed on RFX-mod. The system has been tested during 2007 in a high-vacuum test-bed. The laser has been fired onto a carbon target to test the ablation process (fig. 5.2).

5.3.3 *MSE with Diagnostic Neutral Beam Injector*

During 2007 the optical equipment to be used for the Motional Stark Effect has been completed. It has been verified that the beam emission level is sufficient to yield the value of the magnetic field on the axis. However, the minimum level of plasma current at which this will be possible is difficult to predict.

5.3.4 *Fast CMOS camera*

A fast CMOS camera has been bought and installed on RFX-mod, having a resolution of 1024x1024 pixels when working at frequencies up to 1 kHz and 256x256 pixels up to 10 kHz. The camera has been absolutely calibrated to allow poloidally space resolved fast measurement of H□ emission to better evaluate Hydrogen influx from the wall.

The camera will be installed on the pellet launch port to measure the line emission from the pellet ablation cloud, that will allow evaluating, with good spatial resolution (≈ 2 cm), the magnetic pitch angle. For this task all the equipment is ready and the measurement will be performed in the experimental campaigns of the next year. Conversely, installing the camera on a vessel toroidal view port allows the study of the fast plasma wall interaction.

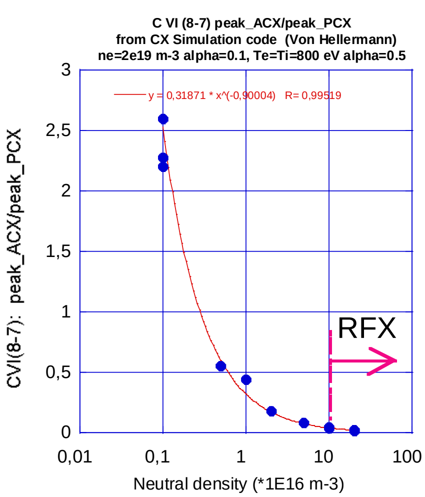

Fig.5.3 Active signal- to-background ratio foreseen for the CV 520 Ang. Emission line in RFX as a function of the edge neutral density.

5.4 Diagnostics for JET-EP

5.4.1 *High Resolution Thomson Scattering (HRTS) for JET*

The HRTS has been successfully operational in JET experimental campaigns from October 2006 till April 2007. Measured profiles, especially of the edge transport barrier, have been used in various physics studies.

The only outstanding problem left was the risk of damaging the input optics by hot spots developed in the laser beam profile: in fact operation had to be constrained to a burst of just 10 pulses, to limit the risk of damage. The remaining of 2007 has been mainly spent to investigate this problem and implement a valid solution. Extensive measurements of the beam profile and damage tests of the optics have better quantified the risk of damage. The laser manufacturer and other experts were consulted to find possible ways of smoothing the beam profile, but all the solutions required to give up a good fraction of the pulse energy, which was not acceptable. Eventually it has been agreed that the best solution to mitigate the risk was a new input path. The new path differs from the previous one only in the roof lab. It still shares the edge LIDAR floor penetration. No modification is required for the optics in the torus hall, which preserves the alignment procedure.

The new path mitigates the risk because of:

a) larger beams both in the roof lab and at the torus window;

b) no optic shared with main LIDAR input optics and negligible impact on collection optics;

c) only 3 optics shared with edge LIDAR (7 before), easily accessible;

d) simpler imaging system, which improves beam quality.

The residual risk has been evaluated more accurately than in the past, using CCD profile monitoring in addition to burn-paper to check profile quality and replicating in the laser room the entire beam path down to the torus window, which has allowed performing damage tests at different locations. These tests indicate that to produce damage the beam diameter has to be reduced 2x at the laser output, but 3.5-4x at the other optics in the beam path. Procurements for the new beam path have started in September and will be completed early in 2008.

In addition, new set of fiber optic delay lines has been ordered, which should also be installed in early 2008, bringing the number of measured spatial positions from actual 37 to 60.

In the original design, 3 spatial positions shared each of the 21 spectrometers (60 total positions), using 10m fiber optic delay lines to separate the TS pulses. Because of spurious signals occurring both before and after the TS pulse, the current layout has been organized with 30m delay lines (three 10m delay lines connected in series), which has restricted the available number of delay lines and then the number of positions to 37. It has then been decided to bring the system to full performance in terms of spatial resolution (60 positions, 1.5cm spatial resolution) purchasing a number of delay lines which, added to those already in house, will allow to accommodate 3 positions for each spectrometer with 30m delay between TS pulses.

5.4.2 Magnetic Diagnostics

The Enhancement Project of the Magnetic Diagnostics aimed at the design, procurement, assembly, installation and commissioning of new sets of magnetic sensors inside and outside the vessel, in order to substantially improve the current capabilities of the JET plasma equilibrium control and reconstruction [Coccorese04]. The project has been managed in the framework of a number of EFDA-JET Orders and Notifications, started in 2002, under the joint responsibility of Consorzio RFX and Consorzio CREATE, in close collaboration with the JET Operator and CRPP.

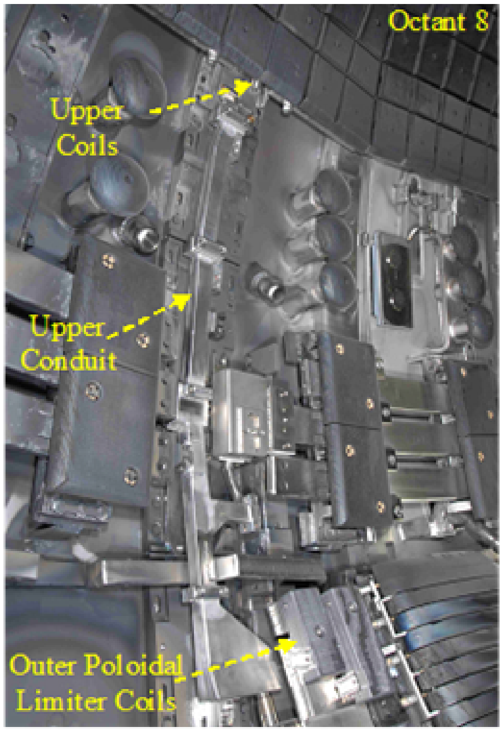

Fig.5.4 Picture of Magnetic Diagnostic system, installed in the JET vessel during the 2007 Shutdown.

Since December 2006 Consorzio RFX has taken the formal leadership of the project. The activities during 2007 were mainly dedicated to Project management, monitoring and interfacing during Operator activities, as foreseen in the running EFDA Tasks JW5-OEP-ENEA-50A and JW7-NEP-ENEA-70. In particular the activities were focused on the following topics:

- in-vessel installation of the system, successfully completed during the 2007 Shutdown (Fig. 5.4);
- preparation of activities related to the commissioning of the diagnostic, to be carried out during the Restart in the first months of 2008 before the Experimental Programme of Campaigns C20-C25, in the frame of the JET 2008 Work-programme [Peruzzo07].

5.4.3 *JET-EP Halo Current Sensors (HCS)*

In 2007 the new JET Halo Current Sensor system has been completed with the final project board and the handover to the operator. This system has been the first JET-EP project that completed the handover process to the operator. The Halo Current Sensor system is able to analyze in more detail the halo current path and allows, for the first time, to study the non-axisymmetric behaviour of the VDEs in JET as shown in fig.4.# A complete set of processed PPF signals are now available for the users in the next experimental campaigns.

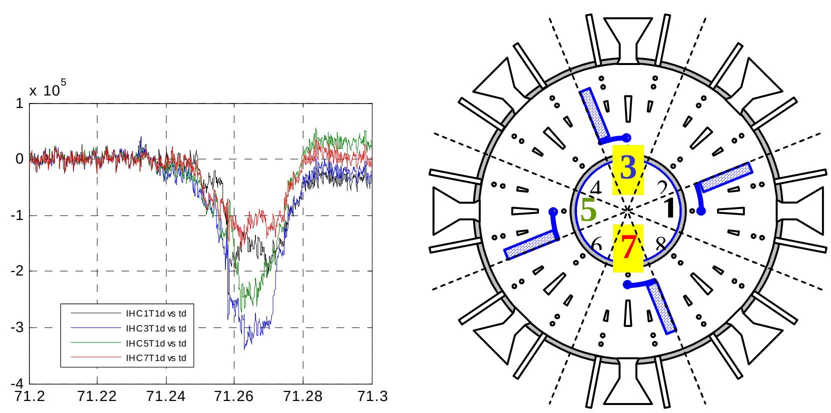

Fig.5.5 Halo currents measured during a disruption by the pick up coils in four different toroidal positions. A non axisymmetric VDE is evident with a maximum in Octant 3 and a minimum in Octant 7

[vonHellermann07] Private communication.

[Serianni04] G. Serianni et al., Rev. Sci. Inst. **75**, 4338 (2004).

6. ITER AND BROADER APPROACH

6.1 Neutral Beam Injector

During 2007 Consorzio RFX has continued the activities aimed to advance the Neutral Beam Injector (NBI) for ITER and the related Neutral Beam Test Facility (NBTF) design and to train the personnel. Most activities have been performed under two EFDA contracts (EFDA/06-1499 and 1426) for a total of 22ppy from December 2006 to April 2008. The advance in the NBI design achieved during 2007 has contributed to provide ITER with the elements to decide for a RF driven ion source and for an alternative Power Supply scheme (originally proposed by RFX and characterized by an air insulated High Voltage deck). Moreover the EU has endorsed the proposal of a Neutral Beam Test Facility (NBTF) to be located in Padova, aimed to install and test the NBI and to support the NBI operation at ITER. As a consequence, the design of the NBI has been oriented to the injector to be installed at the NBTF and the priorities have been related to the NBTF planning, according to which the first system in operation will be an Ion Source operating with low extraction voltage. During 2007 Consorzio RFX has continued accompanying activities aimed to support the ongoing R&D and to train personnel, also by sending researchers to other EU and non EU (Japan) laboratories. Moreover Consorzio RFX has offered support to the design revision of ITER by making available experts in several areas and by participating to several ITER working groups and meetings. In the following, the main activities, grouped into activities related to the NBI development, activities related to the NBTF design and accompanying activities, are reported.

6.1.1 NBI Design Activities

These activities have been performed under EFDA contract for a total of 12ppy. As for previous contracts, the work has been performed in close collaboration with other EU Associations (CEA, IPP, UKAEA, CIEMAT, FZK) and Consorzio RFX has supported EFDA in the overall coordination. The activities have been mainly devoted to the design of the vessels, the accelerator, the ion source and the power supply, to review and to prepare a preliminary assessment of the NBI diagnostics, to develop a conceptual design of an active steering system. All these activities are described in detail in the following.

6.1.1.1 Vessels

The RFX activities in 2007 were aimed to the detailed design of new Beam Source and Beam Line Vessels by developing CAD models and drawings and by carrying out mechanical analyses and verifications.

Following studies and analyses carried out by RFX and CEA during the previous years and further RFX proposals to improve access and space for maintenance and remote handling (RH) operations, it was agreed by EFDA and ITER to develop the design of new vessels for the ITER NB Injectors. The following main changes have been decided for this new design:

- top access for maintenance of Beam Line Components;
- an almost rectangular cross section;
- ~1 m upward shift of the HV Bushing vessel and increased height of the Beam Source Vessel;
- optimized dimensions of Beam Line Vessel to house the highest possible side cryopumps;
- slopes on the bottom part for water drainage.

This work required several preliminary studies of different solutions, developed in the frame of strong interactions with EFDA, ITER and other Associations to comply with a number of varying, uncertain or undefined inputs and requirements and to deal with a large number of complex interfaces with systems and components under development by other EU Associations or by Japan (HV Bushing). The main design constraints and guidelines for the Test Facility vacuum vessels are:

- inner dimensions of Passive Magnetic Shield in ITER;
- ITER Load Conditions to be considered;
- compatibility with the interfaces as foreseen at ITER site;
- fulfillment of RH requirements, but compatibly with Test Facility needs.

The new design has been optimized with iterative static analyses and design changes, in order to limit displacements, stresses and weights within allowable values.

A double shell structure has been chosen to increase the stiffness of lateral walls and suitable stiffening ribs have been added to fulfill the design requirements. Preliminary studies have been also carried out to verify possible design solutions for vacuum tight connection flanges of the top, front and rear accesses of the vessels. The vacuum boundary thickness is 25 – 35 mm, the external stiffening wall 10 mm and the ribs 25 – 35 mm. The total weights of Beam Line and Beam Source Vessels are about 47 t and 40 t respectively. The weight of the top lid is about 13 t.

An example of static analysis of the vessels under vacuum and dead weights is shown in figure 6.1. The maximum static deformation under nominal vacuum condition is lower than 4 mm and the maximum Von Mises stress is lower than 100 MPa, both within acceptable limits. A full set of analyses on the updated model for several normal, upset and fault conditions are still going on and will be completed in the first months of 2008.

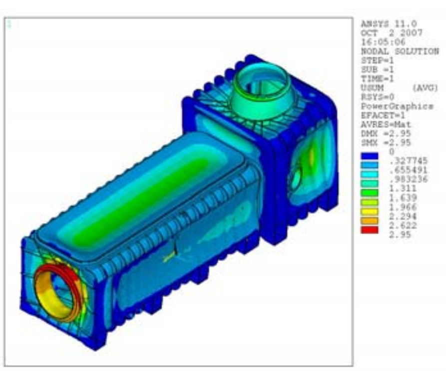

Fig. 6.1 Amplified deformed shape of the vessels under dead weight and vacuum load condition

The CAD model of the vessels developed in 2007 is shown in figure 6.2, with indication of all the different interfaces that have been added as service lines, mechanical actuators and diagnostic access.

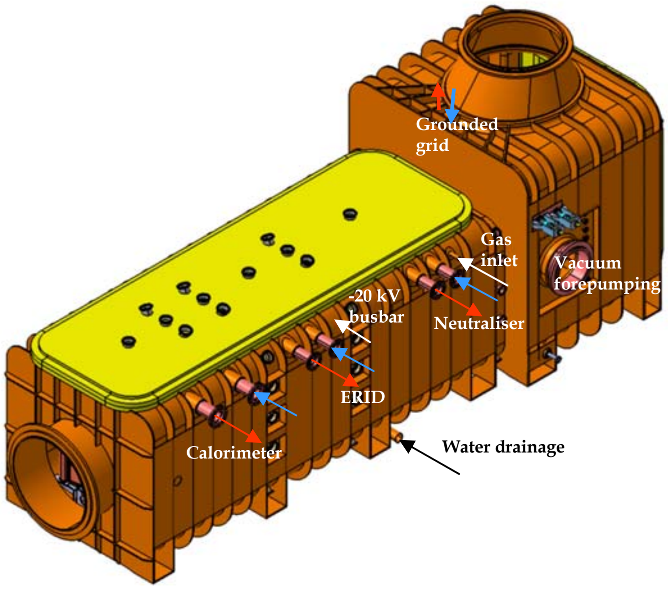

Fig. 6.2 The vessels designed for the ITER NB Injector in the Test Facility configuration

6.1.1.2 Ion sources

During 2007, the detailed design of the RF ion source for ITER NBI has been carried out. In fig 6.3 a scheme of the RF ion source is shown.

The collaboration with IPP-Garching allowed to discuss in detail all design choices, exploiting the progress of the ongoing design activity of the ELISE test bed and the experimental campaigns on the existing facilities.

The previous outline design has been revised, in particular as a consequence of additional heat load deposition onto inner vertical surfaces caused by back-streaming of positive ions.

A thorough revision of cooling circuits for the most-heated components included several detailed thermo-hydraulic analyses, in order to optimize the flow parameters.

The thermo-mechanical evaluation of these components has been carried out according to the new RFX procedure proposed to EFDA/ITER, and fatigue life was verified with reference to all relevant loads. An example of thermal analysis is shown in fig.6.4.

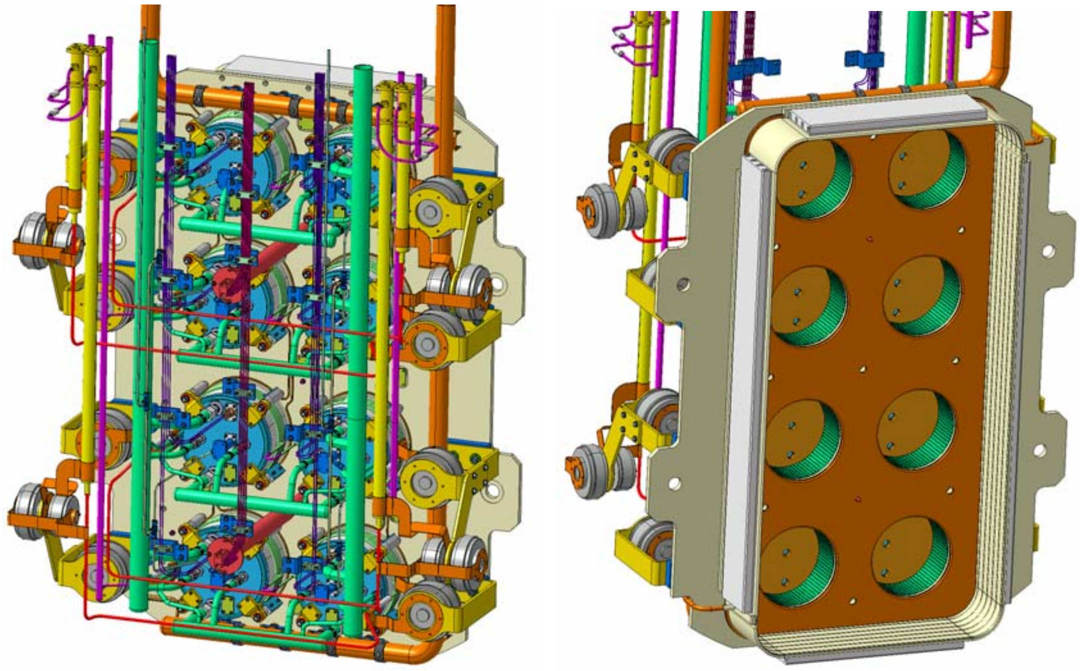

Fig. 6.3 Scheme of the RF ion source

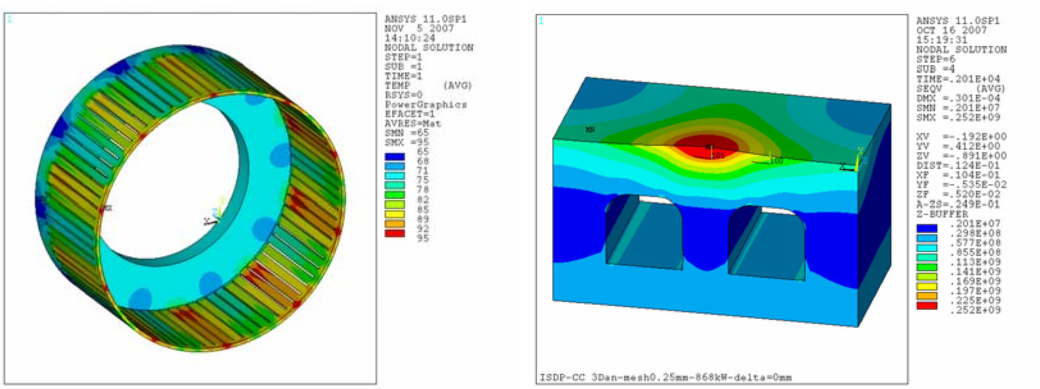

Fig. 6.4 Example of thermal analysis…………..

The electric circuits have been revised, in agreement with the updated requirements from the power supply system. Possible solutions for off-the-shelf components of the electric circuits have been identified (capacitors, connections, …).

Mechanical details for all components have been developed, for example:

- interfaces between components have been defined in order to comply with required alignment tolerances, differential thermal expansion, …
- demountable connections have been foreseen for all hydraulic and gas circuits, in order to ease maintenance interventions in the test facilities;
- a simulation of the assembly sequence has shown no interferences between adjacent parts during assembly/disassembly;

- alternatives for most critical components have been studied, in order to obtain the maximum compatibility with the set of very heterogeneous requirements (mechanical, physics, electrostatic, …).

A comprehensive set of diagnostics has been identified (see 6.1.1.5), and provision for accesses has been made both on the rear and lateral side: the source has been designed in order to maximize the compliance with possible different diagnostic requirements and even with integration in different facilities.

The ion source has been integrated into the SINGAP beam source, MAMuG compatible, with reference to the NBTF configuration, updating support systems and connections for the services.

The replacement of caesium ovens is the only remote handling relevant task in ITER: in collaboration with UKAEA, a preliminary assessment of the procedure and of the required space availability and auxiliary structures has been carried out.

6.1.1.3 Accelerator

Due to the pending decision on the accelerator type (SINGAP or MAMuG) and the possible need of testing both concepts in the Test Facility, the EFDA Task in 2007 was aimed to the design of a SINGAP accelerator that could be compatible with a MAMuG type accelerator, that means a design allowing changes from SINGAP to MAMuG or vice versa with the least consequences in terms of costs and time.

Starting from the previous SINGAP design developed in 2006, the following main activities and design developments have been carried out in 2007:

- integration of the SINGAP accelerator with the RF ion source;
- identification and re-assessment of all the service lines for MAMuG and SINGAP configuration according to RF ion source integration, updated electrical circuits, new heat loads to be removed and cooling requirements, diagnostics requirements;
- optimization of the routing of service lines at different voltages to limit the maximum electric field and to allow RH cut/weld operations;
- design of flexible connections to allow for position adjustment and tilting of the whole source on the vertical plane;
- design of a new support and tilting system that fulfils all the assembly, remote handling and operational requirements;
- electrostatic optimization and addition of several shields to limit local electric field intensity inside and around the beam source;
- design of an overvoltage protection system connected to the grounded grid;
- adaptation of MAMuG mounting flanges, support frames and post insulators to support the SINGAP grids;
- hydraulic assessment and redesign of cooling pipes routes and connections to the grids;

- new thermo-mechanical analyses of SINGAP grids subjected to increased heat loads (new information from updated analyses).

All these activities required a careful design integration and coordination of different design teams, engineers and physicists involved in the design of RF ion source, vessel, diagnostics, power supply and remote handling. In particular, strong collaborations with IPP, CEA and UKAEA laboratories have been put in action.

A 3D cross-sectional view of the whole beam source and details of flexible connections to the HV bushing and new optimized electrostatic screens are shown in figure 6.5.

The main results of the electrostatic optimization of beam source and post insulator shields are shown in figure 6.6. The new screens of post insulators, accelerator flanges and RF ion source significantly reduce the electric field on the screens, on triple points and along the insulator surfaces with respect to the reference design, achieving a larger safety factor and better reliability for in-vacuum high voltage holding.

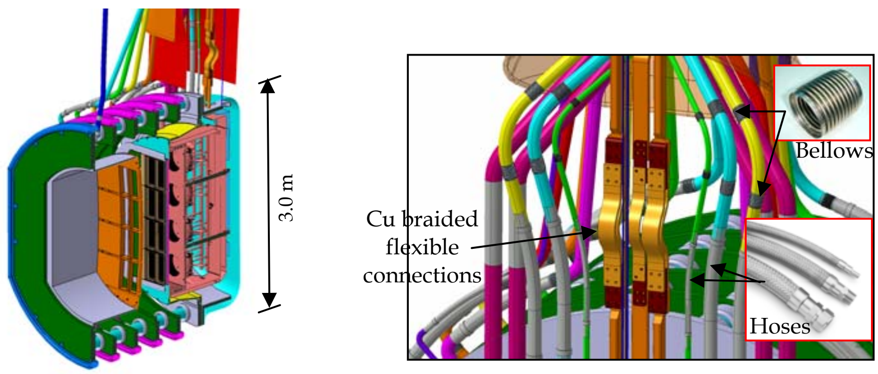

Fig. 6.5 Cross-sectional view of the new beam source and details of the connections between Beam source and high voltage bushing

Details of the new support and tilting system are shown in figure 6.7. The source is hung from the top by means of two hinges connected to a transverse support beam. The beam supports have been designed to guarantee an accurate adjustment of the source position: this is a major requirement in order to achieve the precise aiming of the beam towards the plasma at about 25 m distance from the grounded grid. The system for vertical tilting is located on the bottom part of the vessel and is composed of a linear actuator and hinged leverage to transmit the movement of the source across the vessel wall, with the possibility of remote control of the beam source tilting.

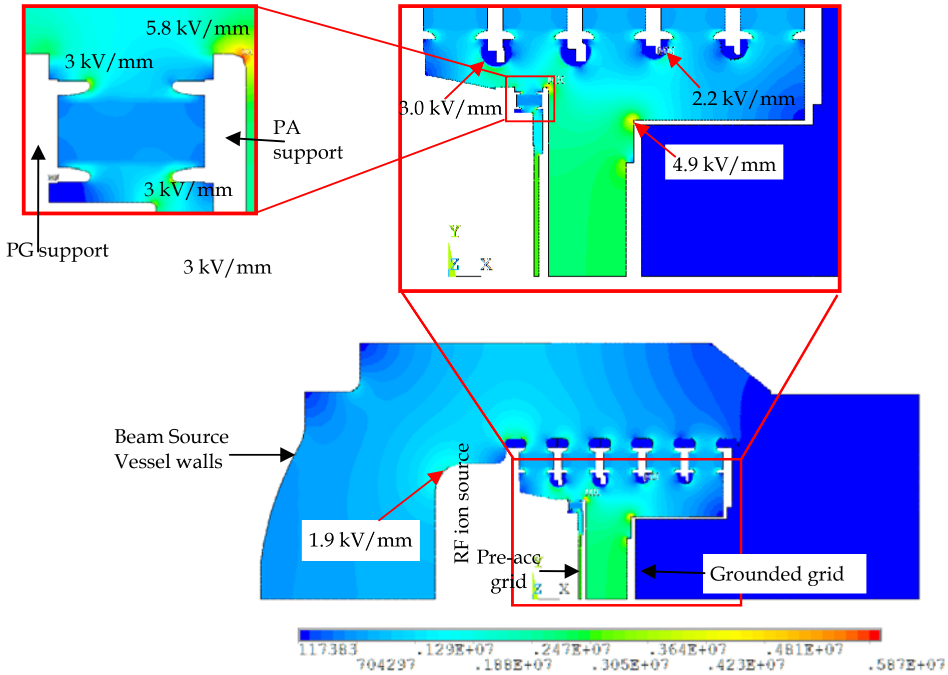

Fig. 6.6 Electric field distribution around the beam source and inside the accelerator after electrostatic optimization

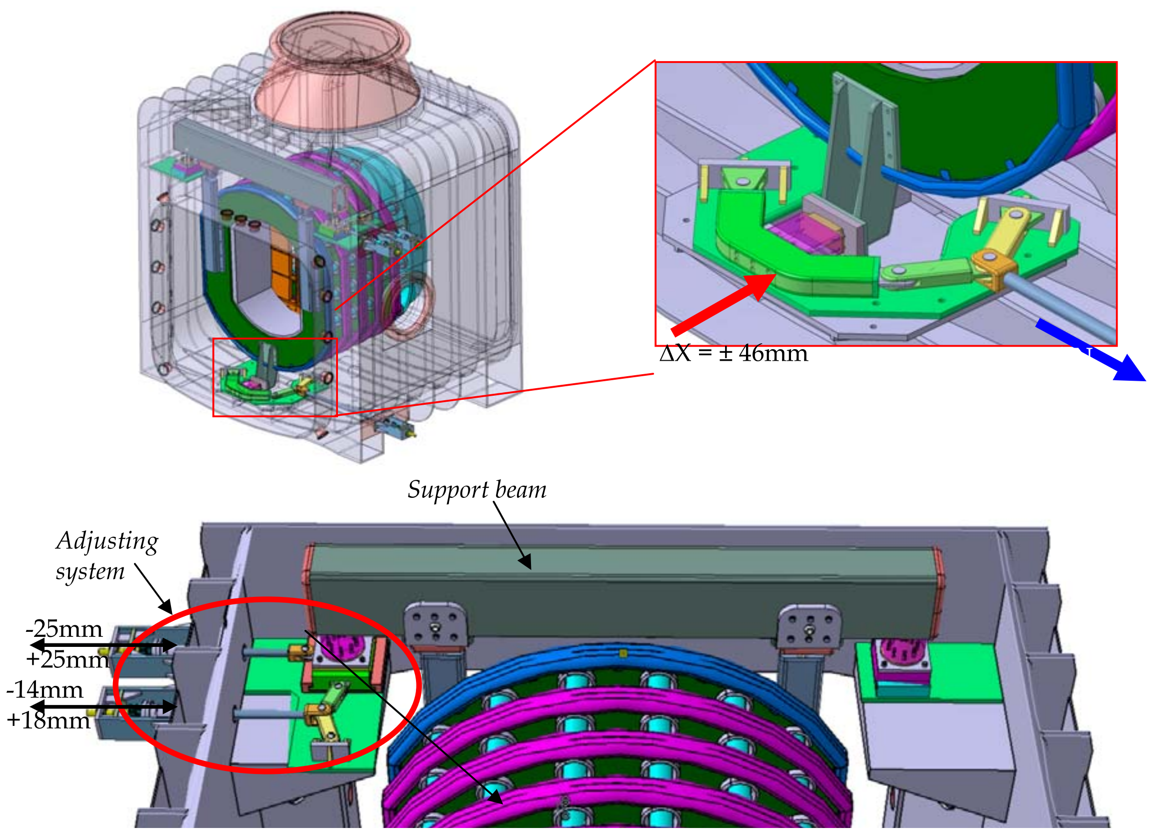

Fig. 6.7 The new beam source support, adjusting and tilting system

6.1.1.4 Electron active steering

The neutral beam injector (NBI) for ITER requires a directional steering of ±9 mrad in the vertical direction in order to compensate residual stray fields. Some additional steering can be envisaged also in the horizontal direction (±2 mrad). According to the present NBI design, such steering is provided by movements of the acceleration grid, which makes alignment a challenging issue (0.2 mm precision over 1.5 m). As an alternative option, an investigation has been carried out about a system of coils located between the Grounded Grid and the Neutraliser. The principle is to control the dissipation of the energy associated to electrons by a suitable magnetic field, bending the electron trajectories towards a material surface; since ion motion would be affected by the magnetic field as well, a second magnetic field should be located behind it to compensate for the first kick on the ions and to provide a degree of freedom on the ion motion. A sketch is presented in fig.6.14.

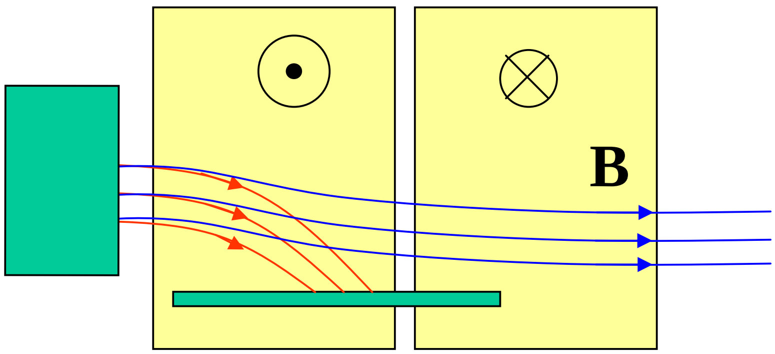

Fig. 6.14 Scheme of the active steering by magnetic field

The whole steerer, including three systems of coils, the dumping plates and the magnetic yoke are shown in fig. 6.15.

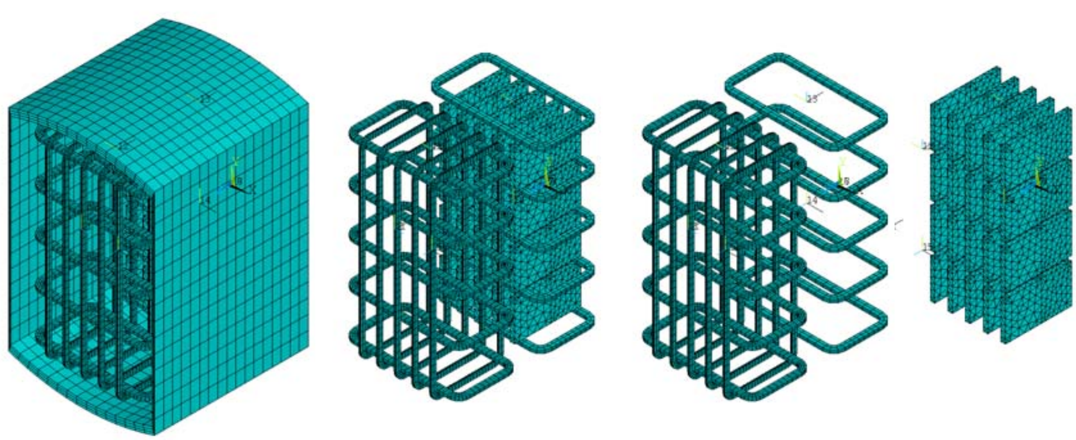

Fig. 6.15 Scheme of the steerer and its components

An ANSYS model has been developed to carry out a preliminary investigation of the power distribution due to electrons impinging over the dumping plates; the flux appears to be tolerable. By using the code COMSOL and the paraxial investigation for ions, the uniformity of the resulting ion beam has been investigated, both in terms of the integral of the magnetic field along the path and by means of ray tracing. The position of the coils has been preliminarily optimised and a new coil configuration ("split-end" coils) has been proposed as a way to further improve uniformity. Fig. 6.16 presents the proposed coil geometry (left) and the resulting magnetic field ripple compared to the normal race-track coils.

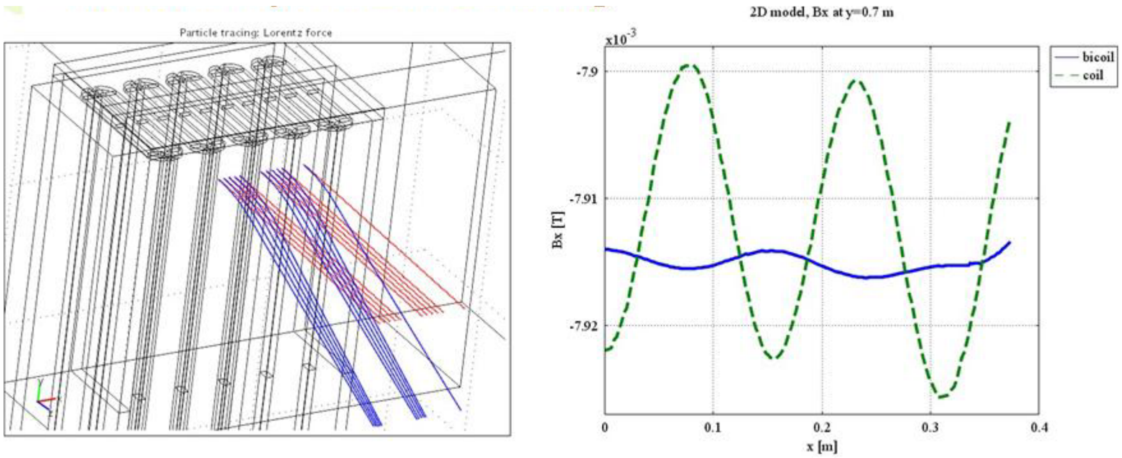

Fig. 6.16 Coils geometry and resulting magnetic field ripple

6.1.1.5 Diagnostics

A complete revision of the diagnostic requirements for the Neutral Beam Injector (NBI) and Neutral Beam Test Facility was carried out during 2007.

In the ITER NBI case, on which previous work had focused, diagnostics will be devoted to protection and to control of a limited set of pre-programmed setups, and emphasis is on reliability and minimum maintenance.

On the contrary, in NBTF the diagnostic set must guarantee adequate protection, but also be able to:

- provide all the information needed to validate the component design;
- allow for complete and flexible control in order to explore and identify optimal operational parameters;
- provide adequate knowledge of all the physical quantities relevant for beam characterization, with the accuracy and resolution sufficient to assess the compliance to

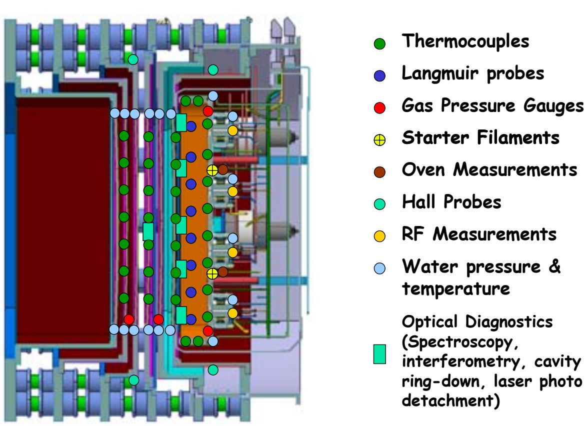

Fig. 6.18 Summary of Source Dignostics

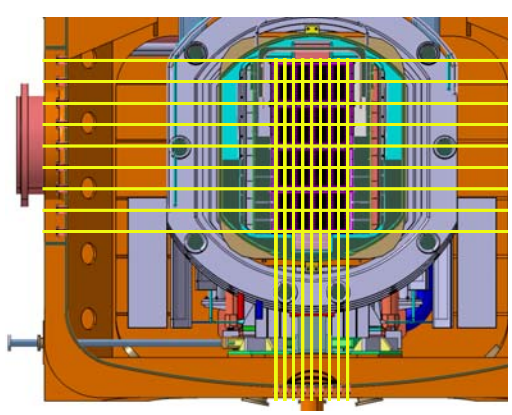

Fig 6.19 Source line Spectroscopy

irements.

To fulfill all the different requirements described above, a wide and complex diagnostic set will be needed, which will include (see fig. 6.17, 6.18, 6.19):

- a large number of calorimetric sensors embedded in all components, for careful monitoring of all parts exposed to the beam, helped by a large set of cooling water measurements (about one hundred independent cooling circuits are present in the NBTF);
- a complete set of electrical measurements in the power supplies, with specific sensors devoted to fast detection of arcs and breakdown events;
- vacuum and RGA (residual gas analyzer) monitors in several parts of the injector (source, vessel, neutraliser);
- optical diagnostics for source and beam chracterisation: line spectroscopy, tomography, doppler spectroscopy, laser cavity ringdown and infrared thermography, with several diagnostic sections distributed along the beam.

Starting from the NBI diagnostic set described in the ITER baseline documentation, and from the diagnostic approaches adopted in existing Neutral Beam Injectors and experiments, a detailed database was realized, containing:

- physical parameters to be measured;
- number and position of sensors;
- required accuracy and resolution of each measurement;
- relevance of the measurement for protection, control, beam characterization, design validation.

In parallel, a Failure Mode Analysis for the whole NBTF plant was performed, based on the FMEA (Failure Mode and Effect Analysis) method, in order to verify the adequateness of the diagnostic set for a reliable protection of the system.

The principal integration aspects of each diagnostic were also addressed, i.e. mechanical modifications for optical access, signal routing and extraction, sensors placement, identifying the critical areas that will require specific design and component adaptation.

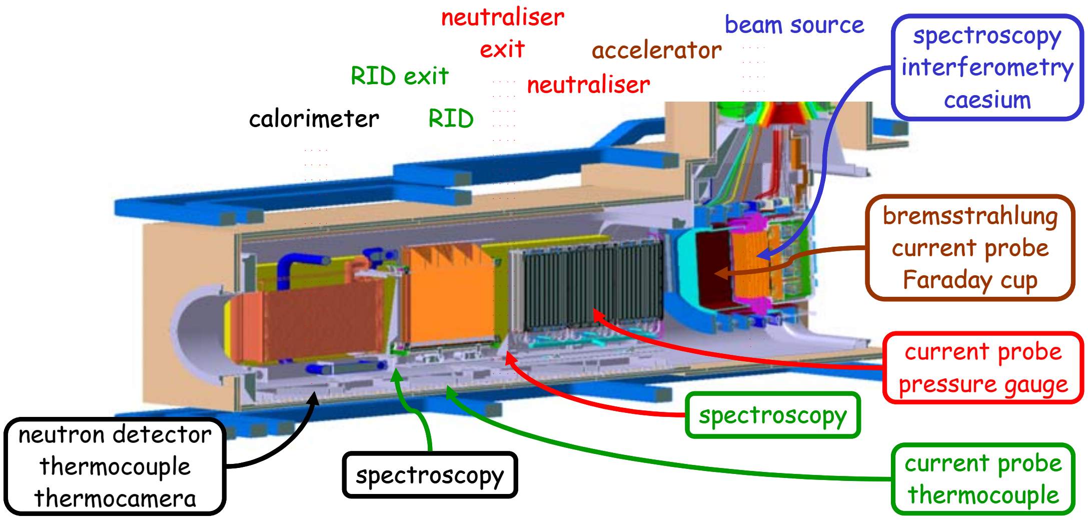

Fig. 6.17 Relevant sections for diagnostics and principal measurements

6.1.1.6 Power supply

The majority of resources working on the ITER NBI power supply (PS) has been concentrated on the development of the integrated design (ID) of the system.

The ID is the basis for the Procurement Arrangement from ITER and for the preparation of the Functional Specifications for the Call for Tender. The scope of this Procurement Arrangement is the supply of all the components of the ITER NBI PS system, which is shared between Europe (38%) and Japan (62%).

Therefore, the ID covers the overall NBI PS system, including the HV components to be procured by JA.

The ID was developed in close cooperation with the JAEA colleagues and with the contributions of CEA (Analyses of the operation scenario), IPP (Support on RF PS design), EFDA and ITER; dedicated meetings to speed up the joint work were held every two months during 2007. The report describing the resulting NBI PS Integrated Design will be finished in January 2008.

The ID is based on the alternative scheme, object of the Design Change Request 58 (DCR-58), which was approved in spring 2007. RFX, who proposed the new design, provided the support necessary for the DCR assessment. Differently from the previous reference design, in this new one the whole Ion Source Power Supply (ISPS) is located in an air insulated High Voltage Deck called HVD1 supplied by a single 1 MV, 50 Hz insulation transformer. In the former HV deck, now called HVD2, no active electronic devices are now present and just the equipment to feed the cooling water and H /D gas required to the injector is hosted. The new reference design is sketched in the block scheme shown in Fig. 6.8.

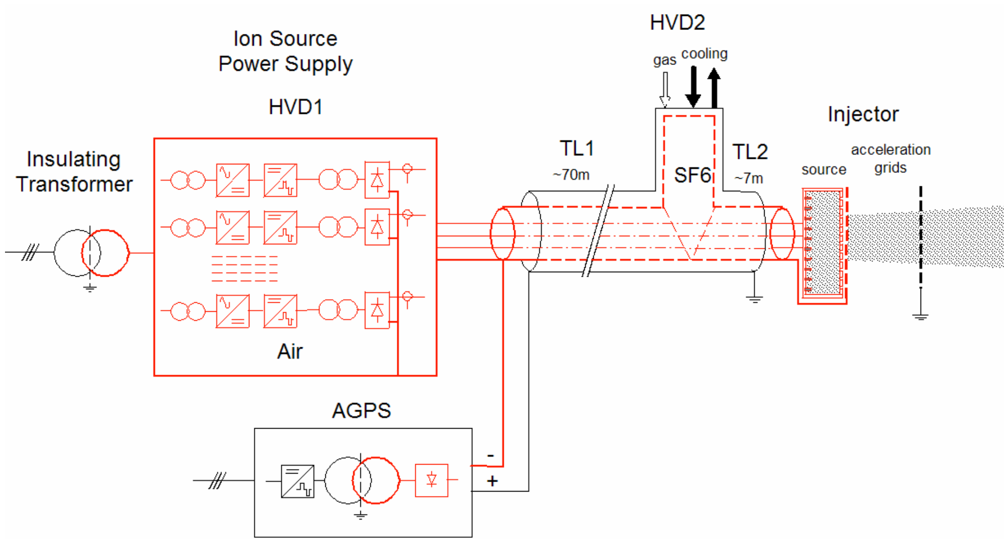

Fig. 6.8 ITER NBI PS scheme adopted with the DCR-58

This NBI PS design, besides offering advantages in terms of higher accessibility to the PS components for maintenance and troubleshooting and saving valuable space in the Tokamak building, allows the adoption of the Radio Frequency (RF) Ion Source. In fact, differently from the previous reference scheme, which required an insulating transformer rated for – 1MV insulating voltage, 1 MW power and 1 MHz operating frequency, whose manufacturing would be well beyond the present industrial experience, in the new NBI PS design this transformer is not necessary.

During 2007, the RF Ion Source was assumed as reference by ITER, as a result of the DCR-64. RFX supported also this DCR with analyses aimed at the assessment and the improvement of the RF Power Supply design, made in cooperation with IPP. The resulting RF PS scheme is shown in Fig. 6.9; the main improvements with respect to that of the previous ITER reference design are the absence of the above mentioned insulating transformer, the use of four RF generators, the removal of the matching transformers inside HVD2 and the adjustment of the matching by varying the frequency of the RF generators.

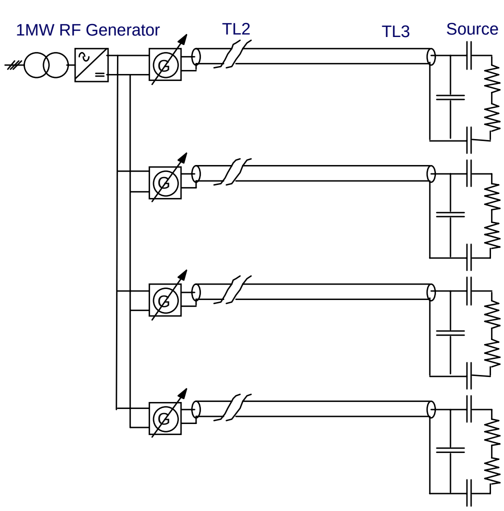

Fig. 6.9 Improved RF PS scheme

The removal of the -1MV, 1 MW, 1 MHz insulating transformer allows increasing the RF generator number from one to four, thus improving the uniformity control of the beam source. The simplification of the matching network, with the removal of the matching transformer and the installation of just fixed capacitors close to the antennas, allows avoiding the presence of electric components inside HVD2 and close to the source and also reducing the HVD2 size. On the other hand, the new design requires longer transmission lines from the HVD1 to the HV Bushing.

On the basis of the analyses of the operating scenario and performance of the beam source provided by CEA, RFX developed the design of the Acceleration Grid Power Supply (AGPS), according to the specification. The resulting reference scheme and main ratings are summarized in Fig. 6.10. Since the reference configuration of the ITER NB accelerator is MAMuG, but the compatibility with SINGAP has to be assured, the AGPS reference design has been worked out accordingly.

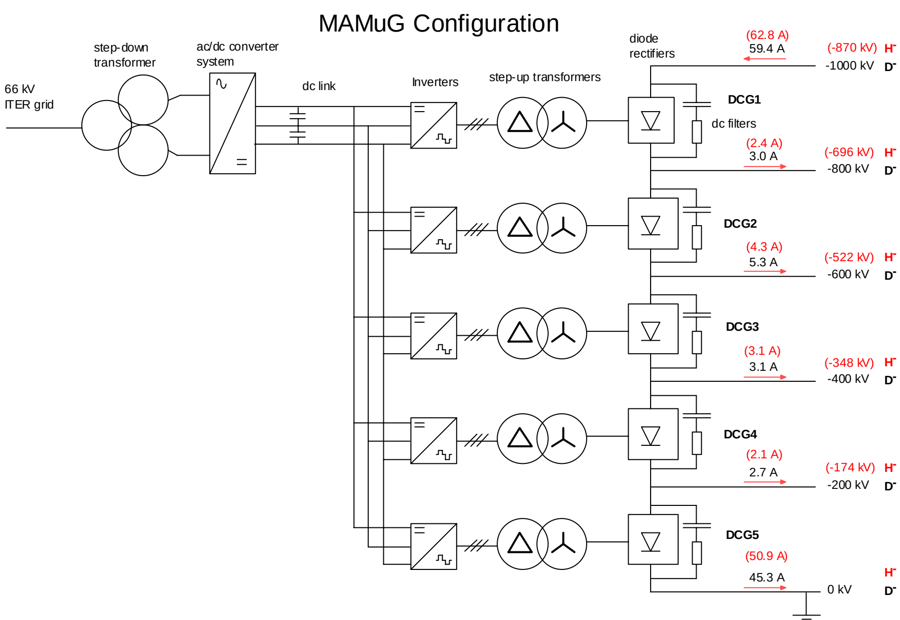

Fig. 6.10 Block scheme of the AGPS reference design.

During this year, significant work was also addressed to analyzing passive and active protection of the NB acceleration grids in case of breakdown, which is an event expected to occur quite frequently. This event is similar to a short circuit at the AGPS output; when it occurs, the PS system should be able to sustain it without any damage, should avoid supplying additional energy to the grids after the breakdown and should restart operation automatically and very quickly.

RFX contributed to the assessment of the specification data for the protection circuits, analyzed and proposed an alternative design for the passive protection system and for breakdown detection and analyzed the effects of the AGPS active protection system by means of numerical simulations. In particular, the design of a damper to reduce the arc energy during breakdown has been developed, combined with a new concept of core snubber; in 2007 the physical properties of this new core snubber concept have been assessed by an experimental campaign on a small scale prototype; furthermore, in the framework of the collaboration with CEA, the tests of a damper prototype have been planned during the Stored Energy Test Campaign scheduled for next year, in which Consorzio

RFX contributes with the damper prototype delivery, electric circuit measurements and modeling. A proposal for the breakdown and partial discharge initiation detection system inside the NBI Transmission Lines and Accelerator has been also developed.

A new operating scenario was also analyzed in 2007, i.e.; operation in Hydrogen at low energy (550 to 600 keV). RFX analyzed in particular how to cope with this particular operating condition with the minimum impact on the present AGPS design and without any power supply re-configuration. The correct operation of the AGPS was also verified by means of numerical simulations on a model of the system; the results showed that this operation is possible, assuring the same dynamic performance as in the reference case.

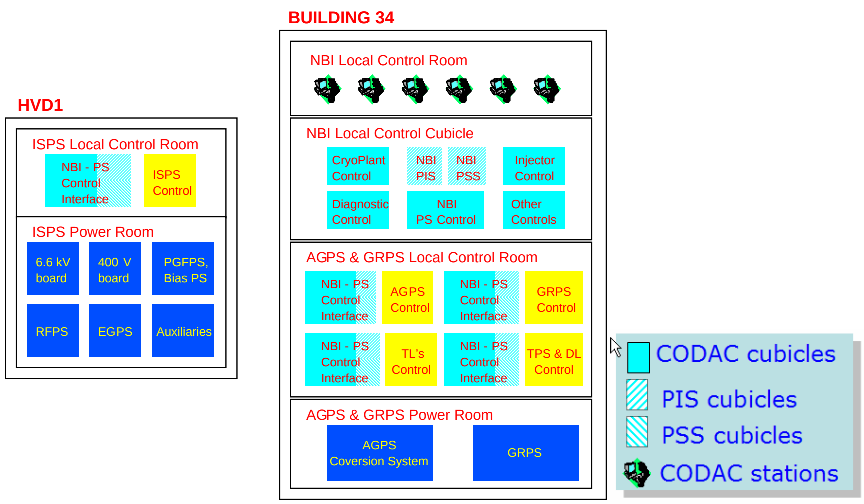

Fig. 6.11 Sketch of the NBI PS Control System and CODAC interfaces

During 2007, RFX also worked out the outline design of NBI PS Control system; a general criterion adopted was: the physical separation between Power and Control Cubicles and between the Remote and Local Control Rooms. Moreover, to reduce the amount of cables/wires to be exchanged with CODAC, local connections from PS's to a specific CODAC interface close to the PS Local Control Cubicles were provided. These criteria are sketched in Fig. 6.11. Of course, this work was strictly connected to the design work for the NBTF (see 6.1.2.3).

Studies were made by RFX also on the layout of the HVD1, the air-insulated deck hosting the ISPS. During normal operation it is kept at the potential of -1MV with respect to ground and it is fed by a single insulating transformer. The HVD1 equipment will be housed on two floors; the mechanical structure must sustain the total equipment load, being about 50 tons and guarantee the mechanical stability in accordance with the specified seismic requirements. The HVD1 will be housed inside a High Voltage Hall (HVH), also containing the insulating transformer, the dummy load and the bushing for the connection of HVD1 to the HV Transmission line; in Fig. 6.12 a plan and a front view of the HVH are shown. Particular attention was paid to the design of the bushing and studies are still in progress; a sketch of the present design and a cross-sectional view of the bushing, showing the internal conductors, is given in Fig. 6.13.

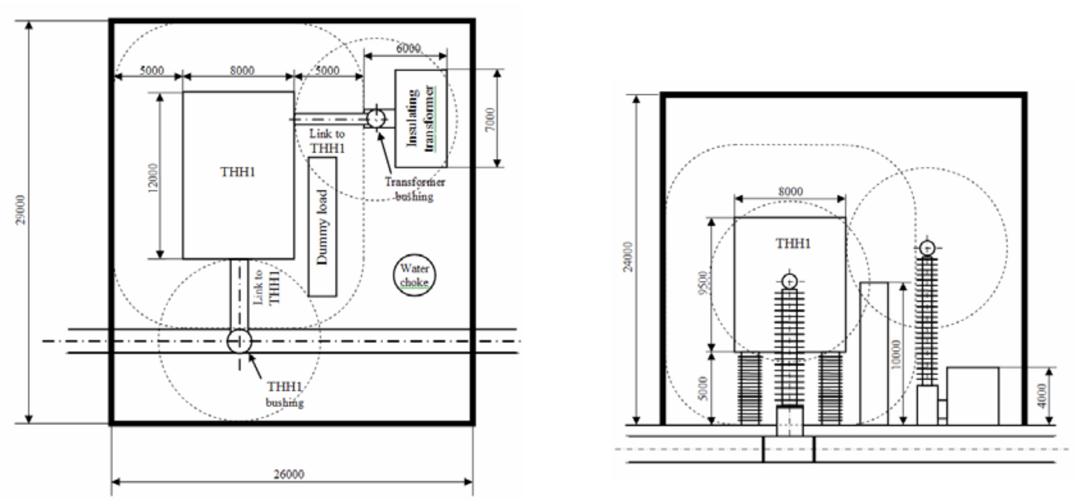

Fig. 6.12 Plan (left) and Front (right) view of the High Voltage Hall

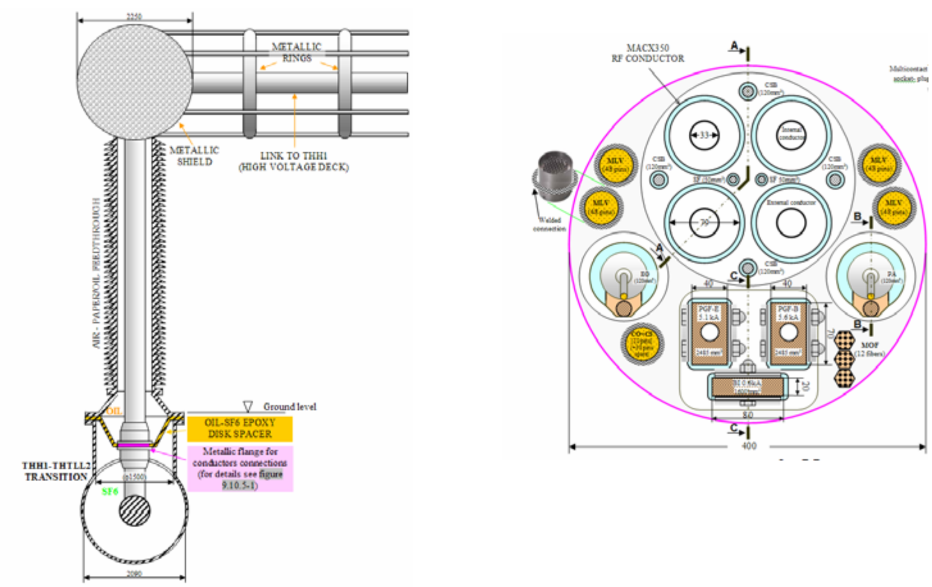

a) b)

Fig. 6.13 1MV feedthrough: a) side view, b) transition cross-section in correspondence to the disk spacer flange

6.1.2 Neutral Beam Test Facility

The studies and design activity on the Test Facility systems and components has been performed in the framework of the contract EFDA/ 06-1426, including buildings and their civil plants, cooling and cryogenic systems, power station adaptation, control systems, licensing and quality assurance. The actions required for the procurement of the most urgent components, in line with the goal to start experiments with the RF source test bed at the end of 2010, have been activated and the contracts with external design offices placed. Some delay in these activities during 2007 was due to late availability of information from ITER concerning the NBI layout.

6.1.2.1 NBTF buildings and civil plants

On the basis of a first assessment of the space necessary to host the plants and of the available area inside the National Research Council Area in Padova, a preliminary layout of the NBTF buildings and plants has been developed, as shown in Fig. 6.14.

The buildings include the main NBI hall with the semi-movable neutron screens, the HV power supply hall which contains the 1 MV HV deck, the building for the low voltage power supplies and control rooms, the auxiliary plant (cooling, cryogenic and gas systems) halls, the RF source (for heating and diagnostic beam) halls with their power supplies and control rooms. Further areas host the cooling towers and the HV transformers. The main constraint in the layout is due to the 1 MV SF_6 transmission line, which represents a rigid connection between the HV transformers, HV deck and the injector; for all these systems the same layout as in ITER must be maintained.

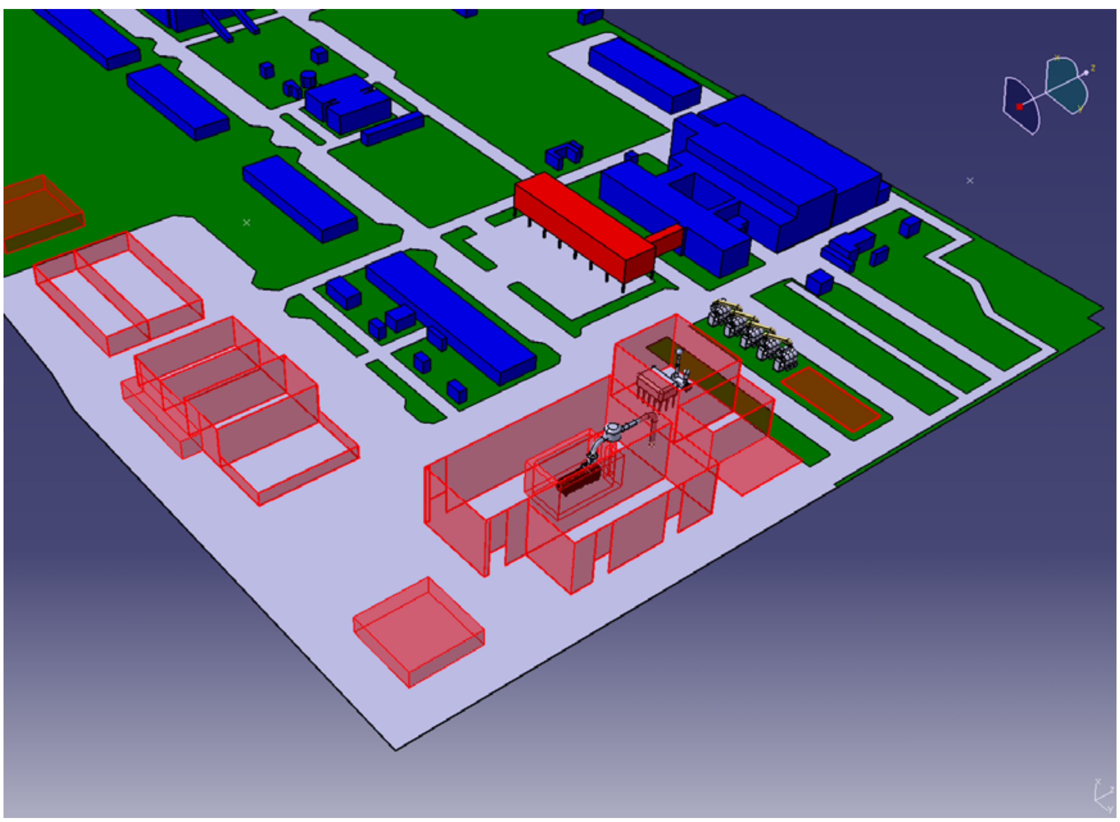

Fig. 6.14 The preliminary layout of the NB Test Facility

6.1.2.2 The cryogenic plant design

The NBTF Injector is equipped with a cryosorption cryogenic pump which needs a cryogenic system for operation.

During 2007, the following activities have been carried out for the design of the NBTF cryoplant and the associated cryogenic process flow:

- design of the External Cryogenic System (ECS);
- conceptual design of the Proximity Cryogenic System (PCS).

The ECS consists of 2 independent systems:

- a 4.5 K cryosystem to cool the cryopanels;
- a 80 K refrigeration module based on a Brayton cycle which is dedicated to the cooling of shields and baffle.

The PCS distributes the refrigerant to the cryopanels and to the chevron baffles. It consists of a Distribution Valve Box (DVB) and of cryogenic piping up to the cryopump interface.

With reference to the ECS, the Technical Specifications for each system have been defined. They state the requirements for the design, manufacture, inspection, installation at Consorzio RFX, commissioning and performance tests of the system in the NBTF. The final data concerning the Cryopump heat loads are not yet available and therefore some of the technical aspects in the definition of cryogenic systems are still open.

Concerning the PCS, the evaluation of different design solutions has been carried out, but the final layout has to be defined. The different alternatives are being assessed in view of achieving the highest flexibility in the system and to meet the requirements of different operative modes with different configurations.

The development of the control and supervision system of the cryoplant has been also started. The solution considered up to now relies on UNICOS (UNified Industrial COntrol System). This is the standard nowadays commonly used at CERN for its cryogenic equipment (e.g. the Large Hydron Collider). It is characterized by a modular and object-oriented structure, that covers both the control (Programmable Logic Controllers) and the supervision layers. The study of the PCS control system has been initiated according to the UNICOS principles: the PCS scheme has been logically divided into modular blocks that represent process control objects inside the control system.

6.1.2.3 The NBTF control systems

The preliminary architecture of the NBTF control system has been defined. Analyses on the NBI plant system have been carried out based on both established and evolving ITER documentation, such as the ITER NBI (2001 DDD5.3 Neutral Beam H&CD) and CODAC baselines (1998 DDD4.5),

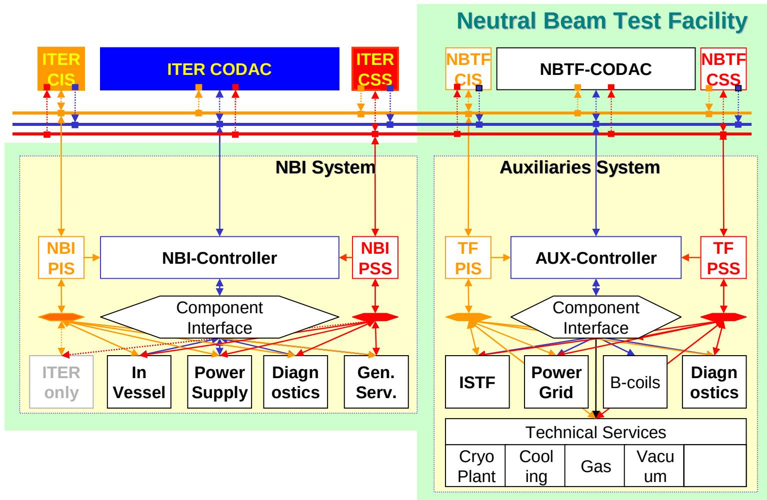

Fig. 6.15 Functional breakdown of ITER neutral beam test facility.

the current design status of the NBI power supplies, diagnostics and in-vessel components and, finally, the status of the ITER CODAC design (Document for the In-Fusion review of the conceptual design of ITER CODAC) and of the instrumentation and control specifications (Plant_Control_Design_Handbook_27LH2V_1_0.doc).

The NBI will be operated through an integrated handling system, referred to as NBI Control, Interlock and Safety System. It will be structured in three tiers, called NBI-Control System, NBI Plant Interlock System (NBI-PIS) and NBI Plant Safety System (NBI-PSS). The NBI-Control System will provide supervisory control, plant control/monitoring and data acquisition for the NBI. The NBI-PIS will be responsible for the coordinated, system-wide protection of the NBI plant system, whereas the NBI-PSS will guarantee the coordinated, system-wide safety of personnel and environment. The separation in three tiers of control, interlock and safety reflects the ITER breakdown structure and corresponds to an approach which is common to both IEC 61508 (non-nuclear) and IEC 61513 (nuclear). The NBTF Control, Interlock and Safety System will also be structured in three equivalent tiers.

A hierarchical functional breakdown, defining systems and subsystems, has been proposed for the NBI and NBTF control systems as shown in fig. 6.15.

A first set of functional and non-functional requirements for the NBI and NBTF control systems have been proposed, including a tentative estimate of the control system design parameters, such as max sampling frequency, number of channels and data throughput. Table I reports a summary of the non-functional requirements for the NBI/NBTF control system.

Table I: NBI/NBTF-Control System requirements

Type	**Quantity**
Sampling frequency	< 5 MHz
Time resolution/precision	<200/50 ns

Nr. of input analogue channels (NBI)	< 1000
Nr. of input analogue channels (NBTF)	< 3000
Control points	10,000 – 30,000
Data acquisition throughput	< 200 MB/s
Data storage per pulse	< 20 GB
Data storage per year	< 60 TB

A preliminary architecture has been outlined to reflect the functional breakdown of the system with the aim to ease integration of the neutral beam injector at the ITER site. Each subsystem will include a slow controller (cycle time > 10 ms), a fast controller if required (cycle time < 10 ms) and a data logger. The controllers are in charge of the reliable operation of the subsystems and will be implemented by using industrial solutions with high proven reliability. The data logger will record data according to their sampling frequency requirements, without responsibility for reliable operation.

The NBI and AUX controllers will supervise the NBI and the Auxiliaries subsystems, respectively. They will share hardware and software technologies. The advantage of this modular approach is that cost for development and prototyping is minimized and integration is easier.

The NBTF Control System will provide a subset of functionalities that ITER-CODAC will provide at the ITER site. It will be interfaced to the system level through the same communication system used by ITER-CODAC to ease integration of NBI into ITER-CODAC.

6.1.2.4 Quality Assurance

As per contract EFDA/06-1426, deliverable 4.13, a quality assurance system has been designed, ready to be implemented, "for the procurement contracts and for the construction of the test facility".

ISO 9001 requirements are at the basis of the system; some "best-practices" have been added, such as FMEA, Problem Solving, competence management, risk management, and other tools also used in project management.

A draft of the documents describing the quality assurance system was sent to EFDA at mid 2007; EFDA comments have been analysed and the final system design is going to be sent to EFDA in January 2008.

At mid 2007, EFDA issued its quality and management requirements and in the second half of 2007 the contract EFDA/06-1499, related to Neutral Beam Injector (NBI) components, was also modified to incorporate those quality and management requirements. As a consequence, a quality plan was developed and applied to the deliverables related to the following 4 components: vessel, RF source, accelerator, power supplies.

This quality plan was completed, together with the related procedures, instructions and forms; the goal was not only to satisfy EFDA requirements but also ISO 9001 requirements. At the end of 2007 the implementation of the quality plan started; in January 2008 EFDA will also receive all the documentation related to this effort.

6.1.3 Accompanying activities

During 2007 Consorzio RFX has increased the efforts in accompanying activities aimed to contribute to R&D. In particular the activities focused on a new HV test facility and on modeling by developing new numerical codes aimed to study the physics of beam extraction and by acquiring existing codes to study thermal loads and pressure distribution in the accelerator.

6.1.3.1 HV test facility

The installation of a HV test facility at the University of Padova premises has been initiated: it will be ready for operation in 2008.

Basically, the experiment test bed consists of a vacuum vessel hosting two insulated electrodes; the vacuum system is based on cryo-pumps, capable to keep the pressure below 10^{-8} mbar; each electrode is fed by a HV power dc power supply, rated for ±400kV - 1mA: in this way the full voltage of 800 kV can be applied across the two electrodes, with a maximum voltage to ground for each electrode of 400 kV. In the first experimental campaign, insulation tests up to 600 kV are planned, using a smaller vacuum vessel with electrode gap up to 150 mm; in a second stage, tests will be carried out on a larger vacuum vessel, in which the electrode gap will be increased up to 300 mm.

The equipment is located inside a concrete screened area (7.60 x 4.30 m), designed to screen the X radiation produced by HV electrical insulation tests in vacuum under the following extreme operational conditions:

Voltage	Current	Hours/year
1000 kV	10 µA	10
1000 kV	1 µA	200
800 kV	20 µA	200
200 kV	300 µA	400

The HV facility is managed by a dedicated Control System. The vacuum system is controlled by a Programmable Logic Controller, in which all the procedures are implemented to control the vacuum quality and to automatically restore the vacuum after shutdown.

The HV power supplies can be operated under both current and voltage control; the current-voltage waveform and voltage-current measurements are exchanged via RS232 protocol through an optical fiber link.

The whole set of measurements (from vacuum system, from HV power supplies and from spectrometers and Xray detectors) are acquired and processed in real time. In this way a great flexibility in defining HV conditioning procedures is achieved, owing to the possibility of implementing feedback control.

The possibility to operate with gas (He or H_2) is also foreseen, in order to test at higher pressure (up to 10^{-4} bar).

The R&D program will mainly cover the issues related to the total voltage effect; in particular, investigation will be carried out on a new anode design concept - transparent anode [Spolaore] which would avoid breakdown due to localized hotspots: it must be pointed out that this problem is relevant not only for the SINGAP configuration, but also applies to the MAMuG configuration, where many vessel regions are directly facing the high potential cathode. Optimization of HV conditioning procedures will be also matter of investigation. Finally, this test facility will be suitable to verify the voltage withstand capability of insulator prototypes, electrode geometries and electrode surface treatments.

Presently, the screened area is ready and all the permissions to operate have been delivered. The auxiliary systems (water and gas supplies, electrical power supply, crane) have been completed as well. The vacuum system is presently under commissioning; at the end of January 2008 the HV facility will be ready to operate. The detailed R&D program for 2008 is under preparation.

6.1.3.2 Numerical modelling

a) Beam formation

The development of a two-dimensional (2D) selfconsistent model to study the formation of a beam of negative ions is in progress. This model describes the trajectories of negative ions and electrons from the sheath region, where ions can be assumed superthermal, to the first acceleration gap, with a space resolution of the order of the Debye length. A continuous map of particle orbits or rays (efficiently generated by interpolation) is used to improve the traditional discrete ray tracing. Plasma presheath (where ions are slowly accelerated) is replaced by a nonlinear boundary condition, according to the classical 1D theory. The model is a stationary 2D model.

All simulation steps are coded for execution with COMSOL Script, an environment adding a powerful programming language to the solvers of nonlinear PDE and graphics, from COMSOL Multiphysics. In Fig. 6.16 an example is shown of preliminary results of negative ion and electron trajecories obtained in a test geometry. The initial tests confirm that the model can perform an efficient and fast self-consistent computation of negative ion trajectories. Work is in progress to optimize the model and to apply it to experimental configurations. A preliminary result is a non uniformity of the meniscus curvature near the extraction edge, at least for simple extraction holes. Moreover, collisional transport in a magnetized presheath was studied with a correlation based

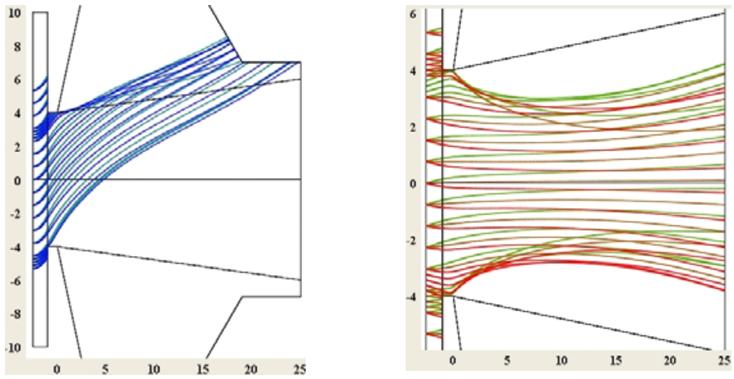

Fig. 6.16 Trajectories (rays) of e and H^- at last iteration; for graph visibility, only first ray refinement is shown.

theory.

b) Other codes

Under contract EFDA/05-995, Task 3, the Russian Federation has developed and adapted for modern ITER NBI and ITER Test Facility applications the three codes, PDP (Power Deposition Profiles), BTR (Beam Transport and Reionisation) and MC GF (Monte Carlo Gas Flow). These codes describe different substantial features of the neutral beam injectors. In particular, the PDP code provides straight trajectory analysis of the beam of neutral particles emerging from a prescribed set of apertures on the grounded grid (GG) of the accelerator. On any surface exposed to the beam, it calculates the power contribution from every beamlet aperture, taking into account beamlet intensity, divergence, aim, misalignment and relative core/halo ratio.

The BTR code studies the transport of the negative, positive and neutral components of the beam, in prescribed profiles of electro-magnetic fields and gas density inside the injector. Small fractions of each beamlet are traced (classical dynamics) from the GG till the first surface along the trajectory. The code considers power deposition due to neutrals and negative ions from beam source and neutraliser, positive ions from the neutraliser and from the reionisation of fast atoms in collisions with background gas molecules. Electrons can also be traced.

The MC GF code provides the gas density profile within the injector and accounts for the following gas sources: gas flow from beam source (external parameter), neutraliser gas flow providing the required gas target thickness for negative ion neutralization, and gas release due to ion recombination and neutral impact on beam line components (including dependence on surface temperature, particle energy distribution in collisions with wall etc.). The gas conductance to the cryopumps located along the beam vessel walls is also computed.

Concerning these codes, during 2007 RFX has attended the various meetings dedicated to discussion and tests prior to the acceptance by EFDA. Intermediate versions of the codes are present in RFX; the final versions are due soon.

CEA Cadarache has developed the code Electrostatic-Accelerator Monte Carlo Code (EAMCC) for the analysis of the physical phenomena occurring in the accelerator region. EAMCC solves the three-dimensional relativistic equation of motion of charged particles in the presence of prescribed electrostatic and magnetic fields and density profile. The code simulates the effect of collisions with grids and residual background gas and follows the corresponding secondary particles. The results include the power and current deposited on each grid, the back-stream of ions and the divergence of the transmitted beam.

The EAMCC code has been acquired by RFX together with some ancillary codes, dedicated to a rough computation of the profile of magnetic fields, electrostatic potential, particle density as well as to the post-processing of the results.

6.2.1 ITER Magnetic Diagnostics

The ITER magnetic diagnostics must provide essential information to be used both for plasma diagnostic purposes, and as feedback signals for the machine control loops. Some sensors must be installed in a hostile environment, characterized by severe neutron irradiation and plasma heat loads, which can reduce the sensor lifetime (due to mechanical and electrical damage) and also generate undesired DC signals, which might compromise the accuracy of the measurements obtained by time-integration.

Consorzio RFX has been working on design studies for ITER magnetic diagnostic since 2003 in the framework of several EFDA Tasks [Chitarin07a]. The activities carried out during 2007 were mainly dedicated to the advancement of the design of in-vessel electromagnetic sensors (essentially pick-up and Rogowski coils) and to the development of an R&D programme on magnetic pick-up coil prototyping. In this period two EFDA Tasks started in 2006 were completed (TW5-TPDS-DIASUP5 and TW5-TPDS-DIADEV) and two further tasks have been initiated and developed (TW6-TPDS-DIADES5, TW6-TPDS-DIASUP12).

The design of the halo sensors for the blanket modules has been developed and reviewed by way of suitable thermal and electric analyses. A design solution proposed by the ITER team for the halo sensors of the divertor modules has also been assessed by means of proper mechanical analyses. The procedure for the reconstruction of the halo current distribution on the blanket modules on the basis of the measurements obtained on the instrumented modules has also been developed, implemented and tested with virtual measurements [Chitarin07b].

The R&D work consisted of the manufacture and test of some prototypes of in-vessel tangential coils, with the aim of assessing the feasibility of a new concept based on a winding pack of ceramic coated conductor, insulated with liquid ceramic filler (fig.6.17), alternative to mineral insulated cable, presently proposed in the ITER reference design. The task was carried out by RFX, taking advantage of the experience gained with previous similar projects developed for RFX and JET, so acquiring new competence on design concepts alternative to mineral insulated cable. With respect to the originally foreseen work-plan, the tests carried out on the prototypes were limited by the unreliability of the ceramic coated wires supplied by two different producers, which both exhibited very poor electrical insulation, at a level that was unacceptable for the proposed applications. Nevertheless, the tests performed gave confidence on the feasibility of the impregnation process with fluid ceramic, even though some open issues indicated the need of further tests on this set-up and suggested to explore further design concepts [Peruzzo07a, Peruzzo07b].

Fig.617 prototype of pick-up coil impregnated with fluid ceramic.

6.2.2 *ITER core LIDAR Thomson scattering*

RFX has participated to a cluster of EU Fusion Associations, coordinated by UKAEA, to develop the specifications of the ITER core LIDAR diagnostic. The EFDA task, which will be concluded in early 2008, asked to develop a project plan for the full implementation of the diagnostic, to address the most urgent design issues and to re-evaluate the diagnostic performance. The areas of responsibility by RFX included: calibration issues, assessment of laser and detector technology, and contribution to optics design in relation to calibration and detector choices.

In particular RFX has investigated high efficiency high speed detector options in the near-IR, such as detectors based on the transferred-electron (TE) III-IV InGaAs/InP photocathode. The need for a detector with adequate sensitivity in the 850-1060 nm wavelength range has been recognized. Such a detector would permit to use a Nd:YAG or Nd:YLF laser system operating at the fundamental wavelength λ=1.06 μm, as the primary laser source, instead of the less efficient Ti:sapphire or 2nd harmonic Nd:YAG systems, with clear benefits in terms of available energy, repetition rate and reliability. A detector that combines sufficient sensitivity in this wavelength range with the other characteristics necessary for the LIDAR TS (primarily speed of response and active area) presently does not exist, but it may be developed by reasonable advancements of the transferred electron (TE) InGaAs/InP photocathode technology pioneered by INTEVAC.

The state of this technology has been reviewed from the available literature, with reference to a possible application in the ITER LIDAR TS. The review of the TE photodetectors showed that this technology may fulfill the requirements for IR sensitive detectors in the ITER LIDAR TS, provided a limited amount of technological advancements are undertaken. Contacts have been taken with

INTEVAC, the leading manufacturer, for a possible demonstration prototype detector. Their proposal is at present under consideration.

The other main task of RFX was to assess the possible calibration methods. The three main methods which had been identified so far have been reviewed with particular attention to the more recent diagnostic design changes and to the development of these and similar methods for calibration of other ITER optical diagnostics.

Relative calibration of spectral channels sensitivity is usually performed with a white light source illuminating all or, more frequently, only part of the collection optics. Because of in-vessel optics degradation, spectral transmission rapidly changes and frequent recalibration is required, but an internal calibration source is difficult to place. The original ITER LIDAR design suggested as preferred solution to use TS measurements from two lasers with different wavelength, which do not require any in-vessel tool and provide both T_e and the relative sensitivities. T_e is calculated from the ratio of TS signals without requiring the knowledge of the relative sensitivities. In addition, the spectral transmission curve is obtained from comparison of measured and expected signals. Restrictions on usable wavelength combinations apply, as a spectral interval with significant scattered signals from both lasers is required to get T_e, while the full spectral range of interest has to be covered by at least one laser to obtain the spectral transmission.

Since the present ITER requirement asks for measuring higher T_e (< 40 keV) than originally assumed, we started revising the proposal, especially the optimum laser combination. Considering that Nd:YAG @ 1064 nm is presently being considered as a good candidate for TS measurements, possibly complemented by doubled Nd:YAG @ 532 nm for lower T_e, two combinations look promising for the dual laser calibration and require further assessment: Nd:YAG @ 1064 nm + Nd:YAG @ 532 nm or Nd:YAG @ 1064 nm + ruby @ 694 nm.

We also investigated other calibration methods, based on retroillumination through the collection optics of a diffuser or a microretroreflector array positioned in front of the plasma facing mirror.

6.3 JT-60 SA

In the framework of the Broader Approach agreement between Europe and Japan, a new plasma experimental device (Satellite Tokamak), named JT60_SA, is being designed and will be installed in Naka, Japan. JT60-SA will be a tokamak with superconducting TF and PF magnets capable of confining high temperature plasmas (current up to 5.5 MA) for 100 s with heating and current drive power up to 41 MW. This device will offer high flexibility in plasma shape and divertor configuration with plasma aspect ratio down to 2.6, elongation up to 1.83, triangularity up to 0.6, single and double null divertor . The construction is expected to require 7 years.

The power supplies will be provided by Europe and Consorzio RFX, in particular, is in charge for the procurement of the “Quench protection system” and of the “In vessel fast control coil power supply”.

During the first half of 2007, RFX continued in contributing to the revision of the JT60-SA Conceptual Design, performing in particular analyses of the JT-60SA poloidal circuit operation both in normal and fault conditions; these activities were concluded in May.

6.3.1 RFX and JAEA joint work to analyze the JT-60SA poloidal circuit operation both in normal and fault conditions

The joint work between Consorzio RFX and JAEA was performed in Naka from the 15th October to 7th December 2007; it was organized in four Tasks. Task 1 was aimed at working out a complete model of the JT-60SA poloidal circuits including the superconducting coils (CS and EF coils), the in-vessel coils, the vacuum vessel, the stabilizing plates and the plasma.

Task 2 was addressed to update the description and the sequences of the operation of the poloidal circuit components in normal conditions on the basis of the present circuit configuration and plasma scenarios.

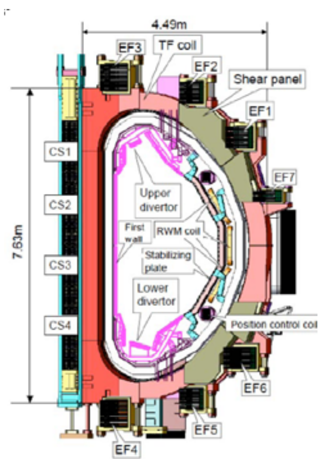

Fig. 6.18 JT-60SA cross section

The target of Task 3 was the analysis of the effects of the plasma disruption and faults in terms of overcurrents in the coils and overvoltages applied across them on the basis of the present machine configuration, plasma scenarios and 78 different snapshots. The fault conditions analyzed with the model worked out in Task1 were the quench, the intervention of a Quench Protection Circuit (QPC) pyrobreaker, and the operation of the QPC of a single circuit in case of protection request different from quench. The sequence of operations of all the poloidal PS component in case of fault were studied and the intervention request of the QPCs in cases different from quench were identified.

Task 4 dealt with the assessment of the specification data for the design of the QPC on the basis of the results of the previous Tasks, which however can not be finalized now being a new JT-60 SA machine design revision still in progress. Nevertheless, the main result is that the tools for the analyses are completed and checked, therefore once the machine configuration will be frozen, the reference scenario for the PS design fixed and the worst snapshots identified, it will be possible to complete easier the work.

6.3.2 Studies to outline the conceptual design of the Quench Protection Circuits (QPC)

During 2007, RFX developed the Conceptual Design of the "Quench Protection System"; the first analyses were devoted to the identification of the technical solution: Vacuum Circuit Breaker (VCB) or semiconductor. No European VCB is available for the required rating (26 kA cw); therefore a mechanical bypass switch in parallel should be necessary, like in the ITER design. These protection units have to sustain steady state currents around 20 kA and interrupt the current diverting it into resistors with reapplied voltage of the order of 5 kV. Once discarded a design solution based on semiconductors only, highly desirable (being almost maintenance free), but affected by high level of losses in normal operation, a new design solution was devised and studied. It is based on a Hybrid Circuit Breaker (CB) composed of a mechanical switch to handle the current in steady state operation paralleled to a static circuit breaker to interrupt the current [Piovan07].

6.3.3 Experimental tests to assess the feasibility of the QPC Conceptual Design

Experimental tests were performed at RFX to assess the feasibility of the QPC Conceptual Design described above. They were in particular addressed at verifying the capability of the Integrated Gate Commutated Thyristors (IGCTs) selected like static CB to assure a safe turn-on with very low voltage applied. The particular operating condition occurring in this application is not quite common in standard industrial applications, therefore it required to be investigated. The tests were concluded with very satisfactory results, which however are still not documented.

6.3.4 First work to identify the main input data for the design of the "In vessel fast control coil power supply"

The design of the RWM control system in JT-60SA has been not assessed so far and studies are still in progress on the main targets of this system, which could also be extended to the ELMs suppression. Recently, a possible collaboration between RFX and JAEA has been proposed with the aim of contribuing to outline the conceptual design of this system, with the consequent definition of the input data for the Procurement of the Power Supply System.

[Piovan07] R. Piovan, E. Gaio, L. Novello, Performance Analysis of a Hybrid IGCTs-Mechanical Dc Circuit Breaker for Quench Protection of Superconducting Magnets, Proc. of 22th SOFE, Nov 2007.

[Chitarin07a] G. Chitarin, L. Grando, N. Pomaro, S. Peruzzo, C. Taccon, "Design developments for the ITER in-Vessel equilibrium pick-up coils and Halo current sensors", Fusion Engineering and Design 82 (2007) 1341–1347

[Chitarin07b] G. Chitarin, E. Alessi, M. Cavinato, S. Dal Bello, R. Delogu, S. Peruzzo, C. Taccon, "Design Study of the ITER magnetic diagnostic: in-Vessel pick-up coils, Blanket Halo sensors and Divertor Halo sensors, numerical model of Halo currents" Final Report EFDA Contract 05-1247 Deliverable 2, RFX Ref. SM-NT-288, EFDA Ref. TW5-TPDS-DIASUP5, 22/6/2007

[Peruzzo07b] S. Peruzzo, G. Chitarin, S. Dal Bello, R. S. Delogu, L. Lotto, A. Sottocornola, C. Taccon, "Development and Testing of in-Vessel Equilibrium Pick-up Coils for ITER", Proceedings of the International Workshop on Burning Plasma Diagnostics, Varenna, Italy, September 24 - 28, 2007.

[Spolaore] P. Spolaore et al. IEEE Trans. DIE, 4 (1997) 389

7. COLD PLASMA APPLICATIONS

7.1 Bipolar low-power plasma source at atmospheric pressure

A new source for the generation of low power (<2W) nonthermal (nonequilibrium) plasma at atmospheric pressure has been developed. The device mainly consists in two coaxial metallic tubes each electrically connected to two gridded electrodes at one end, as shown in Fig. 7.1. A radiofrequency (RF) voltage of some hundreds of volts (up to 600 V peak-to-peak) is applied between the two electrodes in order to ionize a working gas (helium or argon) flowing in the inner tube and partially mixed with air.

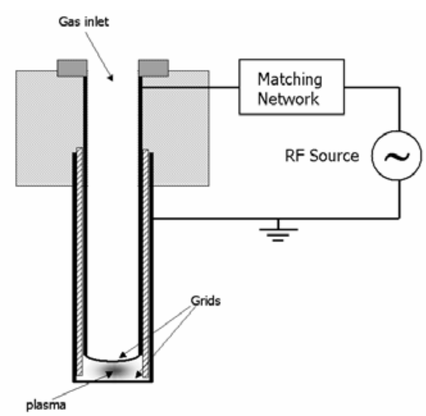

Fig.7.1: Schematic of the low-power atmospheric plasma source.

A cold plasma, with an ion temperature close to the ambient temperature, is thus produced in the inter-electrode region, while the chemical active species (mainly free radicals) generated by the plasma are dragged outside of the device by the gas flow. The device is substantially different from that developed in 2006, which was similar to the one proposed by other groups [Stoffels03] mainly consisting in a single RF powered electrode (a tungsten needle), since in the new device the plasma is produced and confined in a volume delimited by the two metallic grids (see Fig. 7.1). The external grid is grounded, in order to avoid the formation of electric arcs towards the surface to be treated. This is an important care in order to avoid thermal damage to the substrate, as this kind of plasmas is suitable for biological, biomedical and fine surface treatment applications.

In collaboration with the Institute of Ophtalomology and the Department of Microbiology and Histology of the University of Padova, a set of preliminary tests has been performed on cultivated bacteria, porcine corneas with induced bacterial ulcer and cultivated cells in order to test the antibacterial efficacy of this kind of plasmas and their ability of treating living substrates without damaging them. The first encouraging results in the treatment of Escherichia Coli, with a decimal reduction time of the number of colonies of about one minute, are shown in fig. 7.2.

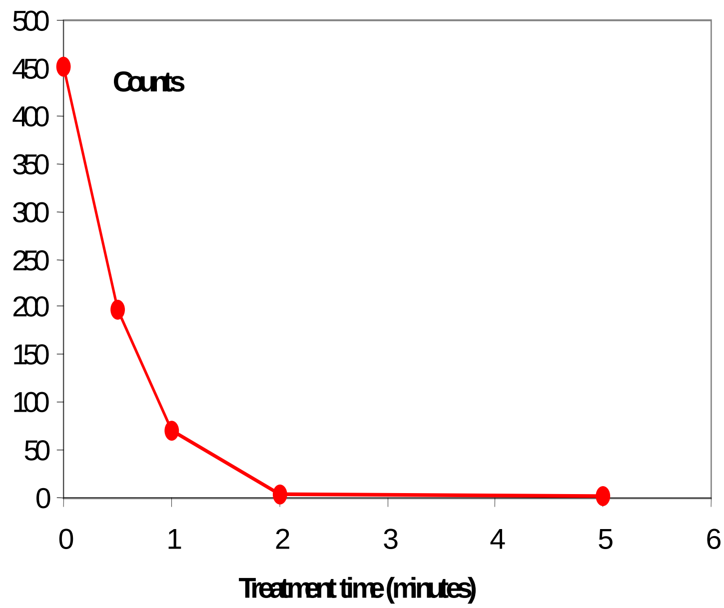

Fig.7.2 Number of E. Coli colonies as a function of the exposure time (t=0 refers to the control case).

An Italian national patent request for the device has been jointly filed by Consorzio RFX and the University of Padova [Leonardi2007].

7b Magneto Plasma Dynamic thrusters

An extensive set of experiments has been performed by Consorzio RFX, in collaboration with Alta/Centrospazio (Pisa), in order to confirm and extend previous results [Zuin06] on the possibility of controlling large-scale MHD instabilities in the plasma channel of a Magneto Plasma Dynamic (MPD) thruster for space applications. The development of MHD instabilities when a critical current level is exceeded is indeed responsible for the loss of efficiency and unstable behavior of this kind of devices. MPD thrusters operate as plasma accelerators by means of the interaction of a current induced in a plasma by the application of a potential difference between two coaxial electrodes, an inner cathode and an anode, and a magnetic field, which can be induced by the plasma current itself or be a combination of the self-induced and of an externally applied one, B_{ext}..

The control technique is based on a reconfiguration of the thruster geometry obtained by means of the insertion in the inter-electrode region of an insulating plate, which divides the plasma channel, intercepting the helical current components produced by the instability. A variety of geometries of the insulating plate have been tested, and the efficacy of each of them in different experimental conditions has been investigated. We observed that, while large plates, extending outside of the inter-electrode region, exhibit a remarkable capability of reducing magnetic fluctuations but have a detrimental effect on the power balance of the discharge, small insulating plates placed in front of the cathode region, or even located in the outer radial positions, are effective in decreasing plasma fluctuations and power losses at high B_{ext} conditions. The effect at low B_{ext} is still not that clear, but in discharges with high B_{ext}, an almost doubled thruster efficiency has been obtained.

[Leonardi2007] A. Leonardi, V. Deligianni, E. Martines, M. Zuin, R. Cavazzana, G. Serianni, M. Spolaore, Domanda di brevetto per invenzione industriale n. RM 2007 A 521.

[Stoffels03] E. Stoffels-Adamowicz, I. E. Kieft, R. E. J. Sladek, Journal of Physics D: Applied Physics, **36**, 2908, (2003).

[Zuin06] M.- Zuin *et al*, Appl. Phys. Lett. **89**, 041504 (2006).

8 LIST OF COLLABORATIONS

A list of the main collaborations active in 2007 follows. Their scientific results were already reported in the previous chapters. This list does not include the collaborations developed under EFDA.

8.1 Collaborations with other RFP laboratories

- Joint experimental campaign for comparison of performances between MST and RFX in RFX mod
- Use of a "multicolour" and "two colours" SXR tomography in MST, University of Wisconsin, Madison
- SXR measurements in PPCD and Pellet Injected PPCD plasmas in MST, University of Wisconsin, Madison
- Pellet experiments on TPE-RX, AIST Tsukuba.
- Edge turbulence statistical analysis in TPE-RX, AIST Tsukuba

8.2 Collaborations with Tokamak laboratories

- MHD studies on ASDEX-Upgrade, IPP Garching
- TAE reconstruction by SXR tomography on ASDEX-Upgrade, IPP Garching
- RWMs active stabilization for FT3
- Diagnostics for FT3
- Electrostatic turbulence control experiments in CASTOR, IPP Prague
- Comparison of L and H-mode edge turbulence by GPI in NSTX, PPPL Princeton
- Statistical edge turbulence analysis in Alcator C-mod, PPPL Princeton

8.3 Collaborations on Theory

- Development of statistical tools for turbulence investigation, Dipartimento di Fisica, Università della Calabria
- Numerical simulations of VDEs in tokamaks, Courant Institute, New York; PPPL, Princeton and SAIC, San Diego
- Effect of toroidicity and shell discontinuities on RWMs, Chalmers Institute of Technology, Goeteborg, and University of Cassino
- Mode locking and plasma control, GA, San Diego
- Orbit code developments, PPPL, Princeton

- Edge modeling, RISO, Roskilde
- MHD modeling, LANL, Los Alamos.

8.4 Other Collaborations

- Collaboration on polarimetry, University College Cork

9. EDUCATION AND INFORMATION TO THE PUBLIC

In 2007 Consorzio RFX finalized the organization of the "Joint Research Doctorate in Fusion Science and Engineering" between the University of Padova and the Universidade Tecnica de Lisboa (Instituto Superior Tecnico). In particular a specific Agreement was signed by the Rector of the Padova University and the President of IST, in September 2007, to activate this joint doctoral degree for five academic years, to guarantee the completion of three doctoral cycles (lasting three academic years each). The public selection process for the admission (15 places) to the first three year's cycle of doctorate was performed in Padova and Lisbon at the end of November. The first doctoral cycle will start on 2nd January 2008.

In parallel, the organization activity of an "European Interuniversity Doctoral Network on Fusion Science and Engineering" among the same two universities and the Ludwig Maximilian University (LMU) of Munich progressed and the final document of Agreement was approved by the Academic Senate of Padova University on 11 Dicember 2008. This Network is aimed at including in the organization of the joint doctoral course Padova-Lisbon also the students of LMU, in order to offer to all three university students a jointly organized and implemented training program, which will create a new high level experts group in the field of Fusion Science and Engineering.

The other educational activity of Consorzio RFX on fusion related disciplines continued with a significant effort also in 2007.

In particular RFX professionals were in charge of 15 postgraduate students of the PhD courses on Physics, Energy Research and Electrical Engineering, of 5 postgraduate students of the annual postgraduate Master course on Engineering and Physics of Plasmas and of about 15 undergraduate students preparing their graduation thesis on fusion related subjects.

Nine regular courses of the Padova University were given by teachers belonging to Consorzio RFX. Four of them have been given at the Faculty of Engineering, in particular "Plasma Physics", "Plasma and Controlled Thermonuclear Fusion", "Industrial Applications of plasmas", "Energy Technology and Economics", and five at the Faculty of Sciences, in particular "Introduction to Plasma Physics", "Experimental and Numerical Methods for Fluid Dynamics and Plasma Physics", "Thermonuclear Fusion and Plasma Physics Applications", "Fluid and Plasma Physics" and "Electrodynamics".

At the Postgraduate level, the annual Master course on "Engineering and Physics of Plasmas" of the Faculty of Engineering was organized for the fourth time and about 300 lessons were given by teachers belonging to Consorzio RFX.

As far as public information is concerned, apart from the permanent organization of visits to the RFX site (that has significantly improved reaching about 2.000 visitors in 2007), Consorzio RFX has the responsibility, under Contract EFDA/03-1056, of running and improving the Fusion Expo. Besides the organization of the exhibitions with the support of the Associations hosting the events, the task included the maintenance and repair of the material, the development of new items where needed, as well as the regular update of the contents according to the last developments.
A full revision of the exhibition, including new content presentation and layout, was also continued in view of its completion in 2008.

10. LIST OF PUBBLICATIONS 2007

International and national journal

R.1. R Cavazzana, G Serianni, P Scarin, M Agostini, N Vianello, Y Yagi, H Koguchi, S Kiyama, H Sakakita and Y Hirano: " Investigation of plasma edge turbulence using a gas-puff imaging system in the reversed-field pinch device TPE-RX"
Plasma Phys. Control. Fusion 49 (2007) 129–143

R.2. P. Zanca: "Self similar current decay experiment in RFX-mod"
Plasma Phys. Control. Fusion 49 (2007) 113-118

R.3. A. Alfier, R. Pasqualotto: "New Thomson scattering diagnostic on RFX-mod"
Rev. of Scien. Instrum. 78, 013505 _2007_

R.4. P Martin, L Marrelli, A Alfier, F Bonomo, D F Escande, P Franz, L Frassinetti, M Gobbin, R Pasqualotto, P Piovesan, D Terranova and the RFX-mod team: "A new paradigm for RFP magnetic self-organization: results and challenges"
Plasma Phys. Control. Fusion 49 (2007) A177–A193

R.5. M. Garcıa-Mu˜noz, P. Martin, H.-U. Fahrbach, M. Gobbin, S. G¨unter, M. Maraschek, L. Marrelli, H. Zohm and the ASDEX Upgrade Team: "NTM induced fast ion losses in ASDEX Upgrade"
Nucl. Fusion 47 (2007) L10–L15

R.6. Leonardo Giudicotti and Matteo Brombin: "Data analysis for a rotating quarter-wave, far-infrared Stokes polarimeter"APPLIED OPTICS _ Vol. 46, No. 14 _ 10 May 2007

R.7. P. Scarin , M. Agostini, R. Cavazzana, F. Sattin, G. Serianni, N. Vianello: "Edge turbulence in RFX-mod virtual-shell discharges", sJournal of Nuclear Materials 363–365 (2007) 669–673

R.8. R Behn, A Alfier, S Yu Medvedev, Ge Zhuang, R Pasqualotto, P Nielsen, Y Martin and the TCV team: "Edge profiles of electron temperature and density during ELMy H-mode in ohmically heated TCV plasmas"

Plasma Phys. Control. Fusion 49 (2007) 1289–1308

R.9. L. Frassinetti, D. Terranova, Y. Hirano, H. Koguchi, F. Auriemma, K. Yambe and H. Sakakita: "Cold Pulse propagation in a reversed-field pinch", Nuclear Fusion 47 (2007) 135-145

R.10. D. Terranova, L. Garzotti, B. Pégourié, H. Nehme, D. Frigione, S. Martini, E. Giovannozzi, O. Tudisco: "Pellet ablation and mass deposition in FTU: Analysis of vertical and low field side injection experiments" , Nucl. Fusion 47 (2007) 288–296

R.11. P. Zanca, D. Terranova, M. Valisa, S. Dal Bello: "Plasma wall interactions in RFX-mod with virtual magnetic boundary", Journal of Nucl. Mater 363-365 (2007) 733-737

R.12. T.C. Hender, J.C Wesley, J. Bialek, A. Bondeson, A.H. Boozer, R.J. Buttery, A. Garofalo, T.P Goodman, R.S. Granetz, Y. Gribov, O. Gruber, M. Gryaznevich, G. Giruzzi, S. Günter, N. Hayashi, P. Helander, C.C. Hegna, D.F. Howell, D.A. Humphreys, G.T.A. Huysmans, A.W. Hyatt, A. Isayama, S.C. Jardin, Y. Kawano, A. Kellman, C. Kessel, H.R. Koslowski, R.J. La Haye, E. Lazzaro, Y.Q. Liu, V. Lukash, J. Manickam, S. Medvedev, V. Mertens, S.V. Mirnov, Y. Nakamura, G. Navratil, M. Okabayashi, T. Ozeki, R. Paccagnella, G. Pautasso, F. Porcelli, V.D. Pustovitov, V. Riccardo, M. Sato, O. Sauter, M.J. Schaffer, M. Shimada, P. Sonato, E.J. Strait, M. Sugihara, M. Takechi, A.D. Turnbull, E. Westerhof, D.G. Whyte, R. Yoshino, H. Zohm and the ITPA MHD, Disruption and Magnetic Control Topical Group: "Chapter 3: MHD stability, operational limits and disruptions", (PROGRESS IN THE ITER PHYSICS BASIS)

R.13. C. Angioni, L. Carraro, T. Dannert, N. Dubuit, R. Dux, C. Fuchs, X. Garbet, L. Garzotti,C. Giroud, R. Guirlet, F. Jenko, O. J. W. F. Kardaun, L. Lauro-Taroni, P. Mantica, M. Maslov, V. Naulin, R. Neu, A. G. Peeters, G. Pereverzev, M. E. Puiatti, T. Pütterich, J. Stober, M. Valovi , M. Valisa, H. Weisen, and A. Zabolotsky: "Particle and impurity transport in the Axial Symmetric Divertor Experiment Upgrade and the Joint European Torus, experimental observations and theoretical understanding " Phys. Plasmas 14, 055905 (May 2007)

R.14. G Van Oost, V V Bulanin, A J H Donné, E Z Gusakov, A Kraemer-Flecken, L I Krupnik, A Melnikov, S Nanobashvili, P Peleman, K A Razumova, J Stoeckel ,V Vershkov, J Adamek, A B Altukov, V F Andreev, L G Askinazi, I S Bondarenko, J Brotankova, A Yu Dnestrovskij, I Duran, L G Eliseev, L A Esipov, S A Grashin, A D Gurchenko, G M D Hogeweij, M Hron, C Ionita, S Jachmich, S M Khrebtov, D V Kouprienko, S E Lysenko, E Martines, S V Perfilov, A V Petrov, A Yu Popov, D Reiser, R Schrittwieser, S Soldatov, MSpolaore, A Yu Stepanov, G Telesca, A O Urazbaev, G Verdoolaege, F Zacek and O Zimmermann: "Multi-machine studies of the role of turbulence and electric fields in the establishment of improved confinement in tokamak plasmas", Plasma Phys. Control. Fusion 49 (2007) A29–A44

R.15. Henry Gardner, Gabriele Manduchi "Design Patterns for e-Science", Springer Verlag

R.16 G. Serianni, R. Cavazzana, M. Agostini, Paolo Scarin, "2D Tomographic Imaging of the Edge Turbulence in RFX-Mod", Plasma and Fusion Research: Regular Articles, Volume 2, S1119 (2007)

R.17 G. Serianni, M. Agostini, R. Cavazzana, P. Scarin: "Application of 2D tomographic imaging techniques to edge turbulence in RFX-mod", Plasma Phys. Control. Fusion 49 (2007) 2075–2086

R.18 G Serianni, M Agostini, V Antoni, R Cavazzana, E Martines, F Sattin, P Scarin, E Spada, M Spolaore, N Vianello and M Zuin: "Coherent structures and transport properties in magnetized plasmas", Plasma Phys. Control. Fusion 49 (2007) B267–B280

R.19 D. F. Escande1,2 and F. Sattin: “When Can the Fokker-Planck Equation Describe Anomalous or Chaotic Transport?”, PRL 99, 185005 (2007)

R.20 G. Spizzo, R.B. White, S. Cappello: “Chaos generated pinch effect in toroidal confinement devices”, PHYSICS OF PLASMAS 14, 102310 _2007

R.21 M. Agostini, S.J Zweben, R. Cavazzana, P. Scarin, and G. Serianni, R. J. Maqueda, D. P. Stotler: Study of statistical properties of edge turbulence in the National Spherical Torus Experiment with the gas puff imaging diagnostic, PHYSICS OF PLASMAS 14, 102305 _2007

R.22 C. Angioni, L. Carraro, T. Dannert, N. Dubuit, R. Dux, C. Fuchs, X. Garbet, L. Garzotti, C. Giroud, R. Guirlet, F. Jenko, O. J. W. F. Kardaun, L. Lauro-Taroni, P. Mantica, M. Maslov, V. Naulin, R. Neu, A. G. Peeters, G. Pereverzev, M. E. Puiatti, T. Pütterich, J. Stober, M. Valovič, M. Valisa, H. Weisen, A. Zabolotsky, ASDEX Upgrade Team, and JET EFDA Contributors: “Particle and impurity transport in the Axial Symmetric Divertor Experiment Upgrade and the Joint European Torus, experimental observations and theoretical understanding”, PHYSICS OF PLASMAS 14, 055905 _2007_

R.23 P. Zanca, L. Marrelli, G. Manduchi and G. Marchiori: “Beyond the intelligent shell concept: the clean-mode-control”, Nucl. Fusion 47 (2007) 1425–1436

R.24 Predebon, R. Paccagnella: “Influence of slow particle dynamics on transport in stochastic plasmas”, PHYSICS OF PLASMAS 14, 082310 _2007

R.25 M Mattioli, G Mazzitelli, M Finkenthal, P Mazzotta, K B Fournier, J Kaastra and M E Puiatti: “Updating of ionization data for ionization balance evaluations of atoms and ions for the elements hydrogen to germanium”, J. Phys. B: At. Mol. Opt. Phys. 40 (2007) 3569–3599

R.26 P. Innocente, A. Alfier, L. Carraro, R. Lorenzini, R. Pasqualotto, D. Terranova and the RFX Team: “Transport and confinement studies in the RFX-mod reversed-field pinch experiment”, Nucl. Fusion 47 (2007) 1092–1100

R.27 D. Terranova, A. Alfier, F. Bonomo, P. Franz, P. Innocente, and R. Pasqualotto: “Enhanced Confinement and Quasi-Single-Helicity Regimes Induced by Poloidal Current Drive”, PRL 99, 095001 (2007)

R.28 R. Lorenzini, D. Terranova, F Auriemma, R. Cavazzana, P. Innocente, S. Martini, G. Serianni and M. Zuin “Toroidally asymmetric particle transport caused by phase-locking of MHD modes in RFX-mod” Nuclear Fusion **47** (2007), No 11, 1468-1475

R.29 R. Paccagnella, D. Terranova and P. Zanca: “Modelling and interpretation of MHD active control experiments in RFX-mod”, Nucl. Fusion 47 (2007) 990–996

R.30 S. Martini, M. Agostini, C. Alessi, A. Alfier, V. Antoni, L. Apolloni, F. Auriemma, P. Bettini, T. Bolzonella, D. Bonfiglio, F. Bonomo, M. Brombin, A. Buffa, A. Canton, S. Cappello, L. Carraro, R. Cavazzana, M. Cavinato, G. Chitarin, A. Cravotta, S. Dal Bello, A. De Lorenzi, L. De Pasqual, D.F. Escande, A. Fassina, P. Franz, G. Gadani, E. Gaio, L. Garzotti, E. Gazza, L. Giudicotti, F. Gnesotto, M. Gobbin, L. Grando, S.C. Guo, P. Innocente, R. Lorenzini, A. Luchetta, G. Malesani, G. Manduchi, G. Marchiori, D. Marcuzzi, L. Marrelli, P. Martin, E. Martines, A. Masiello, F. Milani, M. Moresco, A. Murari, L. Novello, S. Ortolani, R. Paccagnella, R. Pasqualotto, S. Peruzzo, R. Piovan, P. Piovesan, A. Pizzimenti, N. Pomaro, M.E. Puiatti, G. Rostagni, F. Sattin, P. Scarin, G. Serianni, P. Sonato, E. Spada, A. Soppelsa, G. Spizzo, M. Spolaore, C. Taccon, C. Taliercio, D. Terranova, V. Toigo, M. Valisa, N.

Vianello, P. Zaccaria, P. Zanca, B. Zaniol, L. Zanotto, E. Zilli, G. Zollinoand M. Zui~~n~~: "Active MHD control at high currents in RFX-mod", Nucl. Fusion 47 (2007) 783–791

R.31 V. Pericoli-Ridolfini, A. Alekseyev, B. Angelini, S.V. Annibaldi, M.L. Apicella, G. Apruzzese, E. Barbato, J. Berrino, A. Bertocchi, W. Bin, F. Bombarda, G. Bracco, A. Bruschi, P. Buratti, G. Calabrò, A. Cardinali, L. Carraro, C. Castaldo, C. Centioli, R. Cesario, S. Cirant, V. Cocilovo, F. Crisanti, G. D'Antona, R. De Angelis, M. De Benedetti, F. De Marco, B. Esposito, D. Frigione, L. Gabellieri, F. Gandini, E. Giovannozzi, G. Granucci, F. Gravanti, G. Grossetti, G. Grosso, F. Iannone, H. Kroegler, V. Lazarev, E. Lazzaro, M. Leigheb, I.E. Lyublinski, L. Lubyako, G. Maddaluno, M. Marinucci, D. Marocco, J.R. Martin-Solis, G. Mazzitelli, C. Mazzotta, V. Mellera, F. Mirizzi, G. Monari, A. Moro, V. Muzzini, S. Nowak, F.P. Orsitto, L. Panaccione, M. Panella, L. Pieroni, S. Podda, M.E. Puiatti, G. Ravera, G. Regnoli, F. Romanelli, M. Romanelli, A. Shalashov, A. Simonetto, P. Smeulders, C. Sozzi, E. Sternini, U. Tartari, B. Tilia, A.A. Tuccillo, O. Tudisco, M. Valisa, A. Vertkov, V. Vitale, G. Vlad, R. Zagórski and F. Zonca: "Overview of the FTU results" Nucl. Fusion 47 No 10 (October 2007) S608-S621

R.32 D.J. Den Hartog, J.-W. Ahn, A.F. Almagri, J.K. Anderson, A.D. Beklemishev, A.P. Blair, F. Bonomo, M.T. Borchardt, D.L. Brower, D.R. Burke, M. Cengher, B.E. Chapman, S. Choi, D.J. Clayton, W.A. Cox, S.K. Combs, D. Craig, H.D. Cummings, V.I. Davydenko, D.R. Demers, B.H. Deng, W.X. Ding, F. Ebrahimi, D.A. Ennis, G. Fiksel, C. Foust, C.B. Forest, P. Franz, L. Frassinetti, S. Gangadhara, J.A. Goetz, R.W. Harvey, D.J. Holly, B.F. Hudson, A.A. Ivanov, M.C. Kaufman, A.V. Kuritsyn, A.A. Lizunov, T.W. Lovell, R.M. Magee, L. Marrelli, P. Martin, K.J. McCollam, M.C. Miller, V.V. Mirnov, P.D. Nonn, R. O'Connell, S.P. Oliva, P. Piovesan, S.C. Prager, I. Predebon, J.A. Reusch, J.S. Sarff, V.A. Svidzinski, T.D. Tharp, M.A. Thomas, Yu.A. Tsidulko, M.D. Wyman and T. Yates: "Recent improvements in confinement and beta in the MST reversed-field pinch", Nucl. Fusion 47 No 9 (September 2007) L17-L20

R.33 M. Gobbin, L. Marrelli, P. Martin, R. B. White: "Ion and electron local transport inside single helicity islands in the reversed field pinch", Plasma Physics Laboratory, Princeton University, Princeton, New Jersey 08543, Phys. Plasmas 14, 072305 _2007_

R.34 R Behn, A Alfier, S Yu Medvedev, Ge Zhuang, R Pasqualotto, P Nielsen, Y Martin and the TCV team: "Edge profiles of electron temperature and density during ELMy H-mode in ohmically heated TCV plasmas", Plasma Phys. Control. Fusion 49 (2007) 1289–1308

R.35 L. Marrelli, P. Zanca, M. Valisa, G .Marchiori, A. Alfier, F. Bonomo, M. Gobbin, P. Piovesan, D. Terranova, M. Agostini, C. Alessi, V. Antoni, L. Apolloni, F. Auriemma, P. Bettini, T. Bolzonella, D. Bonfiglio, M. Brombin, A. Buffa, A. Canton, S. Cappello, L. Carraro, R. Cavazzana, M. Cavinato, G. Chitarin, S. Dal Bello, A. De Lorenzi, D.F. Escande, A. Fassina, P. Franz, G. Gadani, E. Gaio, E. Gazza, L.Giudicotti, F. Gnesotto, L. Grando, S.C. Guo, P. Innocente, R. Lorenzini, A. Luchetta, G. Malesani, G. Manduchi, D. Marcuzzi, P. Martin, S. Martini, E. Martines, A. Masiello, F. Milani, M. Moresco, A. Murari, L. Novello, S. Ortolani, R. Paccagnella, R. Pasqualotto, S. Peruzzo, R. Piovan, A. Pizzimenti, N. Pomaro, M.E. Puiatti, G. Rostagni, F. Sattin, P. Scarin, G. Serianni, P. Sonato, E. Spada, A. Soppelsa, G. Spizzo, M. Spolaore, C. Taccon, C. Taliercio, V. Toigo, N. Vianello, P. Zaccaria, B. Zaniol, L. Zanotto, E. Zilli, G. Zollino, M. Zuin: "Magnetic Self Organization, MHD Active Control and Confinement in RFX-mod", *Plasma Phys. Control. Fusion* 49 (2007) B359–B369

R.36 S. V. Annibaldi, F. Bonomo, R. Pasqualotto, G. Spizzo, A. Alfier, P. Buratti, P. Piovesan, D. Terranova: "Strong transport reduction in the helical core of the reversed-field pinch", Phys. Plasmas 14 (2007) 112515

R.37 S J Zweben, J A Boedo, O Grulke, C Hidalgo, B LaBombard, R J Maqueda, P Scarin and J L Terry: "Edge turbulence measurements in toroidal fusion devices", Plasma Physics and Controlled Fusion, 49, S1 (2007)

R.38 B. Cannas, A. Fanni, P. Sonato, M.K. Zedda, and JET-EFDA contributors, "Real time prediction of disruptions at JET," *Nuclear Fusion*, 47, 1559-1569, Nov. 2007.

R.39 R. Delogu, A. Fanni, and A. Montisci, "Geometrical Synthesis of MLP Neural Networks," *Neurocomputing* , Elsevier ISSN: 0925-2312. doi:10.1016/j.neucom. 2007.02.006 (in stampa.).

R.40 P. Testoni, F. Cau, P. Sonato "Electromechanical analysis of the ITER Ion Cyclotron antenna structure and components" Fusion Engineering and Design, 82 (2007) 666-670

R.41 P. Testoni, F. Cau, M. Di Mauro, A. Fanni, A. Portone, P. Sonato, E. Salpietro "Electromechanical analysis of the European Superconducting Dipole" Fusion Engineering and Design vol. 82 (2007) pp 1423-1430.

R.42 F. Cau, M. Di Mauro, A. Fanni, A. Montisci, and P. Testoni, "A Neural Networks Inversion–Based Algorithm for Multiobjective Design of a High-Field Superconducting Dipole Magnet," IEEE Trans. On MAG, vol. 43, no. 4, pp. 1557-1560, April 2007

R.43 P. Testoni, F. Cau and P. Sonato: "Electromechanical analysis of the ITER ion cyclotron antenna structure and components", Fus. Eng. and Design, 82, Issues 5-14 (2007) 666

R.44 A. Masiello, A. De Lorenzi, L. Grando and L. Svensson: "Critical issues of HV dc vacuum and pressurized gas environments for the ITER NB injector", Fus. Eng. and Design, 82, Issues 5-14 (2007) 819

R.45 A. De Lorenzi, L. Grando, R. Gobbo, G. Pesavento, P. Bettini, R. Specogna and F. Trevisan: "The insulation structure of the 1 MV transmission line for the ITER neutral beam injector", Fus. Eng. and Design, 82, Issues 5-14 (2007) 836-844

R.46 P. Agostinetti, S. Dal Bello, M. Dalla Palma and P. Zaccaria: "Thermo-mechanical design of the SINGAP accelerator grids for ITER NB injectors", Fus. Eng. and Design, 82, Issues 5-14 (2007) 860-866

R.47 M. Bigi, V. Toigo and L. Zanotto: "Protections against grid breakdowns in the ITER neutral beam injector power supplies", Fus. Eng. and Design, 82, Issues 5-14 (2007) 905-911

R.48 E. Gaio, W. Kraus, C. Martens, R. Piovan, E. Speth and V. Toigo: "Studies on the radio frequency power supply system for the ITER NB injector ion source", Fus. Eng. and Design, 82, Issues 5-14 (2007) 912-919

R.49 S. Peruzzo, G. Anaclerio, S. Dal Bello, M. Dalla Palma, R. Nocentini and P. Zaccaria: "Thermal analyses for the design of the ITER-NBI arc driven ion source", Fus. Eng. and Design, 82, Issues 5-14 (2007) 933-940

R.50 P. Bettini, M. Cavinato and A. De Lorenzi: "Model of the RFX-mod poloidal field circuit", Fus. Eng. and Design, 82, Issues 5-14 (2007) 966-973

R.51 G. Marchiori and A. Soppelsa: "Development and validation of an electromagnetic model of the active control system of MHD modes in RFX-mod", Fus. Eng. and Design, 82, Issues 5-14 (2007) 1015-1022

R.52 T. Bolzonella, M. Cavinato, E. Gaio, L. Grando, A. Luchetta, G. Manduchi, G. Marchiori, L. Marrelli, R. Paccagnella, A. Soppelsa and P. Zanca: "Feedback control of resistive wall modes by saddle coils in RFX-mod", Fus. Eng. and Design, 82, Issues 5-14 (2007) 1064-1072

R.53 L. Zabeo, G. Artaserse, A. Cenedese, F. Piccolo and F. Sartori:" A new approach to the solution of the vacuum magnetic problem in fusion machines", Fus. Eng. and Design, 82, Issues 5-14 (2007) 1081-1088

R.54 B. Cannas, R.S. Delogu, A. Fanni, P. Sonato and M.K. Zedda: "Support vector machines for disruption prediction and novelty detection at JET", Fus. Eng. and Design, 82, Issues 5-14 (2007) 1124-1130

R.55 P. Testoni, F. Cau, A. Portone, M. Di Mauro, A. Fanni, E. Salpietro and P. Sonato: "Electro-mechanical analysis of the European superconducting dipole", Fus. Eng. and Design, 82, Issues 5-14 (2007) 1423-1430

R.56 V. Toigo, L. Zanotto, M. Bigi, E. Gaio, J.H. Hay, R. Piovan and S.R. Shaw: "Conceptual design of the enhanced radial field amplifier for plasma vertical stabilisation in JET", Fus. Eng. and Design, 82, Issues 5-14 (2007) 1599-1606

R.57 A. Masiello, S. Dal Bello, M. Fincato and F. Rossetto: "Performance of modified pulse-operated piezoelectric valves for the gas inlet system of RFX", Fus. Eng. and Design, 82, Issues 15-24 (2007) 2282-2287

R.58 P. Zaccaria, S. Dal Bello and N. Pilan: "Thermo-mechanical analyses of large ceramic rings during brazing process", Fus. Eng. and Design, 82, Issues 15-24 (2007) 2588-2594

R.59 D. Marcuzzi, P. Agostinetti, M. Dalla Palma, H.D. Falter, B. Heinemann, R. Riedl, Design of the RF ion source for the ITER NBI, Fusion Engineering and Design 82 Issues 5-14 (2007) 798–805

R.60 M Leigheb, M Romanelli, L Gabellieri, L Carraro, M Mattioli, C Mazzotta, M E Puiatti, L Lauro-Taroni, M Marinucci, S Nowak, L Panaccione, V Pericoli, P Smeulders, O Tudisco, C Sozzi, M Valisa and the FTU team: "Molybdenum transport in high density FTU plasmas with strong radio frequency electron heating" Plasma Phys. Control. Fusion 49 No 11 (November 2007) 1897-1912

Conference proceedings

P.1 M. Brombin , A. Boboc, C. Mazzotta, L. Zabeo, A. Murari, F. Orsitto, E. Zilli, L.Giudicotti and JET EFDA contributors: "The line-integrated plasma density from both interferometry and polarimetry at JET", 34thEPS Conference on Plasma Physics, 2 - 6 July 2007, Europhysics Conference Abstracts Vol. 31I (2007) P-2.144

P.2 A. Pizzimenti, R. Paccagnella: "Linear control model for m=0 modes in the RFX-mod Reversed Field Pinch", 34thEPS Conference on Plasma Physics, 2 - 6 July 2007, Europhysics Conference Abstracts Vol. 31I (2007) P1.135

P.3 D.F. Escande and F. Sattin: "Limits and potentialities of Fokker-Planck Equation in describing anomalous transport", 34thEPS Conference on Plasma Physics, 2 - 6 July 2007, Europhysics Conference Abstracts Vol. 31I (2007) P4.051

P.4 B. Zaniol, L. Carraro, E. Gazza, I. Predebon, M.E. Puiatti, P. Scarin, M. Valisa: "Impurity flow studies in RFX-mod operation with reduced MHD mode activity.", 34thEPS Conference on Plasma Physics, 2 - 6 July 2007, Europhysics Conference Abstracts Vol. 31I (2007) P1.082

P.5 M.Agostini, R.Cavazzana, F.Sattin, P.Scarin, G.Serianni, M.Spolaore, N.Vianello: "Characterisation of the 2-dimensional edge turbulence of RFX-mod experiment", 34thEPS

Conference on Plasma Physics, 2 - 6 July 2007, Europhysics Conference Abstracts Vol. 31I (2007) P2.044

P.6 M. Agostini, S.J. Zweben, R. Cavazzana, P. Scarin, G. Serianni, R.J. Maqueda, D.P. Stotler: "Comparison of L-mode and H-mode edge turbulence in NSTX with the GPI diagnostic", 34thEPS Conference on Plasma Physics, 2 - 6 July 2007, Europhysics Conference Abstracts Vol. 31I (2007) P2.040

P.7 M. Zuin, N. Vianello, M. Spolaore, T. Bolzonella, R. Cavazzana, E. Martines, D. Terranova, G. Serianni, E. Spada, V. Antoni: "Relaxation event fast dynamics in RFX-mod", 34thEPS Conference on Plasma Physics, 2 - 6 July 2007, Europhysics Conference Abstracts Vol. 31I (2007) P1.118

P.8 V. Igochine, P. Piovesan, A. Flaws, M. García-Muñoz, S. Guenter, , M. Marasheck, L. Marrelli, P. Martin, P. McCarty, K. Sassenberg, H. Zohm: "TAE internal structure through high-resolution soft x-ray measurements in ASDEX-Upgrade", 34thEPS Conference on Plasma Physics, 2 - 6 July 2007, Europhysics Conference Abstracts Vol. 31I (2007) P1.139

P.9 M.Gobbin, L. Marrelli, F. Bonomo, P. Franz, P. Martin, R.B. White: "Implementation in the ORBIT code of radial perturbations in the RFX-mod toroidal geometry", 34thEPS Conference on Plasma Physics, 2 - 6 July 2007, Europhysics Conference Abstracts Vol. 31I (2007) P1.107

P.10 F.Bonomo, P. Franz, M. Gobbin, L. Marelli, G. Spizzo, A. Alfier, P. Martin, R. Pasqualotto, P. Piovesan. D. Terranova: "Imaging of core MHD activity in RFX-mod", 34thEPS Conference on Plasma Physics, 2 - 6 July 2007, Europhysics Conference Abstracts Vol. 31I (2007) P1.130

P.11 A.Alfier, S. Annibaldi, F. Bonomo, P. Buratti, P. Franz, L. Frassinetti, L. Marrelli, R. Pasqualotto, P.Piovesan, G. Spizzo, D. Terranova: "Energy confinement in high current RFX-mod plasmas", 34thEPS Conference on Plasma Physics, 2 - 6 July 2007, Europhysics Conference Abstracts Vol. 31I (2007) P1.065

P.12 P. Martin, M. Gobbin, L. Marrelli, H.-U. Fahrbach , M. Garcia-Munoz, S. Günter, V. Igochine, M. Maraschek, M. Reich, E. Strumberger , R.B. White, H. Zohm and the AUG team: "Numerical study of fast ions transport induced by MHD instabilities in the tokamak", 34thEPS Conference on Plasma Physics, 2 - 6 July 2007, Europhysics Conference Abstracts Vol. 31I (2007) P4.073

P.13 S.Martini, T.Bolzonella, L.Marrelli, R.Paccagnella, D.Terranova, P.Zanca and the RFX Team: "High current RFPs in RFX-mod with induced Locked Mode rotation", 34thEPS Conference on Plasma Physics, 2 - 6 July 2007, Europhysics Conference Abstracts Vol. 31I (2007) P5.134

P.14 P. Innocente, A. Alfier, A. Canton, R. Lorenzini, E. Martines, G. Spizzo, R. Pasqualotto, D. Terranova : "Particles and Energy stochastic transport in the RFX-mod reversed field pinch experiment", 34thEPS Conference on Plasma Physics, 2 - 6 July 2007, Europhysics Conference Abstracts Vol. 31I (2007) P2.051

P.15 F. Auriemma, D. Terranova, R. Lorenzini, P. Innocente,Y. Hirano, H. Koguchi H. Sakakita: "Interaction of pellets with plasma in standard and advanced regimes at TPE-RX reversed field pinch experiment", 34thEPS Conference on Plasma Physics, 2 - 6 July 2007, Europhysics Conference Abstracts Vol. 31I (2007) P4.156

P.16 L. Marrelli, M. Valisa, and the RFX-mod team: "MHD active control and density regimes in RFX-mod", 34thEPS Conference on Plasma Physics, 2 - 6 July 2007, Europhysics Conference Abstracts Vol. 31I (2007) Invited

P.17 L. Carraro, M.E. Puiatti, Valisa, M. C. Angioni ,P. Buratti, R. Buttery, I. Coffey, D. Van Eester , C. Giroud, L. Lauro Taroni, K. Lawson, E. Lerche P. Mantica, M. Mattioli, V. Naulin, and JET-EFDA contributors: "Impurity profile control in JET plasmas with radio-frequency power injection", 34thEPS Conference on Plasma Physics, 2 - 6 July 2007, Europhysics Conference Abstracts Vol. 31I (2007) O4.028

P.18 G. Serianni, M. Agostini, V. Antoni, R. Cavazzana, E. Martines, F. Sattin, P. Scarin, E. Spada, M. Spolaore, N. Vianello, M. Zuin: "Coherent structures and transport properties in magnetised plasmas", 34thEPS Conference on Plasma Physics, 2 - 6 July 2007, Europhysics Conference Abstracts Vol. 31I (2007) Invited

P.19 I Nunes, G Saibene, R Sartori, P J Lomas, C P Perez, S Saarelma, A Alfier, Y. Andrew, G Arnoux, M Beurskens, A Boboc, I Coffey, K Crombe, E Giovannozzi, M. Kempenaars, K Lawson, H Leggate, E de la Luna, C McKenna, V Parail, R. Pasqualotto and the JET EFDA contributors: "Small ELMs in quasi-double null plasmas at JET", 34thEPS Conference on Plasma Physics, 2 - 6 July 2007, Europhysics Conference Abstracts Vol. 31I (2007) P5.137

P.20 E. de la Luna, L. Barrera, L. Figini, A. Alfier, Y. Andrew, M. Beurskens, D. Farina, E. Giovanozzi, M. Kempenaars, A. Loarte, P. Lomas, C. Mckeena, R. Pasqualotto, G. Saibene, R. Sartori, E. R. Solano and JET-EFDA contributors: "Measurements of inboard-outboard asymmetr y of pedestal temperature collapse during Type I ELMs in JET", 34thEPS Conference on Plasma Physics, 2 - 6 July 2007, Europhysics Conference Abstracts Vol. 31I (2007) P5.085

P.21 F. Milani, V. Toigo, L. Zanotto: "Energy storage for power hole mitigation on the electric grid due to the ITER Neutral Beam Injector", 22nd SOFE - Albuquerque - New Mexico (USA) – 17 - 22 June 2007, Proceedings to be published

P.22 P. Agostinetti, S. Dal Bello, M. Dalla Palma ,D. Marcuzzi, P. Zaccaria, R. Nocentini, M. Froeschle, B. Heinemann, R. Riedl: "Thermo-mechanical design of the ITER NB Injector grids for Radio Frequency Ion Source and SINGAP Accelerator", 22nd SOFE - Albuquerque - New Mexico (USA) – 17 - 22 June 2007, Proceedings to be published

P.23 M. Bigi: "An LC output filter with voltage clamp for the Enhanced Radial Field Amplifier", 22nd SOFE - Albuquerque - New Mexico (USA) – 17 - 22 June 2007, Proceedings to be published

P.24 R. Piovan, E. Gaio, L.Novello: " Performance analysis of a hybrid IGCTS- mechanical dc circuit breaker for SC magnet quench protection ", 22nd SOFE Albuquerque - New Mexico (USA) – 17 - 22 June 2007, Proceedings to be published

P.25 M. Cavinato, A. Luchetta, G. Manduchi, G. Marchiori, A. Soppelsa, C. Taliercio: "Control of plasma parameters by the externally applied toroidal field in RFX-mod", Proceedings of Sixth IAEA Technical Meeting on Control, Data Acquisition, and Remote Participation for Fusion Research, 4 - 8 June 2007 , Inuyama, Japan

P.26 G. Marchiori, L. Marrelli, A. Soppelsa, P. Zanca: "Design of a New Controller of MHD Modes in RFX-mod", Proceedings of Sixth IAEA Technical Meeting on Control, Data Acquisition, and Remote Participation for Fusion Research, 4 - 8 June 2007, Inuyama, Japan

P.27 Barbalace, A. Luchetta*, G. Manduchi, A. Soppelsa, C. Taliercio: "Real-Time Communication for Distributed Plasma Control Systems", Proceedings of Sixth IAEA Technical Meeting on Control, Data Acquisition, and Remote Participation for Fusion Research, 4 - 8 June 2007 , Inuyama, Japan

P.28 G. Manduchi, F. Iannone , F. Imbeaux, , G. Huysmans, J. Lister: “A Universal Access Layer for the Integrated Tokamak Modeling Task Force”, Proceedings of Sixth IAEA Technical Meeting on Control, Data Acquisition, and Remote Participation for Fusion Research, 4 - 8 June 2007, Inuyama, Japan

P.29 G.Manduchi, A. Luchetta, C. Taliercio, T.Fredian, J.Stillerman: “Real-Time Data Access Layer for MDSplus”, Proceedings of Sixth IAEA Technical Meeting on Control, Data Acquisition, and Remote Participation for Fusion Research, **4 -** 8 June 2007, Inuyama, Japan

P.30 A.Barbalace, A. Luchetta, G. Manduchi, M. Moro, A. Soppelsa, C. Taliercio: “Performance Comparison of VxWorks, Linux RTAI and Xenomai in a Hard Real-Time Application”, 15th IEEE NPSS Real Time Conference 2007 April 29- May 4, 2007, Fermilab, Batavia, IL USA, proceedings to be published

P.31 O. Barana, A. Luchetta, G. Manduchi and C. Taliercio: “New Architecture for the RFX-mode Machine Control System”, 15th IEEE NPSS Real Time Conference 2007 April 29- May 4, 2007 Fermilab, Batavia, IL USA, proceedings to be published

P.32 O. Barana, A. Murari and I. Coffey: “Artificial Neural Networks for Real-time Diagnostic of High-Z Impurities in Reactor-relevant Plasmas”, Proceedings of 2007 IEEE International Symposium on Signal Processing, 3 - 5 October 2007 , Alcalà de Henares (Madrid), Spain

1

P.33 B. Cannas, R. S. Delogu, A. Fanni, A. Montisci, M.K.Zedda, P.Sonato: “Geometrical Kernel Machine for Prediction and Novelty Detection of Disruptive Events in TOKAMAK Machines”, 2007 IEEE International Workshop on MACHINE LEARNING FOR SIGNAL PROCESSING, Proc to be published

Contributions to international and national conferences

C.1. N.Vianello, E.Spada, R.Cavazzana, E.Martines, G.Serianni, M.Spolaore, M.Zuin and V.Antoni: “Energy balance including turbulence effects in Reversed Field Pinch Plasmas”, presented at 12th US-EU Transport Taskforce Workshop, San Diego CA USA, 17-20 April 2007

C.2. P. Innocente and the RFX Team: "Confinement enhancement with Virtual Shell in RFX-mod", presented at 12th IEA/RFP Workshop, 26-28 march, 2007, Kyoto, Japan

C.3. M.E. Puiatti, M. Valisa, S. Cappello, L. Carraro, L. Frassinetti, P.Innocente, R. Lorenzini, R. Paccagnella, F. Sattin, P. Scarin, G. Spizzo, M. Spolaore, N. Vianelloand the RFX team: "High density limit in hydrogen and helium discharges in RFX-mod", presented at 12th IEA/RFP Workshop, 26-28 march, 2007, Kyoto, Japan

C.4. F. Auriemma, R. Lorenzini, D. Terranova, R. Cavazzana, P. Innocente, S. Martini, G. Serianni, M. Zuin: "Toroidally asymmetric particle transport caused by phase locking of MHD modes in RFX-mod", presented at 12th IEA/RFP Workshop, 26-28 march, 2007, Kyoto, Japan

C.5. F. Auriemma, H. Koguchi, D. Terranova, Y. Hirano, P. Innocente, S. Kyiama, R. Lorenzini, H. Sakakita, K. Yambe, T. Asai: "Pellet injection in TPE-RX", presented at 12th IEA/RFP Workshop, 26-28 march, 2007, Kyoto, Japan

C.6. P. Martin: "Fast ion confinement in RFP and comparison with tokamak", presented at 12th IEA/RFP Workshop, 26-28 march, 2007, Kyoto, Japan

C.7. P. Piovesan, A. Alfier, F. Bonomo, P. Franz, M. Gobbin, L. Marrelli, P. Martin,R. Pasqualotto, G. Spizzo, and the RFX-mod team: "Recent results on QSH in RFX-mod and MST", presented at 12th IEA/RFP Workshop, 26-28 march, 2007, Kyoto, Japan

C.8. P. Zanca, L. Marrelli, G. Manduchi, G. Marchiori: "Beyond the Intelligent-Shell concept: the Clean-Mode-Control for tearing instabilities", presented at 12th IEA/RFP Workshop, 26-28 march, 2007, Kyoto, Japan

C.9. L. Marrelli, A.Alfier,T.Bolzonella, F.Bonomo, M.Gobbin, S.C.Guo, P.Franz, A.Luchetta, G.Manduchi, G.Marchiori, P.Martin, S.Martini,S. Ortolani, P.Piovesan, R.Paccagnella, R. Pasqualotto, A.Soppelsa, G.Spizzo, D.Terranova, P.Zanca and the RFX-mod team: "Active Control of Resistive KinActive Control of Resistive Kink Instabilities and Magnetic self-Organization", presented at 12th IEA/RFP Workshop, 26-28 march, 2007, Kyoto, Japan

C.10. P. Scarin, M. Agostini, R. Cavazzana, F. Sattin, G. Serianni, N. Vianello, Y. Yagi, H. Koguchi, S. Kiyama, H. Sakakita, Y. Hirano:"Intermittent turbulence study in the edge of RFP plasma with GPI diagnostic"

C.11. V. Antoni, M. Spolaore, N. Vianello, R. Cavazzana, G. Serianni,E. Martines, E. Spada, M. Zuin: "Electrostatic transport and coherent structures in RFX-mod", presented at 12th IEA/RFP Workshop, 26-28 march, 2007, Kyoto, Japan

C.12. R. Piovan, S. Cappello, D. Terranova, L. Zanotto, M. Zuin: "First results of RFX-mod test on low-q pinches", presented at 12th IEA/RFP Workshop, 26-28 march, 2007, Kyoto, Japan

C.13. D. Bonfiglio, S. Cappello, R. Piovan, G. Spizzo, D. Terranova: "Preliminary results of 3D nonlinear MHD simulations for ultra-low q plasmas and OPCD RFP discharges", presented at 12th IEA/RFP Workshop, 26-28 march, 2007, Kyoto, Japan

C.14. M. Zuin, N.Vianello, M. Spolaore, R. Cavazzana, E. Martines, G. Serianni, E. Spada, V. Antoni, T. Bolzonella, D. Terranova: "Current structure generation and discrete magnetic relaxation events", presented at 12th IEA/RFP Workshop, 26-28 march, 2007, Kyoto, Japan

C.15 L. Zanotto, M. Barp, M. Bigi, A. Ferro, E. Gaio, F. Milani, L. Novello, R. Piovan, M. Recchia, V. Toigo, A. Zamengo: "Tecnologie di accumulo energetico negli impianti di ricerca sulla fusione e prospettive per il reattore", Giornata di studio "Energy Storage Technologies" EST2007, 8 Ottobre 2007, Bologna

C.16 R. Paccagnella, A. Pizzimenti, "Studies on externally applied m=0 modes in the RFX-mod RFP" presented at the Workshop on Active Control of MHD 18-20 November 2007, Columbia University (New York, Usa)

C.17 F. Bonomo, A. Alfier, S.V. Annibaldi, P. Buratti, R. Pasqualotto, P. Piovesan, G. Spizzo, D. Terranova: "Transport reduction and heating in the helical core of the reversed-field pinch", 49th Annual Meeting of the Division of Plasma Physics - APS, Orlando, Florida, 12 – 16 November, 2007, JP8.00147

C.18 M.E. Puiatti, S. Cappello, F. Carrara, P. Scarin, G. Spizzo, D. Terranova, M. Valisa, B. Zaniol: "Density limit, radiation and magnetic topology in the reversed-field pinch", 49th Annual Meeting of the Division of Plasma Physics - APS, Orlando, Florida, 12 – 16 November, 2007, JP8.00148

C.19 D. Terranova, A. Canton, P. Innocente, R. Lorenzini, P. Zanca, A. Alfier, F. Bonomo: "Enhanced confinement, magnetic topology and diffusion in RFX-mod for poloidal current

drive and pellet injection experiment", 49th Annual Meeting of the Division of Plasma Physics - APS, Orlando, Florida, 12 – 16 November, 2007, TO4.00010

C.20 P. Scarin, M. Agostini, R. Cavazzana, G. Serianni, "Edge turbulence scaling in RFX-mod with the GPI diagnostic", 49th APS 2007, 12-16 November, Orlando

C.21 M. Agostini, S.J. Zweben, R. Cavazzana, P. Scarin, G. Serianni, R.J. Maqueda, D.P. Stotler, "Study of the statistical properties of edge turbulence in NSTX with the GPI diagnostic", 49th APS 2007, 12-16 November, Orlando

C.22 R. Piovan, S. Cappello, L. Zanotto, D. Terranova, M. Zuin, F. Auriemma, P. Scarin**:** "Preliminary Results from ULQ Experiments in RFX-mod", 49th Annual Meeting of the Division of Plasma Physics - APS, Orlando, Florida, 12 – 16 November, 2007, JP8.00143

C.23 P. Franz, F. Bonomo, G.Spizzo, B.E. Chapman, J.A. Goetz: "X-ray emission maps in the MST reversed Field pinch", 49th Annual Meeting of the Division of Plasma Physics - APS, Orlando, Florida, 12 – 16 November, 2007

C.24 H. Koguchi, H. Sakakita, M. Kiyama, K. Yambe, T. Asai, Y. Hirano, F. Auriemma, D. Terranova, P. Innocente: "High beta and high-density operation in TPE-RX", invited session of Japanese Society of Plasma Science and Nuclear Fusion Research Annual Meeting in Himeji, Japan (2007)

C.25 G. Agarici, P. Testoni, et al. "Mechanical design proposal of an Ions Cyclotron Resonant Heating antenna for ITER" 17th Topical Conference on Radio Frequency Power in Plasmas - 7-9 Maggio 2007, Clearwater, Florida, USA

C.26 F. Cau, A. Fanni, A. Portone, P. Sonato and P. Testoni. "3D Electromechanical analyses of the European Superconducting Dipole" 16th International Conference on the Computation of Electromagnetic Fields (COMPUMAG), 24-28 Giugno 2007, Aachen, Germany

C.27 P. Testoni, F. Cau, A. Fanni, A. Portone, P. Sonato. "Static and transient electromagnetic features of the EFDA dipole" 20th Conference on Magnet technology - 27-31 Agosto 2007, Philadelphia, Pennsylvania USA

C.28 S. Cappello, D. Bonfiglio, R. Piovan: "3D nonlinear MHD simulations for ultra-low q plasmas**",** poster contribution for the 49th APS DPP meeting, Orlando (2007)

C.29 S. Cappello, D. Bonfiglio, G. Spizzo, D. Terranova, R. B. White, "Ordered magnetic topology in Reversed Field Pinch configurations**",** poster contribution for the 12th European Fusion Theory Conference, Madrid (2007)

C.30 D.F. Escande and F. Sattin**: "**When can Fokker-Planck equation describe anomalous transport?", poster contribution for the 12th European Fusion Theory Conference, Madrid (2007)

C.31 I. Predebon and R. Paccagnella: "Contribution of slow particle dynamics to chaotic transport in RFP plasmas", poster contribution for the 12th European Fusion Theory Conference, Madrid (2007).

C.32 G. Spizzo1, R. B. White1, S. Cappello1, L.Marrelli1 and F. Sattin: "Pinch effects and chaotic motion in toroidal confinement devices", poster contribution for the 12th European Fusion Theory Conference, Madrid (2007)